

University of Louisville

## ThinkIR: The University of Louisville's Institutional Repository

---

Electronic Theses and Dissertations

---

5-2024

### Porphyromonas gingivalis inactivates anti-viral immunity at the oral and respiratory epithelium.

Carlos J. Rodriguez Hernandez  
*University of Louisville*

Follow this and additional works at: <https://ir.library.louisville.edu/etd>



Part of the [Immunology of Infectious Disease Commons](#)

---

#### Recommended Citation

Rodriguez Hernandez, Carlos J., "Porphyromonas gingivalis inactivates anti-viral immunity at the oral and respiratory epithelium." (2024). *Electronic Theses and Dissertations*. Paper 4305.  
<https://doi.org/10.18297/etd/4305>

This Doctoral Dissertation is brought to you for free and open access by ThinkIR: The University of Louisville's Institutional Repository. It has been accepted for inclusion in Electronic Theses and Dissertations by an authorized administrator of ThinkIR: The University of Louisville's Institutional Repository. This title appears here courtesy of the author, who has retained all other copyrights. For more information, please contact [thinkir@louisville.edu](mailto:thinkir@louisville.edu).

PORPHYROMONAS GINGIVALIS INACTIVATES ANTI-VIRAL IMMUNITY AT  
THE ORAL AND RESPIRATORY EPITHELIUM

By

Carlos J. Rodriguez Hernandez

B.S., Universidad de Puerto Rico, 2017

M.S., University of Louisville, 2020

A Dissertation

Submitted to the Faculty of the  
School of Medicine of the University of Louisville  
in Partial Fulfillment of the Requirements  
for the Degree of

Doctor of Philosophy in Microbiology and Immunology

Department of Microbiology and Immunology

University of Louisville,

Louisville, Kentucky

May 2024

Copyright 2024 by Carlos J. Rodriguez Hernandez

All rights reserved



PORPHYROMONAS GINGIVALIS INACTIVATES ANTI-VIRAL IMMUNITY AT  
THE ORAL AND RESPIRATORY EPITHELIUM

By

Carlos J. Rodriguez Hernandez

B.S., Universidad de Puerto Rico, 2017

M.S., University of Louisville, 2020

A Dissertation Approved on

February 23, 2024

By the following Dissertation Committee:

---

Juhi Bagaitkar, Ph.D. (Mentor)

---

Kevin Sokoloski, Ph.D. (Co-mentor)

---

Richard J. Lamont, Ph.D.

---

Donghoon Chung, Ph.D.

---

Carolyn Casella, Ph.D.

## ACKNOWLEDGEMENTS

I would like to express my deepest gratitude to all of my family but specially to my parents, Irma and Jesus, for their untiring support, encouragement, and love throughout this journey. Your guidance and belief in me have been the cornerstone of my success, and I am endlessly grateful for the sacrifices you have made to help me pursue my dreams.

I extend my heartfelt thanks to all the other friends I have made on this journey, including Hazel, Amanda, Irina, Chris, Caleb, and Ali. Your camaraderie, laughter, and companionship have enriched my life in countless ways, and I am fortunate to have shared this journey with each of you. To Kelley, your encouragement and friendship have meant the world to me. Thank you for your kindness, and for always be there for me. Your friendship and support have been instrumental in helping me overcome obstacles and stay motivated.

I would also like to express my sincere gratitude to my mentor, Juhi, for her unwavering support, guidance, and encouragement throughout my academic journey. Her expertise, patience, and mentorship have been invaluable in shaping my research and personal growth. I am also deeply grateful to my dissertation committee members, Kevin Sokoloski, Richard Lamont, Donghoon Chung and

Carolyn Casella, for their insightful feedback, constructive criticism, and valuable suggestions, which have significantly enriched the quality of my work.

## ABSTRACT

### PORPHYROMONAS GINGIVALIS INACTIVATES ANTI-VIRAL IMMUNITY AT THE ORAL AND RESPIRATORY EPITHELIUM

Carlos J. Rodriguez Hernandez

February 23, 2024

The host microbiome plays an important role in fine-tuning host immune responses in a manner that ultimately impacts outcomes in viral infection. Symbiotic relationships between commensal bacteria and host epithelial and immune cells prime interferon (IFN) signaling, modulating the nature and intensity of the immune response to viral infections at mucosal barrier surfaces. In this doctoral thesis, I explore how dysbiotic shifts in the oral microbial communities modulate antiviral responses at the oral and oro-respiratory mucosal barriers. I identified that in response to a viral challenge, gingival epithelial cells (GECs) preferentially induced type III IFNs (IFN- $\lambda$ ), a newly described family member of the interferon family that plays a superior role in regulating antiviral immunity at barrier surfaces. While IFN- $\lambda$  strongly activated multiple interferon-stimulated genes (ISGs) in human gingival epithelial cells. However, IFN- $\lambda$  responses were significantly dampened in the presence of *Porphyromonas gingivalis*, an oral periodontal pathogen. Mechanistically, *P. gingivalis* virulence factors inactivated IFN-inducing transcription factors and suppressed IFN promoter activity,



subsequently dampening ISG induction. This was coupled with the proteolytic degradation of IFN receptors by *P. gingivalis* proteases, *gingipains*, inducing refractoriness to exogenous IFN stimulation. Overall, *P. gingivalis* induced suppression of IFN signaling significantly enhanced host susceptibility to viral infection of oral epithelial cells. Furthermore, I found that *P. gingivalis* mediated IFN suppression was not limited to the oral epithelium but also impacted airway epithelial cells in a similar manner. In conclusion, my data highlights how a bacterial pathogen associated with oral dysbiosis can significantly impact susceptibility to viral infections at both oral and respiratory barriers.

TABLE OF CONTENTS

**ACKNOWLEDGEMENTS..... iii**

**ABSTRACT..... v**

**LIST OF FIGURES..... x**

**LIST OF TABLES ..... xii**

**CHAPTER 1: ..... 1**

**STRUCTURE AND FUNCTION OF THE ORAL MUCOSAL BARRIER..... 1**

    1.1. Overview of the Oral Mucosal Barrier..... 1

    1.2. The Structure of the Oral Epithelium ..... 2

    1.3. Gingival Epithelial Cells and Immune Surveillance ..... 7

    1.4. Pattern Recognition Receptors ..... 7

    1.5. Antimicrobial Peptides ..... 11

    1.6. Oral Epithelial Chemokine Gradients ..... 12

    1.7. Interferons and antiviral immunity ..... 13

    1.8. IFN- $\lambda$  and Oral Mucosal Antiviral Immunity ..... 17

**CHAPTER 2: ..... 19**

**ORAL DYSBIOSIS AND THE MANIPULATION OF ANTIVIRAL IMMUNITY... 19**

    2.1. Oral Microbial Colonizers and Dysbiosis ..... 19

2.2. <i>P. gingivalis</i> : a “rotten apple” within the gingival polymicrobial “barrel” .....	22
2.3. <i>Porphyromonas gingivalis</i> subverts oral antiviral immunity: .....	24
<b>CHAPTER 3: .....</b>	<b>25</b>
3.1. Introduction .....	25
3.2. Materials and methods .....	27
3.3. Results .....	35
3.4. Discussion.....	46
3.5. Figures:.....	50
<b>CHAPTER 4: .....</b>	<b>73</b>
<b><i>BACTERIAL-VIRAL RIVALRY: INVESTIGATING THE RELATIONSHIP BETWEEN PORPHYROMONAS GINGIVALIS AND RESPIRATORY SYNCYTIAL VIRUS IN MUCOSAL DEFENSE</i> .....</b>	<b>73</b>
4.1. Introduction .....	73
4.2. Materials and Methods: .....	74
4.3. Results .....	78
4.4. Discussion.....	82
4.5. Figures:.....	85
<b>CHAPTER 5: SUMMARY AND FUTURE DIRECTIONS .....</b>	<b>94</b>
<b>REFERENCES.....</b>	<b>102</b>

***CURRICULUM VITAE* ..... 115**

## LIST OF FIGURES

Figure 1.1: Gingival epithelium structure and function .....	3
Figure 1.2: Oral epithelium stratification.....	4
Figure 1.3: Pattern Recognition Receptors signaling.....	9
Figure 1.4: Interferon signaling Pathway.....	14
Figure 2.1. Microbial niches within the oral cavity.....	20
Figure 3.1. IFN- $\lambda$ is strongly expressed in gingival tissues, cell lines, and activates ISG expression in oral tissues.....	50
Figure 3.2. <i>P. gingivalis</i> infection causes IFN paralysis, characterized by the loss of basal and inducible IFN responses and ISG expression.....	52
Figure 3.3. <i>P. gingivalis</i> incapacitates transcription factors that positively regulate IFN- $\lambda$ expression, and up-regulates ZEB1, a transcriptional repressor of IFN- $\lambda$ .....	55
Figure 3.4. <i>P. gingivalis</i> infection reduces responsiveness to exogenous IFN- $\lambda$ .....	58
Supplemental Figure 3.1: IFN- $\lambda$ shows bioactivity in oral tissues.....	60
Supplemental Figure 3.2: Abundance of <i>P. gingivalis</i> in human samples and its effects on IFN production.....	62
Supplemental Figure 3.3: Silencing of IRF1 causes suppression of basal ISG expression.....	64

Supplemental Figure 3.4: Overexpression of IRF1 does not rescue <i>P. gingivalis</i> dependent suppression of ISGs.....	66
Supplemental Figure 3.5: <i>P. gingivalis</i> infection downregulates the expression of members of the IRF family of transcription factors.....	67
Supplemental Figure 3.6: Overexpression of STAT1 does not rescue <i>P. gingivalis</i> dependent suppression of ISGs.....	68
Supplemental Figure 3.7: <i>P. gingivalis</i> degrades STAT1 signaling protein.....	70
Supplemental Figure 3.8: <i>P. gingivalis</i> utilizes a multi-hit strategy to suppress IFN signaling in oral epithelium.....	71
Figure 4.1. <i>P. gingivalis</i> inhibits IFN responses in airway epithelium.....	85
Figure 4.2. <i>P. gingivalis</i> protects HBE cultures against RSV while inhibiting IFN.....	87
Figure 4.3. <i>P. gingivalis</i> protection of HBE cultures against RSV is independent of IFN suppression.....	89
Figure 4.4. Loss of RSV infection in <i>P. gingivalis</i> infected HBE cultures is not due to loss of tissue integrity.....	91
Figure 4.5. Impact of <i>P. gingivalis</i> and Gingipains on RSV infection.....	92

## LIST OF TABLES

Table 1.1: PRR Ligands.....	10
Table 1.2: ISGs mechanisms of antiviral and antibacterial effector functions....	17
Table 3.1: Antiviral restriction factors downregulated by <i>P. gingivalis</i> .....	70

## CHAPTER 1:

### STRUCTURE AND FUNCTION OF THE ORAL MUCOSAL BARRIER

#### 1.1. Overview of the Oral Mucosal Barrier

The oral cavity serves as a primary entry point for microbes into the body, acting as a gateway to the respiratory and gastrointestinal tracts. The mucosal lining of the oral cavity forms a protective barrier that protects the underlying tissues from microbial invasion and insults such as chemical and mechanical trauma. This barrier is formed by a continuous layer of stratified oral epithelial cells, which lines all the soft tissues within the oral cavity. It is supported by the underlying connective tissue or lamina propria that houses blood vessels and immune cells and provides structural support and nourishment to the avascular epithelial layer. The continuous renewal of oral epithelial cells by mitotic division and the formation of inter-cellular junctions regulate barrier integrity and permeability while protecting the host from microbial invasion. Depending on the anatomical region, the oral mucosa undergoes local structural adaptations and functional specialization that aid tissue function. In this chapter, I describe the structure of the oral epithelial barrier and its niche-specific adaptation and discuss epithelial cell-specific factors that guide the maintenance of barrier function and homeostatic immunity. I also discuss how the oral epithelium is more than a



passive barrier but serves as an inductive site for immune responses via expression of pattern recognition receptors and immune mediators.

## 1.2. The Structure of the Oral Epithelium

The entire surface of the oral cavity is lined with a layer of squamous stratified epithelium that forms a barrier and separates the underlying soft tissues from the external environment. The oral epithelium varies in thickness and degree of keratinization in order to adapt to the functional demands of the specific anatomical niche and is semi-permeable. It is classified functionally and histologically into three types. The dorsum of the tongue is covered with specialized epithelium, comprised of keratinized and non-keratinized regions [1, 2]. The 'lining mucosa,' as the name implies, lines the soft tissues such as the cheeks, lips, floor of the mouth, and the soft palate and is non-keratinized in nature. In contrast, the masticatory mucosa, which is found in the gingiva or gums that surround and protect teeth and is tightly attached to the tooth and the underlying alveolar bone is keratinized. Keratinization of the masticatory mucosa and the hard palate enables it to withstand mechanical damage caused by mastication. The gingival epithelium (as shown in Figure 1.1A) forms a V-shaped crevice known as the gingival crevice that surrounds each tooth and has a free margin on the apical side but is bound to the tooth on the basal side. The sulcular epithelium lines the gingival sulcus, while the junctional epithelium attaches to the wall of the tooth (Figure 1.1A) [1, 2]. The gingival sulcus is semi-permeable and allows for the

migration of neutrophils and other chemotactic substances, cytokines, and antimicrobial peptides into the sulcus, which can eventually be found in the saliva[3].

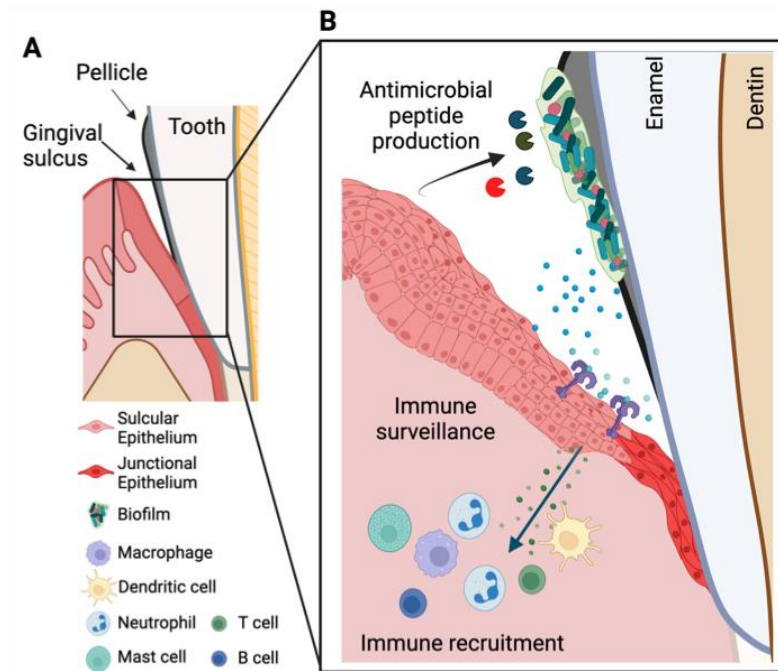


**Figure 1.1. Gingival epithelium structure and function:** (A) Anatomical boundaries and structures of the gingiva (B) GECs produce cytokines, antimicrobial peptides and chemokine gradients that recruit immune cells. These secretory functions are essential for limiting microbial ingress.

In the keratinized oral mucosa, the epithelium is composed of four strata or layers: stratum basale, stratum spinosum, stratum granulosum, and stratum corneum, which show distinct patterns of differentiation (Fig. 1.2). Mitotic division of the cells in the basal layer, their passive migration towards the apical surface, and subsequent shedding or desquamation ensures continuous renewal of the oral epithelium (Fig. 1.2). In the keratinized epithelium, migration is accompanied by keratin synthesis and morphological changes resulting in cellular flattening and progressive loss of organelles as cells differentiate into anucleate squamous cells

found in the stratum corneum [4]. Keratins are a large family of filamentous proteins expressed in differentiated epithelial cells that provide resilience against mechanical stress and maintain structural integrity [4]. They are often distributed in a tissue-specific pattern and vary according to the type of epithelial cell and its stage of differentiation, offering resistance against mechanical stress.

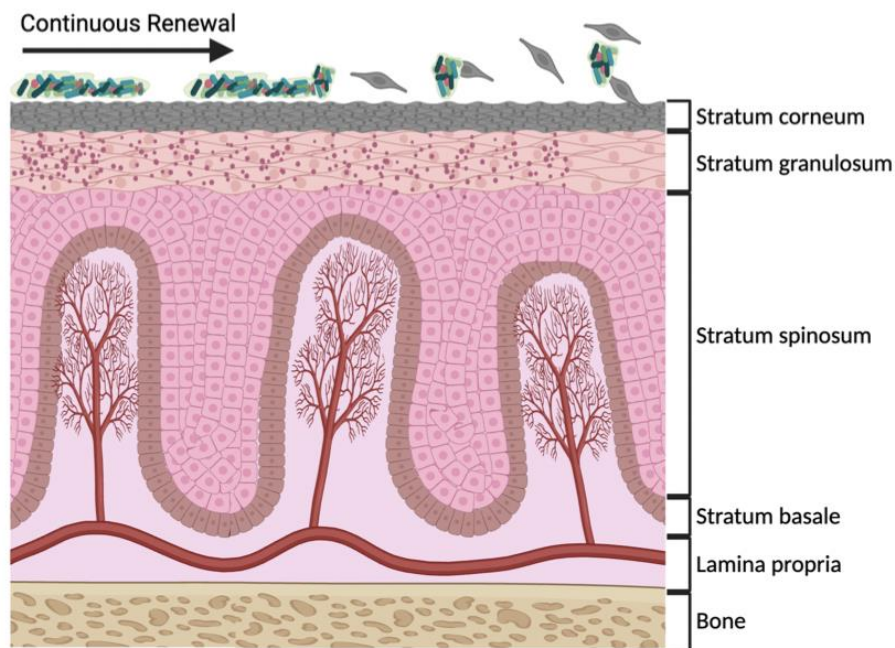


**Figure 1.2. Oral epithelium stratification:** (A) The stratification and keratinization of gingival epithelial cells (GECs) creates a physical barrier provides resistance against mastication induced mechanical trauma.

The structural integrity of the epithelium is further maintained by the presence of inter-cellular molecular protein complexes that form cell-to-cell junctions and allow for selective permeability. Broadly, cell junctions are classified into three groups: tight, gap, and anchoring junctions [4]. Tight junctions directly join two neighboring cells and obstruct the intercellular space. In the stratified

epithelium of the oral mucosa, tight junctions are present in the superficial layers, providing structural support and limiting the free flow of microbial ligands and other antigens across the oral mucosal barrier [5]. In contrast to the tight junctions that impart selective permeability, gap junctions are formed by transmembrane channels that permit direct exchange of ions, metabolites, and nutrients between adjacent cells, facilitating communication [6]. Lastly, anchoring junctions are multi-protein complexes formed between neighboring cells that link the cytoskeleton of one epithelial cell to the neighboring cell or the extracellular matrix. Thus, anchoring junctions serve as scaffolds between epithelial cell layers, providing strength and resilience [7, 8]. Anchoring junctions are further classified into adherens junctions, which bind to actin filaments, and desmosomes, which attach to intermediate filaments.

Interestingly, the intercellular junctions seem to be less developed in the junctional epithelium making it more permeable compared to other epithelial sites. It is characterized by larger intercellular spaces. Cellular junctions are continuously remodeled in the oral cavity and proteolytically degraded during desquamation, inflammation, or by the action of host or microbe-derived proteases[9]. The breakdown of claudin strands and decreased levels of E-cadherin with adherens junctions have been linked with large intercellular spaces within the junctional epithelium, making it permeable and allowing for the efflux of gingival crevicular fluid and other mediators[10, 11]. Furthermore, the recognition of microbial ligands can directly influence inflammatory responses, causing barrier breaches and microbial invasion into the tissue, ultimately disrupting barrier permeability. During

inflammation, pro-inflammatory cytokines such as tumor necrosis factor (TNF) and interleukin-1 beta (IL-1 $\beta$ ) can trigger the internalization and redistribution of tight junction proteins such as occludin and claudins, weakening the epithelial barrier [12] and exacerbating inflammatory tissue damage [13].

The epithelial layer is avascular and is supported by an underlying connective tissue or lamina propria, which contains neuronal structures, blood vessels, and lymphatic vessels and is infiltrated by immune cells. Broadly, the lamina propria is divided into the papillary layer and the deeper reticular layer. The papillary layer forms papillae ridges that interdigitate and connect with the epithelial layer. This layer is formed by irregularly oriented thin collagen and elastin fibers and capillary loops that allow for nutrient transport. The underlying reticular layer connects to the underlying structure and is formed by thicker collagen fibrils. Fibroblasts are the most abundant cells within the stroma/ lamina propria and aid in the deposition of the extracellular matrix [14, 15]. All regions of the oral mucosa are highly vascularized, allowing for an influx of leukocytes that play important roles in warding off microbial invaders. The gingival sulcus is constantly patrolled by neutrophils that come out of circulation and translocate into the gingival crevicular fluid due to the permeability of the junctional epithelium (Figure 1.1B) [16]. The mucosal-associated lymphoid tissue (MALT) that typically is found at other mucosal surfaces is absent in the oral mucosa. Instead, lymphoid aggregates have been observed around the epithelial invagination sites [17, 18]. These lymphoid foci and other infiltrating immune cells, such as macrophages, mast cells, neutrophils, dendritic cells, and Langerhans cells, all contribute towards inductive

and effector immune responses to a diverse antigenic load (Fig. 1.1B). Several lines of evidence show that the oral epithelium is an inductive site that actively senses microbes by dedicated receptors [19] and plays an important role in oral antimicrobial immunity against bacterial pathogens and viruses [20].

### 1.3. Gingival Epithelial Cells and Immune Surveillance

Under homeostatic conditions, the microbial community within the gingival biofilm lives in a complex network of interactions between the microbes themselves and also with the host [21]. This crosstalk between biofilms and the host is primarily mediated by the recognition of the microbial ligands by host pattern recognition receptors (PRRs). Oral epithelial cells respond to these diverse microbial assaults by the calibrated and synergistic activation of downstream signaling pathways, culminating in the release of inflammatory mediators.

### 1.4. Pattern Recognition Receptors

GECs detect conserved microbe-associated molecular patterns (MAMPs) via a series of membrane-restricted or cytosolic PRRs located either on the plasma membrane, endosomal membranes, or the cytosol. The strategic location of PRR facilitates the detection of extracellular as well as intracellular pathogens and the activation of downstream signaling cascades and transcriptional factors that mediate effector responses. Depending on the structural characteristics, sub-cellular location, and ligand specificity, PRRs are classified into 3-4 broad categories. Toll-like receptors (TLRs) are transmembrane dimeric receptors

located on the plasma or endosomal membranes that recognize microbial ligands from viruses, bacteria, and fungi with high specificity (Table 1.1). Upon ligand binding, TLRs signal by the recruitment of adaptor molecules MyD88 and/or TRIF. MyD88 activation induces the activity of NF- $\kappa$ B and the expression of inflammatory cytokines, whereas TRIF engagement preferentially induces the activation of IFN Regulatory Factors (IRFs) and the production of Type I IFNs (Fig 1.3).

Another category of receptors expressed by GECs belongs to the Nucleotide Oligomerization domain-like receptors (NLRs) family of cytosolic PRRs that have evolved to recognize pathogen ligands released into the cytosol. NLRs are particularly adept at recognizing microbial ligands from intracellular bacteria, such as LPS, lipoteichoic acid, and bacterial RNA [3, 27]. They also play an important role in antiviral immunity by recognizing viral RNA and proteins, eliciting robust immune responses to combat viral infections [22, 23] (Table 1.1). NLR activation results in the activation of RIP2 kinase and/or the assembly of the inflammasome complex, leading to the processing and the release of IL-1 $\beta$  [24] (Fig. 1.3).

Retinoic Acid Inducible Gene I (RIG-I)-like Receptors (RLR), are cytosolic receptors that undergo conformational changes and multimerization upon ligand binding, which allows for the binding of the adaptor protein MAVS. Signaling through MAVS links the RLR activation to the activation of IRF3/IRF7 and NF- $\kappa$ B, leading to the production of Type I and Type III IFNs and the initiation of the antiviral response [25] (Fig. 1.3). While RLRs primarily recognize viral RNA, intracellular sensors AIM2 (Absent in Melanoma 2), IFI16 (IFN Gamma Inducible

Protein 16), and the cGAS (Cyclic GMP-AMP synthase) / STING (Stimulator of IFN Genes), play important roles in the recognition of viral DNA.

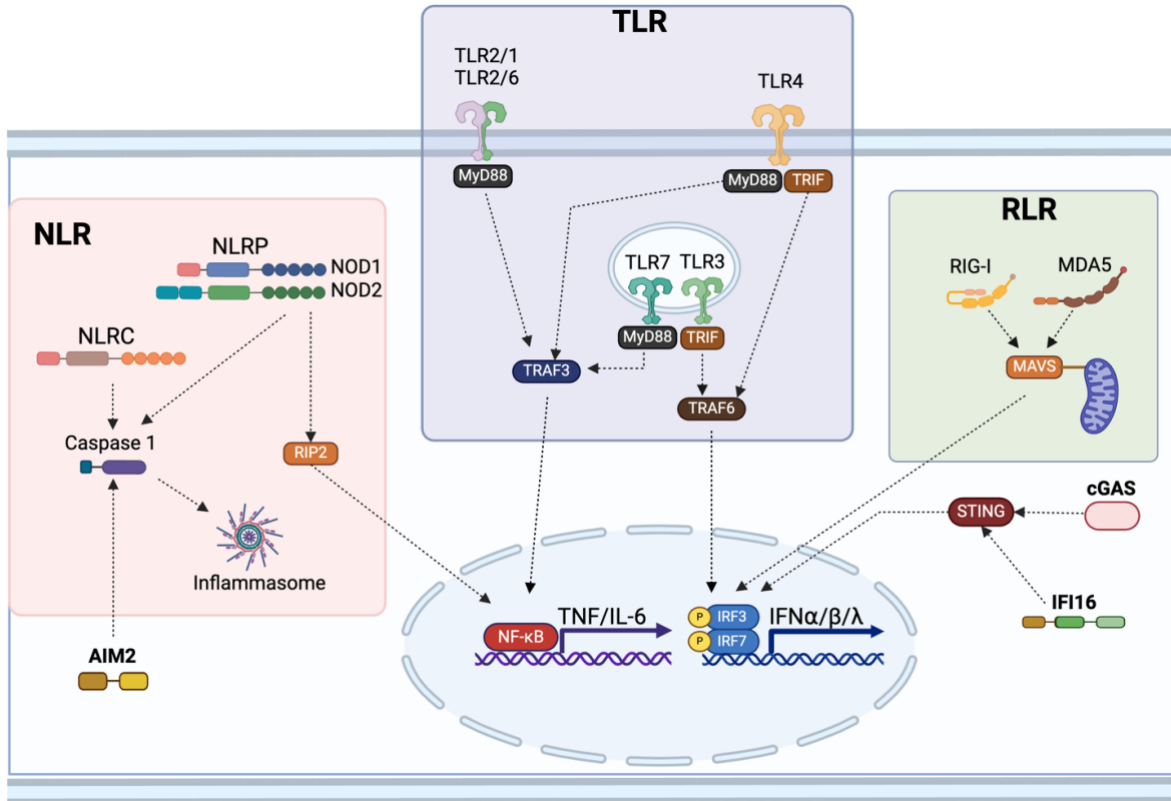


**Figure 1.3: Pattern Recognition Receptors signaling:**

Signaling pathways of innate immune receptors Toll-like receptors (TLRs), NOD-like receptors (NLRs), RIG-I-like receptors (RLRs), and DNA sensors including AIM2, IFI16, and cGAS/STING. Upon ligand recognition, these receptors initiate downstream signaling cascades leading to the activation of transcription factors such as NF-κB, ultimately resulting in the production of pro-inflammatory cytokines, or IRF3, and IRF7, resulting in the expression type I/III interferons (IFNs).

These sensors lack a shared common structure but are capable of eliciting robust immune responses upon ligand binding [26, 27]. For example, AIM2 senses cytosolic double-stranded DNA (dsDNA) and forms an inflammasome complex, activating caspase-1 and subsequent production of pro-inflammatory cytokines IL-1β and IL-18 [28]. IFI16, primarily localized in the nucleus, can also detect



cytoplasmic DNA, particularly from herpesviruses, initiating the expression of type I IFNs and inflammatory cytokines through the STING-TBK1-IRF3 axis [29].

The cGAS-STING pathway, on the other hand, detects cytosolic dsDNA and cyclic dinucleotides (CDNs) derived from bacteria, viruses, and endogenous sources. Upon DNA binding, cGAS synthesizes cyclic GMP-AMP (cGAMP), which activates STING, leading to the phosphorylation of TBK1 and subsequent phosphorylation and activation of IRF3. This cascade culminates in the induction of IFNs and other pro-inflammatory cytokines, orchestrating an effective antiviral response [29] (Table 1.1; Fig. 1.2).

Table 1.1: PRR ligands:

PRR		Ligand		
		Viral	Bacterial	Fungal
TLRs	TLR1/2		Triacyl lipoprotein	Oligomeric chitin
	TLR2/6		Peptidoglycan, lipoteichoic acid (LTA)	Phospholipomanan
	TLR3	dsRNA		
	TLR4		Lipopolysaccharide (LPS)	
	TLR5		Flagellin	
	TLR7	ssRNA		
	TLR9	non-methylated CpG DNA	non-methylated CpG DNA	
NLRs	NOD1		iE-DAP	
	NOD2	dsRNA/OAS complex	Muramyl dipeptide (MDP)	
	NLRP3	dsRNA	RNA, LPS, LTA, MDP	
	NLRC4/NAIP	HIV gp41		

RLRs	RIG-I	5'-triphosphorylated dsRNA		
	MDA5	5'-triphosphorylated dsRNA		
	LGP2	5'-triphosphorylated dsRNA		
DNA sensors	c-GAS/STING	Cyclic dinucleotides (CDNs)	Cyclic dinucleotides (CDNs)	
	AIM2	dsDNA	dsDNA	
	IFI16	DNA	DNA	

TLRs: [30-36]; NLRs: [22, 23, 37-40]; RLRs: [41] DNA sensors: [26, 27, 29]

### 1.5. Antimicrobial Peptides

Antimicrobial peptides (AMPs) are an essential component of homeostatic immunity at the oral mucosal barrier. Their constitutive production by oral epithelial cells is essential for limiting oral bacterial load. The engagement of PRRs by plaque bacteria can further amplify AMP production in oral epithelial cells. Cathelicidins and defensins are the two main families of AMPs.

$\beta$ -defensins, produced by GECs, have been shown to be effective against a variety of oral bacterial and viral colonizers [20, 42].  $\beta$ -defensins disrupt membrane integrity by forming pores or channels within the bacterial membranes, resulting in the leakage of intracellular contents and, ultimately, bacterial cell death [43]. Similarly, oral epithelial cells produce the LL-37/hCAP-18 peptide [44], which has varying antibiotic activity against a number of oral bacterial commensals or pathogens, such as *Streptococcus sanguinis* and *Porphyromonas gingivalis* [45]. Upon encountering bacterial membranes, LL-37 inserts itself into the lipid bilayer,

forming pores or channels that compromise membrane integrity and induce bacterial cell lysis. This process is facilitated by LL-37's amphipathic nature, with hydrophobic and cationic regions facilitating interaction with the lipid bilayer [46]. Calprotectin, a heterodimeric protein complex consisting of S100A8 and S100A9 subunits, normally associated with myeloid cells, has been shown to be constitutively expressed by gingival epithelium [47]. By sequestering transition metals such as zinc and manganese, calprotectin deprives bacteria of these essential nutrients, thereby exerting bacteriostatic or bactericidal effects. Homeostatic release of antimicrobial peptides into the saliva and gingival crevicular fluid curtails and trims biofilms, thus playing an important role in regulating microbial burden. While these peptides are primarily known for their antibacterial activity, some studies suggest they may also possess antiviral properties. LL-37, for instance, has been shown to inhibit the entry and replication of certain viruses, including human immunodeficiency virus (HIV) [48] and herpes simplex virus 1 (HSV-1) [49], by interacting with viral envelopes and impeding viral attachment or fusion. Similarly,  $\beta$ -defensins have been reported to inhibit SARS-CoV-2 viral entry by blocking the spike-ACE2 interaction [50]. However, the specific mechanisms underlying the antiviral activity of antimicrobial peptides may vary depending on the virus and the context of infection.

## 1.6. Oral Epithelial Chemokine Gradients

Homeostatic or controlled activation of PRR maintains tolerance to the commensal microbiota and supports the development of mucosal barrier immunity.

For example, PRR-mediated detection of microbial ligands by epithelial cells under homeostatic conditions facilitates the establishment of chemokine gradients that recruit immune cells into foci that are essential for immune surveillance. Interleukin 8 (IL-8/CXCL8) secretion by GECs mediates the steady-state recruitment of neutrophils to the gingival crevice, where they play an important role in tissue homeostasis [51, 52]. Neutrophil recruitment can be further enforced by the production of CXCL1 and CXCL6[19]. Neutrophils form a protective wall between the plaque and gingival epithelium, release antimicrobial peptides ( $\alpha$ -defensins and LL-37), and actively phagocytose adjacent bacteria [53, 54]. GEC-mediated production of lymphocyte-recruiting chemokines such as CXCL10 and 11 facilitate lymphoid foci formation and intraepithelial lymphocyte recruitment without inducing damaging inflammation[55, 56].

#### 1.7. Interferons and antiviral immunity

Interferons (IFN) are potent antiviral cytokines that play an important role in limiting viral infection, especially at barrier surfaces, which are frequent sites of viral entry. Autocrine or paracrine IFN signaling downstream of IFN receptors results in the activation of a large number of IFN-stimulated genes (ISGs) that play critical roles in blocking viral replication and dissemination and prime innate and adaptive immunity. They are broadly classified into three families (Type I, Type II, and Type III) and function synergistically to activate anti-viral responses in epithelial cells.

IFN- $\alpha$  and IFN- $\beta$  are the two prototypical members of the Type I IFN family, along with lesser recognized IFN- $\kappa$ , IFN- $\omega$ , IFN- $\epsilon$ , IFN- $\tau$ , and IFN- $\delta$ . Type I IFNs can be produced by a large number of cell types, such as epithelial cells, macrophages, T cells, and NK cells, with plasmacytoid dendritic cells being the most potent source. They signal via the activation of the Type I IFN receptor (IFNAR), expressed by all nucleated cells, and thus are capable of mediating a systemic response and immunopathology associated with viral infections [57, 58]. IFN- $\gamma$  is the sole member of the Type II IFN family, which is produced by immune cells

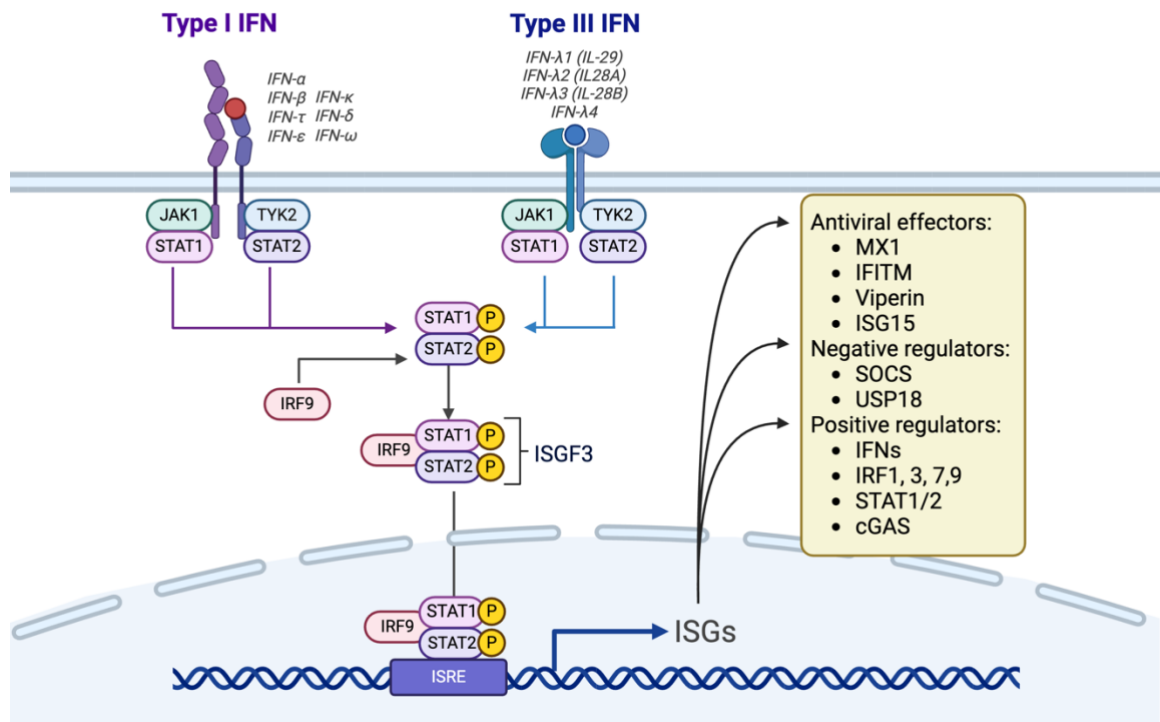


**Figure 1.4: Interferon Signaling Pathway:** Signaling through the Type I and III IFN receptors causes an almost identical signaling cascade. Binding of the cognate cytokine causes the activation of the adaptor molecules JAK1 and TYK2, which in turns phosphorylates STAT1 and STAT2. Active dimers of STAT1/2 join with IRF9 to form the ISGF3 complex, which translocates into the nucleus. ISGF3 binds to ISRE in the promoter regions of ISGs and induces their expression. ISGs include antiviral effectors that restrict all stages of the virus life cycle, along negative and positive regulators, including the IFN genes creating a positive feedback loop.

primarily of the lymphocytic lineage (innate lymphoid cells, natural killer (NK) cells, and T cells) in response to IL-12 signaling or through antigen stimulation of the T cell receptor. Although the expression of IFN- $\gamma$  is limited to immune cells, the IFNGR is expressed in most cells, causing very cell-specific responses. In non-hematopoietic cells, IFN- $\gamma$  signaling can upregulate the expression of major histocompatibility complexes (MHC) and antigen presentation that promotes the recognition of transformed or virally infected cells by T cells [59]. IFN- $\gamma$  signaling is also critical in immune responses against fungal and bacterial pathogens [60, 61].

Type III IFNs of IFN- $\lambda$  are the most recently identified IFN family with 4 members IFN- $\lambda$ 1-4 in humans. IFNAR and IFNLR activate almost identical downstream signaling pathways that lead to the activation of very similar ISG signatures (Fig 1.4). Signaling downstream of IFNAR and IFNLR results in the phosphorylation of STAT1 and STAT2 and the formation of the heterotrimeric complex with IRF9, also known as the IFN-stimulated gene factor 3 (ISGF3) complex. Nuclear translocation of the ISGF3 complex and DNA binding at the IFN-stimulated response element (ISRE) results in the robust transcription of a large number of ISGs, including the IFN genes themselves, creating a feedforward loop that potentiates the antiviral response. ISGs include a broad family of chemokines, antiviral restriction factors, and inflammatory cytokines that play diverse roles in the antiviral response. Certain ISGs can block the viral replication cycle by targeting specific steps in the viral replication cycle. For example, IFN-induced transmembrane proteins (IFITM) restrict the release of Zika virus particles from the endosome to the cytosol. In Influenza B infections, the ubiquitin-like protein ISG15

disrupts viral replication machinery by conjugating itself with the viral nucleoprotein [62]. ISGF3 signaling also mediates the transcription of positive and negative regulators of IFN signaling that further fine-tune IFN response and limit damage (Fig 1.3).

Although the IFN response is predominantly antiviral in nature, accumulating evidence suggests that IFNs also play an important role in clearing bacterial infections [63, 64] (Table 1.2). The involvement of IFN stimulation in bacterial infections can have both protective and damaging effects in a context-dependent manner.

Table 1.2: ISGs mechanisms of antiviral and antibacterial effector functions

ISG	Gene	Anti-viral	Cell type	Anti-bacterial	Cell type
Tripartite Motif Containing 14	TRIM14	TRIM14 increased IRF3 phosphorylation and NF-κB DNA-binding activity after SeV infection	Airway epithelium (A549)	Inhibits <i>L. monocytogenes</i> infection via incompletely understood mechanisms	Fibroblasts
IFN induced transmembrane proteins	IFITM1, 2, 3	Restrict the release of ZIKV particles from the endosome to the cytosol	HEK and Vero	Restricts <i>M. tuberculosis</i> by enhancing acidification of Mtb containing phagosomes	Monocytic and alveolar/epithelial cells
Viperin	RSAD2	Delays Rotavirus Release by Inhibiting NSP4-Induced Intrinsic Apoptosis	Intestinal epithelial cells, HEK and Vero	Limits the intracellular lifecycle of <i>Shigella flexneri</i> and <i>L. monocytogenes</i> via its radical SAM enzymatic functions	Epithelial cells (HeLa, HEK293T, Huh7)
Interferon stimulated gene 15	ISG15	Restrict the replication of IAV by modifying the active site of the viral NS1A	A549 HEK293T	Restricts <i>L. monocytogenes</i> infection by enhancing cytokine secretion	HeLa, murine hepatocytes, fibroblasts
OAS-regulated RNaseL	RNASEL	Inhibition mRNA export inhibits influenza protein synthesis	A549	Essential for the cytokine production in response to <i>B. anthracis</i>	Macrophages

TRIM14:[65, 66]; IFITM:[67, 68]; RSAD2:[69, 70]; ISG15[71, 72]; RNASEL[73, 74]

### 1.8. IFN-λ and Oral Mucosal Antiviral Immunity

IFN-λ has emerged as an important regulator of antiviral immune responses at mucosal barrier surfaces due to the ‘focused nature’ of its signaling. Even



though Type I IFNs and IFN- $\lambda$  activate overlapping downstream signaling pathways, the mostly restricted expression of IFNLR on barrier epithelial cells enables it to modulate antiviral responses without activating damaging inflammation typically seen with Type I IFNs [75, 76]. For example, high expression of the IFNLR in intestinal epithelial cells results in type III IFN responses being the primordial defense against norovirus, reovirus, rotavirus, and enterovirus [77-79]. The superior role of IFN- $\lambda$  at these sites is further reinforced by the differential kinetics of activation and blunted recruitment and/or dampened activation of inflammatory cells (neutrophils), all of which contribute toward antiviral immunity while preventing collateral damage [76, 80-83]. Thus, Type III IFNs have emerged as the “guardians” of anatomic barriers.

Type III IFNs have been shown to play important roles in antiviral defenses at the intestinal, respiratory, and vaginal mucosal barriers [84]. However, their role at the oral mucosal barrier, which is often an initial site of viral infection and functions as a portal of entry to other barrier sites, was unknown. DNA viruses, such as members of the Herpesviridae, Papillomaviridae, and Poxviridae families, are known to cause recurrent oral lesions. Cytomegaloviral infections have been associated with painful ulcerations in the oral cavity. RNA viruses, including enteroviruses and paramyxoviruses, can also infect the oral cavity. Despite its diverse virome, very little is known about the regulation of antiviral immunity in the oral mucosa [85, 86].

## CHAPTER 2:

### ORAL DYSBIOSIS AND THE MANIPULATION OF ANTIVIRAL IMMUNITY

#### 2.1. Oral Microbial Colonizers and Dysbiosis

The oral cavity serves as a reservoir for many microbes, including bacteria, archaea, fungi, protozoa, and several prokaryotic and eukaryotic viruses. From birth, progressive colonization of the mouth occurs, and the diversity of colonizing communities increases with age. At homeostasis, bi-directional interactions (co-adhesion, metabolite exchange and signaling) between the host and colonizing communities regulate local oral immune responses and have implications for systemic health. Dysbiosis, or the pathogenic shifts in the oral microbiome towards a community of organisms dominated by pathobionts and opportunistic pathogens, results in inflammation of varied severity and the destruction of oral tissues.

The oral microbiome houses diverse bacterial and viral species which include commensals and opportunistic pathogens that inhabit specific microniches within the mouth (Figure 2.1). Due to the nature and structure of the gingival sulcus, a rich bacterial biofilm forms attached to the pellicle of the tooth (Figure 1.1A) and spans the subgingival and supragingival surfaces. However, aside from the supragingival and subgingival biofilms, microbes can colonize other areas in the mouth, such as

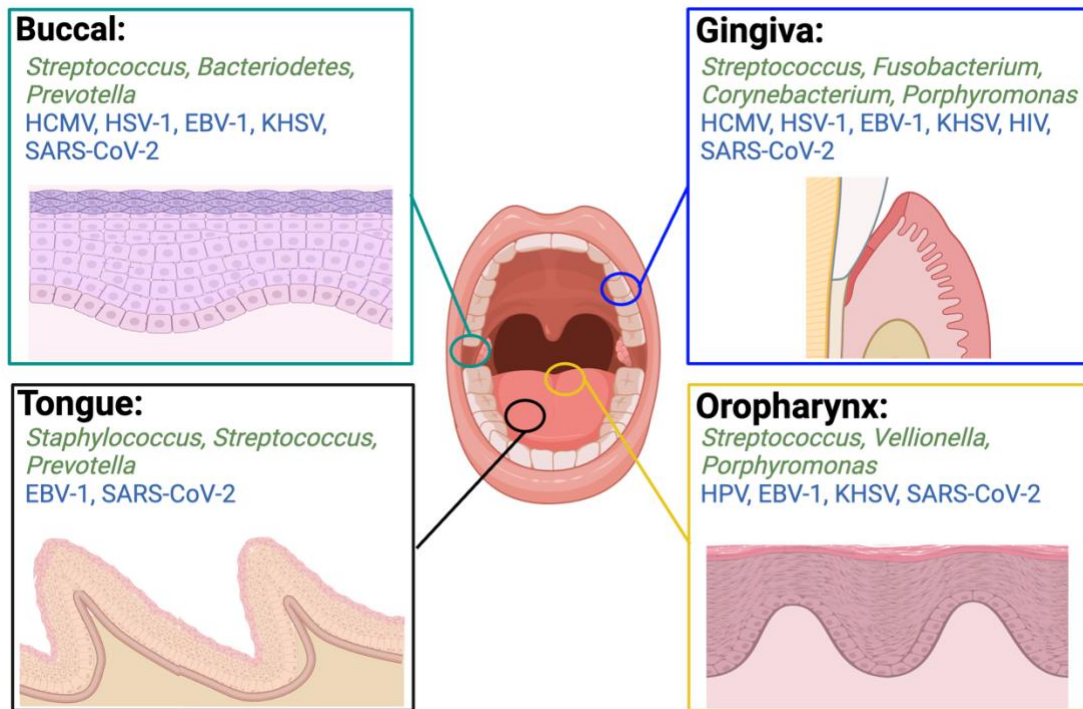


**Figure 2.1. Microbial niches within the oral cavity:** The buccal mucosa, tongue surface, gingival crevices, and oropharynx represent distinct microniches harboring diverse microbial communities. Examples of common bacteria and viruses found in each niche are depicted, showcasing the complex microbial ecosystem of the oral cavity.

the tongue, salivary glands, and buccal surface [87, 88] (Figure 2.1). Synergistic interactions within these commensal communities of microbes and the host maintain tissue homeostasis and protect the host by preventing colonization of other pathogenic species and limiting the virulence of opportunistic pathogens [89, 90]. However, alterations in diet, smoking habits, and other immune stresses result in alterations in local pH, redox potential, and nutrient availability within the microniche mediate dysbiosis, which is associated with a shift from commensals to pathogenic species [91, 92]. Immune subversion or inactivation further increases the bacterial burden and the overrepresentation of specific microbial

community members. Several studies now show that the oral cavity can also harbor microbes that do not cause disease within the oral cavity but are associated with pathogenesis at other mucosal surfaces, such as the respiratory pathogens SARS CoV-2, *Pseudomonas aeruginosa*, *Klebsiella pneumoniae*, *Staphylococcus aureus* [93-96] and the gastrointestinal pathogens *Helicobacter pylori* and Rotavirus [88, 97].

Dysbiotic heterotypic communities of microorganisms in the oral cavity activate host inflammatory responses and subsequent tissue damage. Gingivitis is associated with gingival bleeding, immune cell recruitment, and inflammation and can be reversible. The progression of gingivitis into periodontitis is accompanied by irreversible alveolar bone resorption and deepening of the sub-gingival pocket, tissue damage, and tooth loss [98, 99]. Etiologically, anaerobic Gram-negative, proteolytic bacteria such as *Fusobacterium nucleatum*, *Treponema denticola*, and *Porphyromonas gingivalis* are found within the dysbiotic oral plaque bacteria in periodontitis. These pathogens employ diverse virulence strategies to dysregulate host inflammatory pathways possibly contributing towards the chronic inflammation observed in periodontitis. Recent studies have added other Gram-positive bacteria, *Filifactor alocis*, and *Peptoanaerobacter stomatis*, to the list of periodontal pathogens [100, 101]. While each pathogen utilizes unique virulence strategies to evade immune clearance, *P. gingivalis* has emerged as a significant periodontal pathogen due to its ability to subvert host immune responses and remodel the sub-gingival microbial communities towards those enriched in pathobionts that aid disease progression [102].

## 2.2. *P. gingivalis*: a “rotten apple” within the gingival polymicrobial “barrel”

*P. gingivalis* is a non-motile, gram-negative, obligate anaerobe that colonizes the deep anaerobic regions of the periodontal pocket, often adhering to primary colonizers such as *Streptococcus gordonii* [103, 104] as well as other periodontal pathogens such as *T. forsythia*, and *F. nucleatum* [105]. Although *P. gingivalis* is a member of oral biofilms, it can actively adhere to and invade GECs, and opt for an intracellular lifestyle that allows for protection from immune clearance [106]. Even in low numbers, *P. gingivalis* can significantly manipulate oral microbial communities by a series of molecular interactions that mediate cross-species signaling, resulting in the upregulation of virulence factors such as proteases, oxidative stress response genes, hemolysins, and adhesins that impart resilience to the dysbiotic community against immune clearance [107].

*P. gingivalis* is particularly adept at disarming host immune responses by producing a large number of virulence factors and bacterial effectors such as hemolysins, fimbriae (FimA and Mfa1), lipopolysaccharide (LPS), capsule, proteases and outer membrane vesicles (OMVs) that subvert or dysregulate host immune responses leading to the persistence of the pathogen. Production of proteolytic enzymes, gingipains, allows these bacteria to not only break down proteins for nutrition but also to degrade immunoglobulins, complement proteins, cytokines, extracellular matrix proteins, and immune receptors, resulting in significant attrition in microbial clearance and dysregulated inflammatory response [108-110]. In order to invade gingival epithelium, *P. gingivalis* produces two main

effectors: the fimbrial adhesin (FimA) and a haloacid dehalogenase family serine phosphatase (serB) [111, 112]. SerB is secreted by the bacterium and taken up by the epithelial cell, where it interacts with the host actin depolymerase, cofilin [111]. Loss of stability in the actin cytoskeleton allows the bacteria to cause invaginations in the membrane, giving it access to the cytoplasm. Similarly, FimA interaction with  $\beta$ 1-integrin receptors leads to the activation of complex signaling pathways that result in the successful invasion of the bacterium into the host cell by means of actin and microtubule reorganization [111-113]. In epithelial cells, *P. gingivalis* invasion induces epithelial-mesenchymal transition (EMT) [114], blocks apoptosis [115], and programs cells toward mitosis [116]. These changes are consistent with oncogenic transformation and are in part orchestrated by the upregulation of zinc finger E-Box binding homeobox1 ZEB1, a transcription factor that drives EMT [114]. Similarly, *P. gingivalis* has also been described to interfere with the function of p53 and manipulate cyclin/CDK activity [117], both of which can promote cancer development. Indeed, a large amount of clinical data links *P. gingivalis* with several types of cancers, such as oral and esophageal squamous cell carcinomas [114, 118]. *P. gingivalis* also actively manipulates leukocyte responses to dysregulate host inflammatory responses and enhance susceptibility to rheumatoid arthritis [119], cardiovascular disease [120], Alzheimer's disease [121], and other inflammatory conditions.

### 2.3. *Porphyromonas gingivalis* subverts oral antiviral immunity:

Several recent studies show that bacterial colonizers at anatomic barrier sites can profoundly influence host antiviral immunity by either boosting or suppressing IFN responses, thereby modulating host susceptibility to viral infection. Microbial colonizers and their ligands are important 'microbial triggers' that play an inductive role in the development and maintenance of IFN responses and ISG expression, as well as IFN-regulated cellular and humoral anti-viral immunity [122-130]. On the flip side, dysbiosis, which enriches certain bacterial pathogens, can debilitate IFN signaling. Certain bacterial metabolites [131] and toxins [132, 133] have been previously shown to resurrect latent viruses of Herpesviridae family (EBV and HSV). As these are diffusible, co-infection of a cell with bacteria and viruses is not necessary.

Previous studies have shown that *P. gingivalis* can manipulate IFN- $\gamma$  signaling, impairing the efficacy of downstream T-cell immunity. *P. gingivalis* suppress the expression of IP-10 expression by downregulating IRF-1 and STAT1, two molecules directly linked with the IFN-mediated antiviral response [56]. It has been suggested that this bacterium have the ability to promote the reactivation of Epstein-Barr virus on oral epithelial cells [134]. Taking into consideration the capabilities of *P. gingivalis* to manipulate various immune functions and to induce viral reactivation made us believe that infection with this periodontopathogen could be restricting antiviral responses in the oral cavity, leaving it susceptible to viral infection. Thus, we determined whether common oral colonizers influenced the ability of GECs to respond to viral agonists and produce IFNs.

## CHAPTER 3:

### MICROBIOME-MEDIATED INCAPACITATION OF INTERFERON LAMBDA PRODUCTION IN THE ORAL MUCOSA<sup>1</sup>

#### 3.1. Introduction

Recent clinical studies show an increased prevalence of several viruses in inflamed oral tissues and sites of active periodontal inflammation [136, 137]. Viruses can either directly infect oral epithelial cells that line the buccal and gingival surfaces of the oral mucosal barrier or have a transient presence in the oral cavity due to replication and release from other tissues[138]. These include Herpes simplex virus (HSV-1), cytomegalovirus (CMV), varicella-zoster virus, as well as oncogenic viruses such as Epstein–Barr Virus (EBV), and human papillomaviruses [138-143]. Despite the high prevalence of oral viral infections, little is known about the nature of antiviral immune responses and their regulation in the oral cavity.

Recent studies show that the microbial colonizers at anatomic barrier sites can either stimulate or suppress IFN responses and ISG expression and thereby

---

<sup>1</sup> This chapter has been modified from a recent publication: 135. Rodriguez-Hernandez, C.J., et al., *Microbiome-mediated incapacitation of interferon lambda production in the oral mucosa*. Proc Natl Acad Sci U S A, 2021. **118**(51).



influence host susceptibility to viral infection[124, 126, 144-148]. Detection of bacterial ligands by epithelial TLRs can stimulate IFN- $\lambda$  expression in a manner that reinforces epithelial barrier integrity [123]. Certain bacterial commensal species such as segmented filamentous bacteria play a more direct role in protecting against rotavirus infection and maintaining barrier integrity by inducing epithelial turnover and epithelial ISG expression[144]. While antibiotic depletion of microbiota enhanced susceptibility to flavivirus infections[149], it protected the mice from murine norovirus infections[127]. This protection was conferred by antibiotic-mediated deletion of microbial colonizers that limited the efficacy of IFN- $\lambda$ -mediated antiviral pathways. Thus, the nature of colonizing bacterial species can either activate or disarm epithelial IFN responses and impact host antiviral immunity.

In this chapter, we show that detection of viral agonists by various cytosolic and membrane-restricted PRRs preferentially induced IFN- $\lambda$  by GECs, resulting in the activation of multiple ISGs. Data from human primary tissues, cell lines, and mouse models show that IFN- $\lambda$  production and downstream antiviral pathways were severely compromised in the presence of *P. gingivalis*, a bacterial periodontal pathogen and resident of the subgingival microbial niche. Synergetic inactivation of multiple transcription factors, cleavage of IFN receptors, and global downregulation of canonical IFN response genes by *P. gingivalis* severely compromised host IFN-mediated antiviral immunity. Our observations were specific to *P. gingivalis*, as other oral periodontal pathogens that are commonly associated with periodontal inflammation did not affect IFN production.

### 3.2. Materials and methods

#### *Bacteria.*

*P. gingivalis* 33277, W83, and MP4-504 were cultured in trypticase soy broth (TSB) supplemented with hemin (5 µg/mL) and menadione (1 µg/mL) and 1 mg/mL yeast extract. Isogenic mutants were cultured in supplemented TSB with the appropriate antibiotics:  $\Delta rgpA$ ,  $\Delta kgp$ , and  $\Delta serB$  had 10 µg/mL erythromycin;  $\Delta rgpAB$  had 10 µg/mL erythromycin and 1 µg/mL tetracycline;  $\Delta rgpAB\Delta kgp$  had 10 µg/mL erythromycin, 1 µg/mL tetracycline, and 20 µg/mL chloramphenicol [90]. *F. nucleatum* 25866 was cultured in brain heart infusion broth with yeast extract (1 mg/mL), hemin (5 µg/mL), and menadione (1 µg/mL). *S. gordonii* DL1 was cultured in TSB with yeast extract. *T. denticola* 35405 was cultured in new oral spirochete media. All strains were grown anaerobically (85% N<sub>2</sub>, 10% H<sub>2</sub>, and 5% CO<sub>2</sub>) at 37 °C.

#### *Processing of Human Gingival Tissues.*

Deidentified gingival tissue specimens were obtained from healthy individuals that needed gingival tissue excision for aesthetic or functional purposes and periodontal disease patients undergoing periodontal surgeries. All studies were approved by the University of Louisville's Institutional Review Board (IRB No. 15.0163). Tissues were subdivided and fixed in formalin as well as cryopreserved in Optimal Cutting Temperature Embedding Medium for Frozen Tissue Specimens

(OCT) for histology and immunofluorescence staining. A total of 10 to 50 mg tissue was also homogenized in phosphate-buffered saline (PBS) containing protease inhibitors using a Bead Beater and the lysing matrix D (MP Biomedicals). Tissue homogenates were used for ELISA.

#### Cell Culture.

Primary GECs were isolated from human gingival specimens as previously described [150]. Briefly, tissues were treated with 5 mg/mL Dispase II overnight at 4 °C, followed by mechanical separation of the epithelial layer from the underlying connective tissue. Tissues were further dissociated by enzymatic digestion with Trypsin-EDTA at 37 °C for 10 min and then minced to obtain single-cell suspension. Cells were cultured in keratinocyte basal serum-free media with Gentamicin (30 mg/mL) and Amphotericin B (15 ng/mL) and used for assays between passages 2 and 6. GECs (TIGKs)[151] and human oral keratinocyte (OKF6) cell lines were cultured in keratinocyte basal serum-free media (Invitrogen) supplemented with 0.4 mM calcium chloride, 25 µg/mL bovine pituitary extract, and 0.2 ng/mL epidermal growth factor at 37 °C and 5% CO<sub>2</sub>.

#### *Immunofluorescence and Confocal Laser Scanning Microscopy.*

GECs were grown on glass coverslips in 24-well plates. Cells were fixed in 4% paraformaldehyde for 10 min and permeabilized with 0.2% Triton X-100 for 10 min at room temperature (RT). After blocking with 5% bovine serum albumin (20 min), cells were incubated with either anti-human IRF-1 (Cell Signaling Technologies)

primary antibody 1:200 dilution (0.165 µg/mL) overnight at 4 °C and Alexa fluor 488–conjugated anti-rabbit secondary (Invitrogen) antibody at 1:1,000 dilution (2 µg/mL) at RT for 30 min or anti-human ZEB1 primary antibody (Novus Biologicals) 1:100 dilution (100 µg/mL) overnight at 4 °C and Alexa fluor 488–conjugated anti-mouse secondary antibodies at 1:2,000 dilution (1 µg/mL) at RT for 30 min. Cells were labeled with Texas Red-phalloidin for 40 min at RT. OCT-embedded gingival tissues were sectioned at 5 µm in a cryotome and fixed with ice-cold 100% methanol. Slides were permeabilized with 0.4% Triton X-100 , blocked with 5% goat serum, and stained with anti-human IFNLR antibodies. The presence of *P. gingivalis* in gingival tissues was measured using IgG isolated from rabbits immunized with *P. gingivalis* 33277[114]. After 2 h of staining at RT, slides were washed three times with PBS, and then incubated with Alexa Fluor 488–conjugated anti-rabbit secondary antibody (1:1,000) for 1 h. Following this, slides were counterstained with DAPI (4'6-diamidino-2-phenylindole). Formalin-fixed paraffin-embedded gingival tissues were sectioned at 5 µm in a microtome, dewaxed, and rehydrated. Unmasking of antigens was performed using citrate-based antigen unmasking solution (Vector Laboratories). Tissue sections on slides were then blocked with blocking buffer (2.5% goat serum, 1% bovine serum albumin (BSA), 0.05% Tween 20, and 0.05% Triton X-100). Slides were stained with APC-conjugated mouse anti-human EpCAM (Biolegend) at 1:50 dilution, anti-human IFNLR 1:50 dilution, or rabbit anti-*P. gingivalis* antibody[152] at 1:500 dilution overnight at 4 °C. Slides were washed three times with PBS and then incubated further with Alexa Fluor 488–conjugated anti-rabbit secondary antibody

at 1:1,000 dilution for 1 h. Slides were counterstained with DAPI (4',6-diamidino-2-phenylindole) and mounted using ProLong antifade mounting media. Images were visualized using LAS X Life Science software (Leica Microsystems) and analyzed using Imaris software (OXFORD instruments). Mean fluorescence intensities were determined by enumerating positive pixel intensity as described by Shihan et al. [153].

#### *RNA Scope.*

Transcript expression was determined in formalin-fixed paraffin-embedded gingiva tissues (sectioned at 5  $\mu\text{m}$ ) using transcript-specific probes and RNAscope Fluorescent Multiplex Assay version 2 kit (Advanced Cell Diagnostics Inc.) as per the manufacturer's protocol.

#### *Oral Infection of Mice.*

Mx1<sup>gfp</sup> mice[154] were purchased from Jackson Laboratory and maintained in specific pathogen-free conditions. Male and female mice, 8 to 12 week old, were orally infected with  $10^9$  cfu *P. gingivalis* 33277 suspended in 2% carboxymethylcellulose (CMC) on alternate days for a total of three infection cycles. The bacterial suspension was directly applied to the gingival margin of each mouse under brief isoflurane anesthesia. Sham-infected mice received 2% CMC alone. At 48 h after last inoculation, mice received either 50  $\mu\text{g}$  poly I:C or 40  $\mu\text{g}$  IFN- $\lambda$  in 100  $\mu\text{L}$  PBS intraperitoneally and euthanized after 36 h. The maxilla and mandible were surgically dissected from each mouse and tissues digested using

the tumor dissociation Kit (Miltenyi Biotech) as per the manufacturer's instructions. Soft tissue was harvested and minced through a 70- $\mu$ m strainer to obtain a cell suspension. Cells were then washed and stained for flow cytometry using antibodies against CD45-BV605 (1:400) and EpCAM-APC (1:400). Cells were processed using FACSCelesta, and data were analyzed using FlowJo Software. Alternatively, total RNA/protein was isolated from dissected gingival tissues from maxillary molars using the Nucleospin dual extraction kit (Takara Biosciences) as per manufacturer's instructions.

#### *Western Blots.*

Cells were lysed in radio immunoprecipitation (RIPA) buffer containing protease inhibitor mixture, phosphoStop phosphatase inhibitors (Roche), and 50  $\mu$ M gingipain inhibitor N $\alpha$ -Tosyl-L-Lysine chloromethyl ketone hydrochloride (Sigma Aldrich). Protein concentration was estimated by a bicinchoninic acid assay. Samples were separated by SDS-PAGE and electroblotted onto nitrocellulose (0.2  $\mu$ m) membranes. Membranes were blocked in PBS-Tween (PBST) containing 5% nonfat dried milk and incubated with primary antibodies. Anti-human IL-28R (IFNLR) antibody was purchased from Novus Biologicals, while anti-human IFNAR, phospho-STAT1 (Y701), STAT1, MX1, ISG15, and GAPDH antibodies were purchased from Cell Signaling Technologies. ZEB1 and IRF-1 antibodies were purchased from ThermoFisher. MDA5 and IFNAR antibodies were purchased from ENZO Life Sciences and Santa Cruz Biotechnology, respectively. For mouse gingival tissue lysates, IFNLR expression was determined using anti-

mouse IL-28R antibody from Lifespan Biosciences and HRP conjugated goat anti-rabbit secondary antibody from Invitrogen.

#### *qPCR.*

Total RNA was extracted using the RNAeasy kit (Qiagen) and converted to cDNA using the high-capacity cDNA reverse transcription kit (ThermoFisher). Transcript expression was determined by TaqMan assays using TaqMan mastermix. All prevalidated primer sets and probes were purchased from ThermoFisher.

#### *Dual Luciferase Assay.*

GECs were transfected with pGL4.45-luc2P/ISRE Vector (Promega) containing five copies of the ISRE element that drives the transcription of the *luc2P* firefly luciferase reporter gene using Lipojet (SignaGen). Cells were also transfected with the pRL vector that provides constitutive expression of Renilla luciferase as an internal control. At 24 h after transfection, cells were stimulated with 10 µg/mL HSV60 with or without *P. gingivalis* infection. Cells were also stimulated with 100 ng/mL recombinant IFN-λ. Cells were lysed 24 h poststimulation, after which dual luciferase reporter assays were performed using Stop & Glo dual luciferase reporter kit from Promega as per the manufacturer's instructions. Luciferase activity was measured using a 10-s integration time in a Luminometer (Molecular Devices). Firefly luciferase activity was normalized over Renilla luciferase activity from the same lysates.

*Transfection Studies: siRNA and Overexpression Vectors.*

GECs were transfected with siRNA (75  $\mu$ M) against IRF-1 or ZEB1 or scrambled control RNA (Life Technologies) using Lipojet. At 24 h post transfection, cells were stimulated with *P. gingivalis* (multiplicity of infection [MOI] 100) for 5 h, washed once with PBS, and then stimulated with HSV60 for additional 18 h. Immunoblots confirmed siRNA-mediated knockdown. For overexpression, pcDNA-GFP-STAT1 (Addgene No. 11987) was a gift from Alan Steven Johnson, and pcDNA3.2 [155] vector control was a gift from Jan Rehwinkel (Addgene No. 120833). pCMV-IRF-1 [56] and pCMV empty vector control were from Panomics.

*RNA-seq.*

RNA was extracted using the RNAqueous-Micro Total RNA Isolation kit (ThermoFisher Scientific). The TruSeq Stranded Total RNA with RiboZero Gold kit (Illumina) was used to generate a sequencing library from 1  $\mu$ g total RNA. Paired-end sequencing was performed on an Illumina NextSeq 500 at the University of Louisville core, using the NextSeq 500 High-Output Kit (150 cycles) (Illumina). Base calls were made using the BaseSpace FastQ version 1.0.0 application (Illumina, Inc.). For the analysis of differentially expressed genes, demultiplexed paired-end fastq files were aligned to reference GRCh38 by top-level assembly with STAR (version 2.6.1). Gene counts were produced by RSEM (version 1.3.1). We used DESeq2 R/Bioconductor package to obtain differential expression between *P. gingivalis*-treated and control samples ( $n = 3$  per sample). DESeq2



guidelines were used to identify differentially expressed genes, and all *P* values were adjusted for testing multiple genes (Benjamini–Hochberg procedure, alpha = 0.1). For gene set enrichment analysis, we used fgsea Multilevel function from fgsea R/Bioconductor package (<https://doi.org/10.1101/060012>). RNA-seq datasets have been deposited in the NCBI GEO database under Accession Nos. [GSE184456](#) and [GSE184463](#).

#### *Viral Assays.*

To determine if *P. gingivalis* infection influenced viral replication, GECs were seeded in 24-well plates at 80% confluency. Cells were infected with *P. gingivalis* WT or the gingipain-deficient mutant at MOI of 10 for 5 h. GECs were washed once with PBS and fresh media added. Cells were then infected with Toto1101-derived SINV strains containing either nsP3-GFP (nsP3-green fluorescent protein) or nsP3-Nanoluc at an MOI of 10 plaque-forming units (PFU) per cell (as determined in BHK-21 cells)[156]. After a 1 h adsorption period, the inoculum was removed, and the cells were washed twice with 1× PBS to remove unbound viral particles and incubated at 37 °C in a humidified incubator in the presence of 5% CO<sub>2</sub>. For assaying viral susceptibility and permissivity (which together amount to infectability), the cells were examined at 24 h post infection via a GFP-capable epifluorescence microscope. The assessment of viral gene expression was identical to that described; however, after the removal of any unbound viral particles, the infectious process was limited to a single round via the addition of media supplemented with 40 µM ammonium chloride. At the indicated

times post infection, the cells were lysed by the addition of 1× PBS supplemented with 0.5% Triton X-100. The lysate was frozen until the completion of the experimental time course. The samples were thawed and clarified by centrifugation at 16,000 × *g* for 5 min, and equal cell volumes of the nanoluciferase samples were processed using a Nano-Glo nanoluciferase assay system (Promega) according to the manufacturer's instructions. Luminescence was recorded using a Synergy H1 microplate reader (BioTek).

#### *Statistics.*

Statistical analyses utilized GraphPad Prism 6.0 (GraphPad). A *P* value <0.05 was considered statistically significant. A detailed description of the statistical tests used is stated in each figure legend.

### 3.3. Results

#### *Oral Mucosal Epithelial Cells Preferentially Induce IFN-λ in Response to Viral Agonists.*

We determined levels of IFN-λ transcript as well as IFN-λ receptor (IFNLR) expression in healthy human gingival tissues. Similar to the respiratory and intestinal epithelium [157], our data show robust expression of IFN-λ transcripts (Sup. Fig. 3.1A) as well as IFNLR (Fig. 3.1A) toward the apical side of the tissue, largely localized within the epithelial cell adhesion molecule (EpCAM)-positive region. GECs, unlike gingival fibroblasts, specifically and strongly express EpCAM [150]. To determine responsiveness of viral pathogen-associated molecular

patterns (PAMPs), GECs were isolated from human gingival tissues and challenged in vitro with poly I:C, a synthetic double-stranded RNA analog and TLR3 agonist, as well a 60 base pair oligonucleotide sequence derived from HSV-1 (HSV60) recognized by cytosolic DNA sensors. IFN- $\lambda$  was preferentially induced in human GECs with very little IFN- $\beta$  (Fig. 3.1B). Significantly higher levels of IFN- $\lambda$  were also observed with human oral keratinocytes (OKF-6 cells) that line buccal surfaces of the mouth and also in the telomerase immortalized human gingival keratinocyte (TIGKs) cell line [150] (Fig. 3.1B). Thus, our observations are not limited to a single epithelial cell type. We did not detect any IFN- $\alpha$  or IFN- $\gamma$ . In order to overcome the low yield and passage number limitations of primary GECs, we used immortalized GECs (TIGKs) for the rest of our studies. TIGKs faithfully mimic the responses observed in primary GECs cells [150], express IFNLR (Sup. Fig. 3.1B), and are responsive to viral agonists (Fig. 3.1B). RNA sequencing (RNA-seq) profiles of TIGKs stimulated with recombinant IFN- $\lambda$  or IFN- $\beta$  showed overlapping transcriptional signatures consistent with the induction of multiple ISGs that inhibit early viral infection, replication, and release (Fig. 3.1 C and D). Common and uniquely expressed transcripts from either treatment are shown in Sup. Fig. 3.1C–F.

We determined whether viral agonists or IFN- $\lambda$  activated ISG expression in the oral epithelium in vivo. Most viruses with tropism to oral epithelium are human specific and poorly or transiently infect mice. To overcome this, we used the Mx1<sup>gfp</sup> knock-in mouse model, where inducible green fluorescent protein (GFP) expression occurs specifically in response to IFN-mediated activation of the ISRE

that is upstream of ISGs, such as Mx1 [154]. First, we confirmed that IFNLR is expressed in mouse gingival tissues (Sup. Fig. 3.1G). Injection of recombinant IFN- $\lambda$  strongly induced GFP expression in oral murine GECs but not in the infiltrating leukocytes in gingival tissues (Fig. 3.1E and Sup. Fig. 3.1H), consistent with the preferential expression of IFNLR in epithelial cells. In contrast, the Type I IFN receptor (IFNAR) is expressed in all nucleated cells and drives systemic responses to Type I IFN. In accordance with this, mice challenged with poly I:C, an agonist known to induce both Type I ( $\alpha/\beta$ ) and Type III ( $\lambda$ ) IFNs, showed robust GFP expression in GECs as well as leukocytes (Fig. 3.1E). Thus, our data show that similar to respiratory and gastrointestinal barriers, IFN- $\lambda$  is induced at the oral epithelial barrier and activates ISGs in barrier epithelial cells.

*Periodontal Disease and Associated Dysbiosis Dampens Inducible IFN Responses and Antiviral Immunity in Oral Epithelial Tissues.*

A significant predisposing factor for viral infections, or reactivation of latent viruses, in the oral cavity is chronic inflammation associated with periodontal disease [158-160]. Interestingly, GECs isolated from periodontitis patients ( $n = 3$ ) had significantly lower IFN- $\lambda$  responses concomitant with lowered ISG expression to viral agonists compared to GECs isolated from healthy individuals ( $n = 4$ ) (Fig. 3.1F and G). These observations were consistent across multiple periodontitis patients and could not be attributed to differences in apoptosis, growth rates, or differences in passage numbers between donors.

We determined whether microbial dysbiosis, which is associated with periodontal disease in humans and actively contributes to chronic inflammation, can impact IFN- $\lambda$  responses. Specifically, we challenged TIGKs with HSV60 in the presence of various oral commensal and pathogenic bacterial species. Periodontal pathogens such as *F. nucleatum* had no effect on HSV60-induced IFN- $\lambda$  production, while *Treponema denticola* moderately reduced IFN- $\lambda$  production but did not completely abolish it. In contrast, stimulation with the Gram-positive commensal *Streptococcus gordonii* (Sg) enhanced IFN- $\lambda$  production (Fig. 3.2A). Unlike other oral colonizers, *P. gingivalis* completely abolished IFN- $\lambda$  in response to HSV60 (Fig. 3.2A). *P. gingivalis* resides in subgingival biofilms and is highly associated with chronic periodontitis in both humans and murine models of periodontal disease [161]. Interestingly, published clinical data show an increased presence of HSV-1, CMV, and EBV in patients with active periodontal lesions, which correlated with the presence of *P. gingivalis* in the same lesion [139, 140]. As previously reported [162, 163], we found that *P. gingivalis* was present in gingival tissues of healthy individuals ( $n = 10$ ) and periodontitis patients ( $n = 8$ ). However, immunofluorescence staining showed *P. gingivalis* was significantly more abundant in periodontitis tissue samples (Fig. 3.2B and Sup. Fig. 3.2A). We confirmed these findings using an enzyme-linked immunofluorescent assay (ELISA)-based quantitative approach to enumerate *P. gingivalis* in tissue homogenates and found a significant increase in total colony forming units (cfu) per milligram of tissue in patients with periodontitis (Sup. Fig. 3.2B).

We found that *P. gingivalis* infection inhibits IFN- $\lambda$  induced by multiple viral PAMPs and PRRs such as poly I:C (TLR3 agonist), the TLR-7 agonist ORN06 (single-stranded RNA analog), and also 2'3'-cGAMP (stimulator of IFN genes [STING] agonist) (Fig. 3.2C). The cyclic GMP-AMP synthase (cGAS) and STING pathway is central to recognition of cytosolic DNA from DNA viruses such as HSV-1 [164, 165]. *P. gingivalis* infection also blocked IFN- $\beta$  responses in oral keratinocytes in response to HSV60 (Sup. Fig. 3.2C and D), indicating that our observations were not limited to TIGKs or a singular viral agonist. We also tested other *P. gingivalis* strains such as W83, another common laboratory strain of *P. gingivalis*, as well as the clinical isolate MP-504, and found these strains also strongly inhibited IFN responses (Sup. Fig. 3.2E). In contrast to *P. gingivalis* and other periodontal pathogens, stimulation with *S. gordonii* slightly augmented inducible IFN production to HSV60 stimulation (Fig. 3.2A). None of the tested oral bacteria by themselves induced IFN. However, they were able to differentially modulate HSV60 IFN (Fig. 3.2A). As *S. gordonii* often co-colonizes with *P. gingivalis* in mixed oral biofilms, we determined whether *S. gordonii* can prevent or reprogram IFN suppression induced by *P. gingivalis*. Costimulation of TIGKs with the two bacteria suppressed IFN- $\lambda$  production, indicating that *P. gingivalis* is able to inhibit the stimulatory effect of *S. gordonii* (Sup. Fig. 3.2F). Further insight into IFN genes/pathways modulated by *P. gingivalis* was gained through RNA-seq. *P. gingivalis* infection led to a massive down-regulation of several genes implicated in IFN responses related to all aspects of viral infection. These include families of antiviral restriction factors essential in blocking select steps in viral replication such

as ribonuclease L (RNaseL), IFIT (IFN-induced proteins with tetratricopeptide repeats) family members, ISG15 (IFN-stimulated protein of 15 kDa), protein kinase R (PKR), GTPase Mx1 (myxovirus resistance 1), and the tripartite motif (TRIM) family members (Fig. 3.2D and E and Table 2.1). IFIT proteins degrade viral RNAs during infection [166], while tetherin/BST2 protein prevents budding of virions from the plasma membrane and blocks the release of coronaviruses, herpesviruses, paramyxoviruses, and flaviviruses from infected cells. Also, down-regulated was SAMHDI (SAM and HD domain containing deoxynucleoside triphosphate triphosphohydrolase), which is critical in fighting retroviral infections. Significant down-regulation of transcription factors such as IFN regulatory factors (IRFs) and signal transducer and activator of transcription (STAT1, 2) was consistent with loss of IFN and ISG expression. Several genes essential in immune cell recruitment (CCL5, CXCL10) and antigen presentation (HLA) were also down-regulated. Overall, we found that the extent of IFN paralysis induced by *P. gingivalis* infection was broad and affected genes involved in immune responses against a wide range of RNA and DNA viruses. For example, growth/dissemination of a model positive-sense RNA virus, Sindbis virus (SINV), which is known to be highly controlled by the IFN response, was significantly elevated in *P. gingivalis*-infected cells (Fig. 3.2 F and G).

Consistent with our RNA-seq data sets, we found that *P. gingivalis* colonization of Mx1<sup>gfp</sup> mice resulted in a loss of IFN-inducible GFP expression in oral epithelial tissues (Fig. 3.2H). These data were striking for several reasons. First, we did not antibiotic treat these mice prior to colonization

with *P. gingivalis* in order to avoid any selective advantage or disruption of the natural microbiome. Second, *P. gingivalis* not only successfully colonized the oral cavities of these mice (as confirmed by 16S rRNA nested PCRs using *P. gingivalis*-specific primers) [151] but was able to specifically down-regulate IFN-induced ISG expression in vivo. These data confirm our in vitro observations and establish that the presence of *P. gingivalis* in the oral microbiome reduces the effectiveness of IFN responses, potentially contributing to clinical observations in periodontitis patients. Specifically, increased titers of DNA viruses such as EBV, HSV1, and CMV, were found in deep periodontal pockets where *P. gingivalis* normally resides [138-140, 143], as well as increased susceptibility to RNA viruses such as SARS-CoV-2 [167, 168].

*IRF-1 Regulates Cell-Intrinsic Antiviral State by Maintaining Basal Expression of ISGs.*

To determine how *P. gingivalis* blocks IFN responses in a cell-intrinsic manner, we looked at the activation of several transcription factors that either maintain the cell-intrinsic antiviral state and/or actively induce IFN expression in response to viral PAMPs. IRFs are a family of transcription factors that play critical roles in several aspects of host antiviral immunity. TLR and RIG-I-like-receptor (RLR) activation drives nuclear translocation of IRFs 1, 3, 5, and 7 and Type I IFN [169, 170] and Type III IFN production [123, 171]. Recently, it was shown that unlike IRFs 3 and 7, IRF-1 expression was critical in the maintenance of constitutive or



basal levels of multiple ISGs in epithelial cells independently [172-174]. Thus, IRF-1 provides early protection against viral infection by maintaining a cell-intrinsic “antiviral state” [174]. We previously showed that *P. gingivalis* transcriptionally down-regulates IRF-1 levels [56], thus we investigated whether loss of IRF-1 expression (using silencing RNA (siRNA)) was sufficient to down-regulate ISG transcripts in TIGKs. Silencing IRF-1 indeed down-regulated several IFN response genes and antiviral restriction factors (Fig. 3.3A and Sup. Fig. 3A and B). Select genes from the RNA-seq datasets were confirmed by qRT-PCR (Sup. Fig. 3C) and immunoblotting (Fig. 3.3B and C). Hence, *P. gingivalis*-mediated down-regulation of IRF-1 can be predicted to compromise the antiviral state in GECs by a significant reduction in basal ISG signatures. During an infection, viral agonists induce IFN production, which via paracrine and autocrine signaling, reinforces antiviral defenses by driving ISG expression to levels several-fold higher than those observed in the basal state. Loss of IRF-1 did not negatively impact inducible IFN- $\lambda$  expression (Sup. Fig. 3D) in response to HSV60. Consistent with this, we found that stimulation with HSV60 led to activation of antiviral genes as measured by differential transcript expression in RNA-seq datasets (Sup. Fig. 3E) and immunoblots (Fig. 3.3B and C). ISG levels induced were comparable to those induced in TIGKs treated with scrambled control siRNA, indicating the presence of additional mechanisms of IFN- $\lambda$  regulation in response to viral agonists (Fig. 3.3B and C and Sup. Fig. 3D). Thus, we show that while IRF-1 was essential for the maintenance of basal ISGs levels in GECs, inducible IFN production and consequent ISG expression was not affected by IRF-1 deficiency. *P.*

*gingivalis* infection not only down-regulated IRF-1 levels, but it also blocked its nuclear translocation (Fig. 3.3D). Stimulation with HSV60 did not augment IRF-1 levels or ISG expression in HSV60-treated cells. Furthermore, in *P. gingivalis*-infected cells, we did not see any restoration of ISG expression even after overexpressing IRF-1 (Sup. Fig. 3.4). Collectively, these results indicate that *P. gingivalis* has additional targets for antagonism of IFN- $\lambda$ .

*P. gingivalis* Transcriptionally Represses IFNL1 by Up-Regulating ZEB1.

Multiple transcription factors, including other IRF family members (IRF-3 and IRF-7), Nuclear Factor kappa-light-chain-enhancer of activated B cells (NF- $\kappa$ B), and Activator Protein 1 (AP-1) can all cooperatively induce Type I and Type III IFN transcription independent of IRF-1 [169, 170, 175]. All the aforementioned transcription factors potentially could contribute to IFN- $\lambda$  production in response to HSV60. To further investigate the mechanistic basis of *P. gingivalis*-mediated IFN- $\lambda$  repression, we looked at other transcription factors that positively regulate IFN- $\lambda$  expression. Consistent with our RNA-seq data in Fig. 2D and E, *P. gingivalis* infection down-regulated IRFs 3, 7, and 9 that bind to PRD1 and ISRE elements on *IFNL1* promoter to induce Type III IFN production [123, 171] (Sup. Fig. 3.5A). Thus, we turned our attention on NF- $\kappa$ B, which binds to  $\kappa$ B sites on the *IFNL1* promoter [176] and also plays a role in reinforcing IFN pathways by augmenting the expression of various IRFs [177]. We have previously shown that SerB, a serine phosphatase produced by *P. gingivalis*, dephosphorylates the serine 536 residue on the RelA subunit of NF- $\kappa$ B, preventing its nuclear

translocation and blocking subsequent expression of NF- $\kappa$ B-regulated genes such as *IL8/CXCL8* [178]. We assessed the extent to which restoration of NF- $\kappa$ B activation would rescue IFN- $\lambda$  responses to viral agonists. GECs were infected with either the wild-type (WT) or  $\Delta$ *serB* strains of *P. gingivalis* and challenged with HSV60 DNA. IRF-1 expression was reduced on infection with either strain (Sup. Fig. 3.5B). However, IFN- $\lambda$  production remained repressed even when cells were stimulated with  $\Delta$ *serB* (Fig. 3.3E and F). These data establish that non-NF- $\kappa$ B-dependent mechanisms predominate in the suppression of IFN- $\lambda$  production by *P. gingivalis*.

One such candidate is up-regulation of the zinc finger E-Box binding homeobox1 ZEB1, a transcription factor involved in epithelial-mesenchymal transition [114]. ZEB1 transcriptionally represses *IFNL1* by binding to E-box-like sites on the *IFNL1* promoter [176] and also by epigenetically silencing IRF-1 [179]. Unlike *P. gingivalis*, HSV60 stimulation did not significantly change ZEB1 expression (Fig. 3.3G and H). Moreover, targeted knockdown of ZEB1 by siRNA significantly enhanced *IFNL1* transcription in response to HSV60 and prevented *P. gingivalis* antagonism of *IFNL1* expression (Fig. 3.3I). Thus, these data demonstrate that *P. gingivalis* represses IFN- $\lambda$  both by disarming IRFs and by up-regulating the transcriptional repressor ZEB1.

#### *P. gingivalis*-Mediated Cleavage of IFN Receptors Enforces IFN Paralysis.

In vivo, *P. gingivalis*-induced IFN- $\lambda$  paralysis could be circumvented by IFN- $\lambda$  secreted from noninfected epithelial cells or from additional cell types. Hence,

we determined whether exogenously added IFN- $\lambda$  would restore ISG expression. The heterodimeric IFN- $\lambda$  receptor (IFNLR) is composed of the IL-28 receptor chain and the IL-10 receptor  $\beta$ -chain and on binding to IFN- $\lambda$  family members, induces phosphorylation of signal transducer and activator of transcription (STAT) proteins STAT1 and STAT2. Phosphorylated STATs along with IRF-9 form the heterotrimeric transcription factor complex ISGF3 (ISG factor 3) that binds to the ISRE within the promoters of IFN-inducible genes [81, 180]. GECs incubated with recombinant IFN- $\lambda$  rapidly phosphorylated STAT1; however, *P. gingivalis* infection blocked STAT1 phosphorylation in the presence of exogenously added IFN- $\lambda$ , suggestive of an additional component to the *P. gingivalis* antagonistic process (Fig. 3.4A).

*P. gingivalis* produces several cysteine proteases, the arginine-specific gingipains A and B (RgpA and RgpB) as well as the lysine-specific gingipain (Kgp), that proteolytically degrade cellular proteins and attenuate signal transduction pathways [152, 181-183]. We examined the role of gingipains in preventing IFN- $\lambda$ -induced activation of STAT1 by infecting GECs with a triple mutant strain ( $\Delta rgpAB\Delta kgp$ ) of *P. gingivalis* lacking expression of all gingipains. Loss of gingipain activity prevented attenuation of STAT1 phosphorylation by *P. gingivalis* upon IFN- $\lambda$  stimulation (Fig. 3.4A) and also restored expression of ISGs (Fig. 3.4B). Even in GECs overexpressing STAT1 protein, phosphorylation levels remained low in cells infected with *P. gingivalis* (Sup. Fig. 3.6). We hypothesized that the loss of phosphorylation following *P. gingivalis* challenge was mediated by an upstream target sensitive to gingipain-mediated proteolytic cleavage. Thus, we

tested the ability of *P. gingivalis* to cleave IFN receptors and thereby limit STAT1 phosphorylation. GECs were incubated with the parental strain of *P. gingivalis* or mutants lacking either Kgp, RgpA/B, or the triple mutant. Our data show that cleavage of IFNLR (IL-28R) was mediated predominantly by the arginine-specific gingipains RgpA/B (Fig. 3.4C). Although Type I and III IFNs bind to distinct receptors, they activate overlapping downstream signaling pathways leading to ISG expression [81]. Thus, we also looked for cleavage of the Type I IFN receptor (IFNAR) by Western blotting. *P. gingivalis* arginine gingipains also cleaved IFNAR (Fig. 3.4D). Interestingly, IFNLR was also cleaved in periodontitis patients (Fig. 3.4E and F), with cleavage evident toward the apical epithelial side that interfaces with colonizing bacteria such as *P. gingivalis* (Fig. 2B). At later timepoints, *P. gingivalis* also cleaved STAT1 protein (Sup. Fig. 3.7), compromising the formation of ISGF3, the heterotrimeric transcription factor complex that binds to the ISRE sites found on promoters of several ISGs. Additionally, viral agonists (HSV60) as well as exogenously added IFN- $\lambda$  failed to stimulate the ISRE promoter element in *P. gingivalis*-infected GECs (Fig. 3.4G), further enforcing IFN- $\lambda$  paralysis.

### 3.4. Discussion

Here, we report a previously unknown role for IFN- $\lambda$  in modulating ISG expression and antiviral immunity at the oral mucosal epithelium of humans and mice. Modulation of viral infection by the indigenous microbiota is well-established [124, 143-148], and one recently documented mechanism involves microbial priming of antiviral IFN pathways [127, 144, 146]. We find here a

mechanism by which an indigenous bacterial colonizer of the oral cavity can suppress IFN- $\lambda$  responses and increase susceptibility to viral infection. Interestingly, the concerted action of multiple *P. gingivalis* virulence factors blocked IFN pathways (summarized in Sup. Fig. 3.8) using molecular strategies that are similar to those used by certain viruses. For example, *P. gingivalis* infection suppressed the activation of multiple IFN-driving transcription factors such as IRFs 1, 3, 7, and 9, NF- $\kappa$ B, and STAT-1, subsequently blocking ISGF3-driven ISG expression. Additionally, an increase in ZEB1, a negative regulator of *IFNL1*, synergistically blocked transcription of IFN- $\lambda$ . The targeting of IFN-activating transcription factors by *P. gingivalis* is similar to the strategies by various viral pathogens to antagonize IFN transcription and IFN receptor-mediated activation of ISGs. For example, viral proteins can directly bind to IRF-3 and -7 in a manner that blocks IFN transcription either due to dephosphorylation of IRFs themselves or by preventing their interaction with other binding partners required for IFN transcription[184]. NS5 from the yellow fever virus, upon binding to STAT2, prevents the formation of the ISGF3 complex and ISG induction[185]. In addition to misdirection of signaling, viral proteases can also cleave and degrade host proteins by targeting them for proteasomal degradation[186]. In our model, IFN paralysis was further reinforced by *P. gingivalis* via proteolytic degradation of INFL-R and IFNAR making GECs insensitive to exogenous IFNs produced by other cells such as plasmacytoid dendritic cells in tissues. The NS5 protein of West Nile and tick-borne encephalitis virus inhibits the expression of these receptors on the plasma membrane[187]. Thus, there are several parallels between *P.*

*gingivalis*-mediated antagonism of IFN responses and mechanisms used by viral pathogens.

Our findings are of broad relevance not only for oral health but also for host responses to a wide range of viral pathogens that infect various mucosal surfaces. Translocation of *P. gingivalis* to other mucosal surfaces such as the gut and surfaces of the digestive tract is associated with dysbiosis and other complications including gastric and esophageal cancers[188, 189]; translocation to the respiratory epithelial tissues exacerbated aspiration-induced pneumonia[190-192] in patients and mouse models. In periodontitis patients, increased titers of EBV, HSV1, and CMV were observed in deep periodontal pockets[138, 140, 143], the predominant niche of *P. gingivalis*. While the contribution of these viruses to periodontitis is unclear, *P. gingivalis*-mediated IFN paralysis might promote reactivation or replication of these and other viruses within the subgingival epithelium. Extension of this work in vivo to test specific viral pathogens will require technological advances, as genetically tractable mouse models that phenocopy the oral epithelial tropism of these viruses as seen in human cells have not been described. However, data from our human tissues and the Mx1<sup>gfp</sup> reporter mice strongly correlates with our observations in multiple oral epithelial cell lines.

IFN- $\lambda$  has been investigated for the treatment of viral diseases given its focused role on epithelial cells. In patients with hepatitis C infection, IFN- $\lambda$  treatment was efficacious in lowering viral titers, similar to IFN- $\alpha$  but with lower side effects and toxicity in comparison to IFN- $\alpha$ [193]. Pegylated IFN- $\lambda$  is also being investigated as a broad-spectrum antiviral to provide immediate or early protection

to healthcare workers against the SARS-CoV2 outbreak[194]. While it is premature to state that *P. gingivalis* infection might be a risk factor in exacerbating clinical symptoms of COVID-19, our data do demonstrate that it can certainly enhance susceptibility by compromising the “antiviral state.”



### 3.5. Figures:

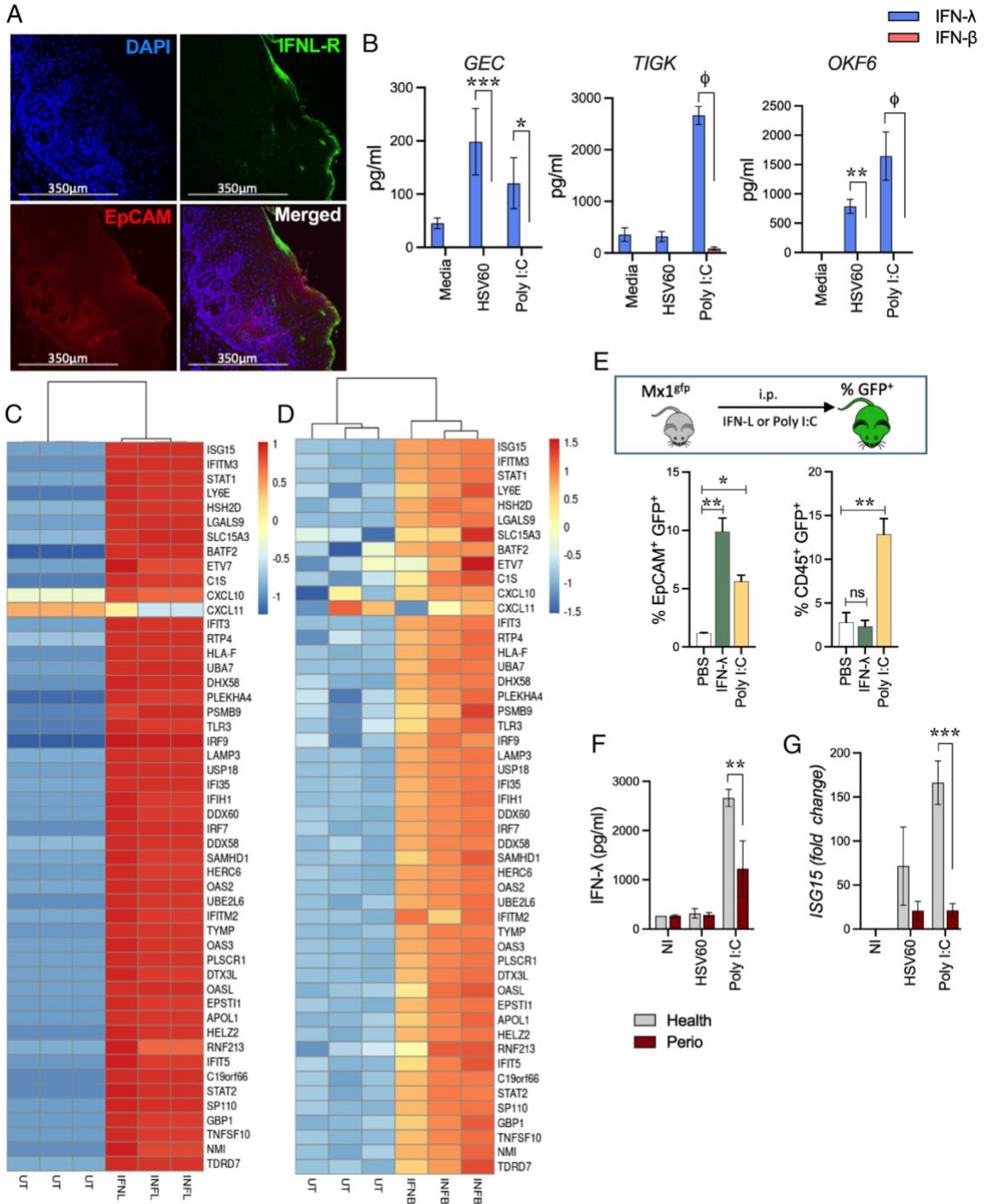


*Figure 3.1. IFN-λ is strongly expressed in gingival tissues, cell lines, and activates ISG expression in oral tissues.*

(A) IFNLR expression was determined in fixed human gingival tissues from healthy donors by immunofluorescent staining (epithelial cells were identified by EpCAM expression and cell nuclei with DAPI staining). (B) Oral epithelial cells were stimulated with 5 µg/mL HSV60 or 50 µg/mL poly I:C for 24 h and IFN-λ and IFN-β levels measured in cell-free supernatants by ELISA. Data are shown as mean ± SD and statistical differences determined by two-way ANOVA with Holm–Sidak multiple comparison test (\*\*P < 0.01; †P < 0.001). (C) TIGKs were treated with 20 ng/mL IFN-λ1 or (D) 0.25 ng/mL IFN-β for 24 h and analyzed by RNA-seq. Hierarchical clustering heatmap (based on log [RPKM] values) of the top 50 ISGs induced by IFN-λ1 or IFN-β compared to untreated cells are shown. Color intensity denotes level of gene expression. (E) Mx1<sup>gfp</sup> mice were intraperitoneally (i.p.) injected with 50 µg poly I:C or 4 µg IFN-λ and euthanized after 36 h. GECs (EpCAM<sup>+</sup>, CD45<sup>-</sup>) and leukocytes (EpCAM<sup>-</sup>, CD45<sup>+</sup>) were analyzed by flow cytometry and % GFP-positive cells (mean ± SD) determined by flow cytometry for each population from three mice per group. Statistical differences determined by one-way ANOVA with Holm–Sidak multiple comparison test (\*P < 0.05; \*\*P < 0.01). (F) IFN-λ responses to 5 µg/mL HSV60 or 50 µg/mL poly I:C were measured by ELISA in supernatants of GECs isolated from healthy donors or periodontitis patients. (G) ISG15 expression was determined by qRT-PCR, normalized to GAPDH ( $2^{-\Delta\Delta CT}$ ), and is shown as mean ± SD. Statistical differences were determined by two-way ANOVA with Holm–Sidak multiple comparison test (\*\*P < 0.01; \*\*\*P < 0.005).

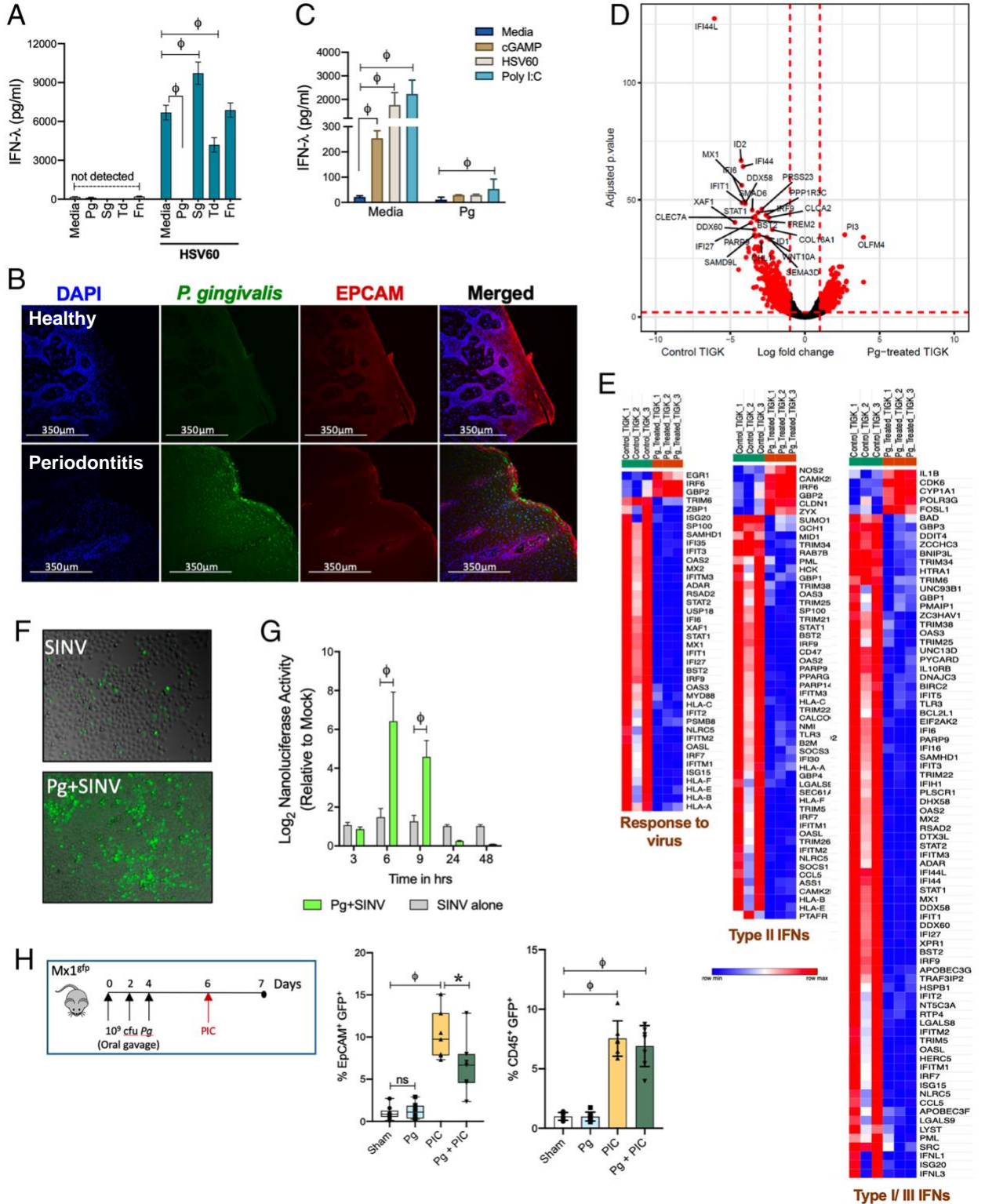


*Figure 3.2. P. gingivalis* infection causes IFN paralysis, characterized by the loss of basal and inducible IFN responses and ISG expression.

(A) IFN- $\lambda$  responses were measured by ELISA in TIGKs challenged either with *P. gingivalis* (Pg), *T. denticola* (Td), or *F. nucleatum* (Fn) at MOI 100 or *S. gordonii* (Sg) MOI 10 for 5 h, washed once with PBS, and then stimulated with 5  $\mu$ g/mL HSV60 for additional 18 h. (B) *P. gingivalis* colonization was determined in gingival tissues by immunofluorescence staining (top healthy donor; bottom periodontitis patient). (C) TIGKs were either left untreated or infected with *P. gingivalis* as described above with subsequent stimulation with 50  $\mu$ g/mL poly I:C (TLR3 agonist), 5  $\mu$ g/mL ORN06 (TLR7 agonist), 5  $\mu$ g/mL HSV60, or 25  $\mu$ g/mL 2'3'-cGAMP (STING agonist) for 18 h. IFN- $\lambda$  levels in cell-free supernatants are shown as mean  $\pm$  SD. Statistical differences were determined by two-way ANOVA (\*\*P < 0.01;  $\Phi$ P < 0.001). (D) Volcano plot of differentially expressed transcripts between GECs infected with *P. gingivalis* (MOI 100) and uninfected control cells. X-axis shows log-fold change between the two conditions, with positive values showing up-regulation and negative values showing down-regulated genes. Y-axis denotes P values for corresponding genes. Significantly different genes are shown highlighted in red (P < 0.001 as determined using the DESeq package in R). (E) Gene enrichment analysis of top 300 down-regulated genes was performed as described in [Materials and Methods](#), and hierarchical clustering heatmaps (based on RPKM values) for response to virus pathway, Type II IFNs, and Type I/III IFNs pathways are shown. Color intensity denotes level of 3gene expression. (F) Viral growth/dissemination was measured in mock and *P. gingivalis*-treated GECs infected with SINV nsP3-GFP strain at an MOI of 10 PFU per cell and cultured under normal conditions for a period of 24 h prior to GFP and brightfield microscopic imaging. Data shown are representative of three independent biological replicates. (G) Viral

gene expression was assessed in mock and *P. gingivalis*-treated GECs infected with SINV nsP3-Nanoluc at an MOI of 10 PFU per cell and cultured in the presence of ammonium chloride to limit infection to the initial single-round entry event. At the indicated time points, the cells were harvested and the level of Nanoluc activity was assayed. Statistical differences were determined by two-way ANOVA (\*\*P < 0.01; †P < 0.001). (H) Mx1gfp mice were colonized by *P. gingivalis* before intraperitoneal (i.p.) challenge with poly I: C. GECs (EpCAM<sup>+</sup>, CD45<sup>-</sup>) and leukocytes (EpCAM<sup>-</sup>, CD45<sup>+</sup>) were analyzed by flow cytometry, and %GFP-positive cells (mean ± SD) determined by flow cytometry. Each data point represents one mouse (n = 7 to 5 per group). Statistical differences determined by one-way ANOVA (\*P < 0.05; \*\*P < 0.01).

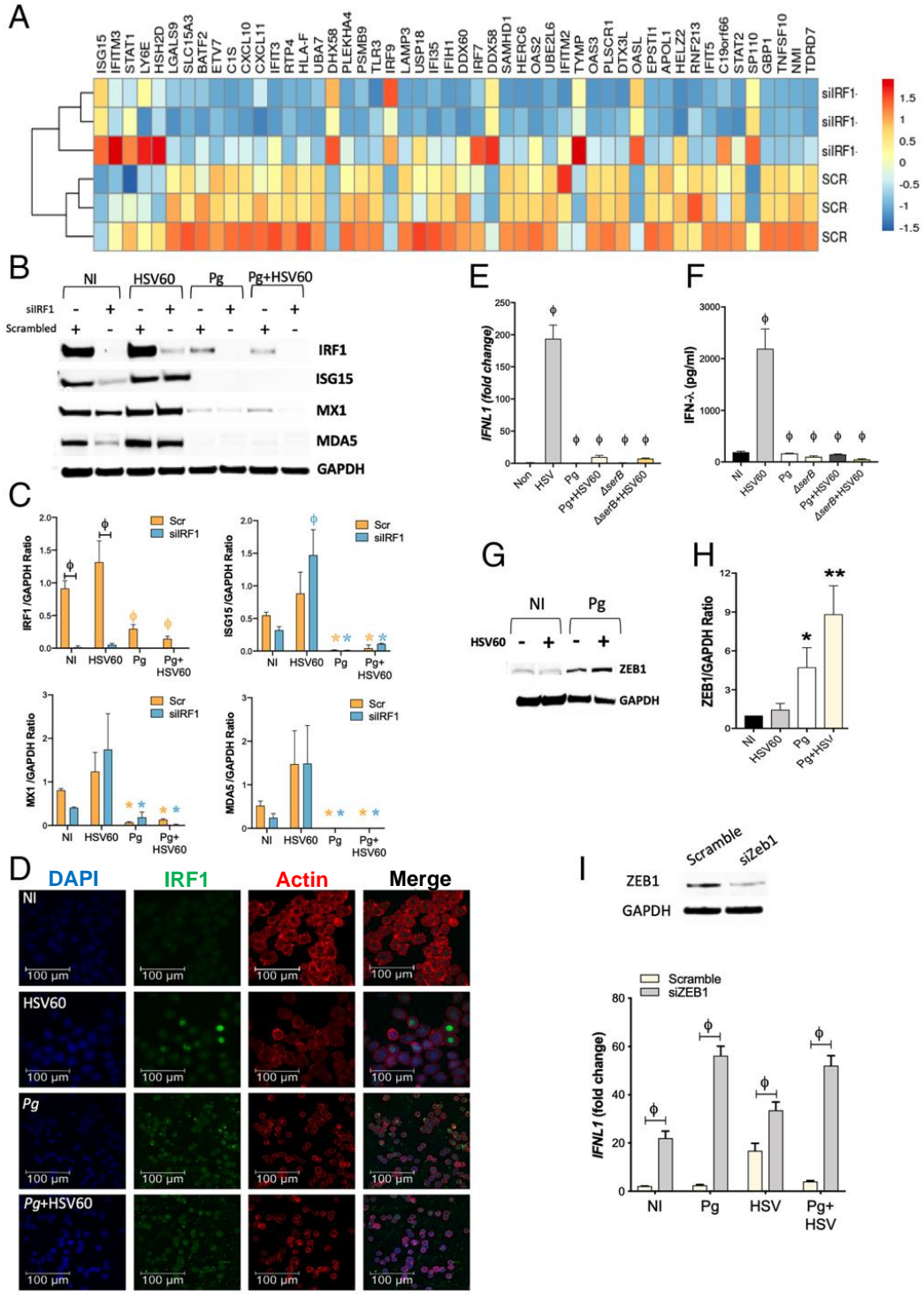


*Figure 3.3. P. gingivalis* incapacitates transcription factors that positively regulate IFN- $\lambda$  expression, and up-regulates ZEB1, a transcriptional repressor of IFN- $\lambda$ .

(A) TIGKs were transfected with siIRF1 or scrambled control siRNA and differentially expressed transcripts determined by RNA-seq. Hierarchical clustering heat map (based on log RPKM values) of the top 50 ISGs differentially expressed on IRF-1 silencing. Color intensity denotes level of expression. (B) TIGKs were transfected with siIRF1 (si) or scrambled control siRNA (scr) and infected with *P. gingivalis* or stimulated with 5  $\mu$ g/mL HSV60 and immunoblotted for IRF-1, ISG15, MX1, MDA5, and GAPDH. (C) Band intensities of immunoblots were determined, and ratios of IRF1, ISG15, MX1, and MDA5 normalized to GAPDH from three different blots are shown (mean  $\pm$  SD). Statistical differences were determined by two-way ANOVA ( $^{\#}P < 0.001$ ;  $*P < 0.05$ ). Orange and blue symbols depict comparisons between NI (not infected) scr control and siIRF1, respectively. (D) TIGKs were infected with *P. gingivalis* and/or stimulated with 5  $\mu$ g/mL HSV60, labeled with anti-IRF-1 antibodies (green), and analyzed by confocal microscopy. Actin was labeled with phalloidin (red) and nuclei stained with DAPI (blue). Merged images are shown on the Right. Magnification (63 $\times$ ) of 20 z-stacks of 0.3  $\mu$ m. TIGKs were infected with *P. gingivalis* WT or serB-deficient isogenic mutant ( $\Delta$ serB) for 5 h, followed by 5  $\mu$ g/mL HSV60 for additional 18 h. (E) Transcript levels of IFNL1 determined by qRT-PCR, normalized to GAPDH ( $2^{-\Delta\Delta CT}$ ) and are shown as mean  $\pm$  SD; (F) secreted IFN- $\lambda$  in cell-free supernatants determined by ELISA and shown as mean  $\pm$  SD. (G) ZEB1 and GAPDH were detected by immunoblotting. (H) Band intensities were determined, and ratios of ZEB1 to GAPDH from three different blots are shown (mean  $\pm$  SD). (I) GECs were transfected with siZEB1 or scrambled control siRNA. After 48 h, media was replaced, and cells were challenged with *P. gingivalis* (MOI 100) for 5 h and then stimulated with 5  $\mu$ g/mL

HSV60 for 16 h. Transcript levels of IFNL1 were determined by qRT-PCR normalized to GAPDH ( $2^{-\Delta\Delta CT}$ ) and are shown as mean  $\pm$  SD (n=3). Statistical differences were determined by two-way ANOVA ( $P < 0.001$ ).



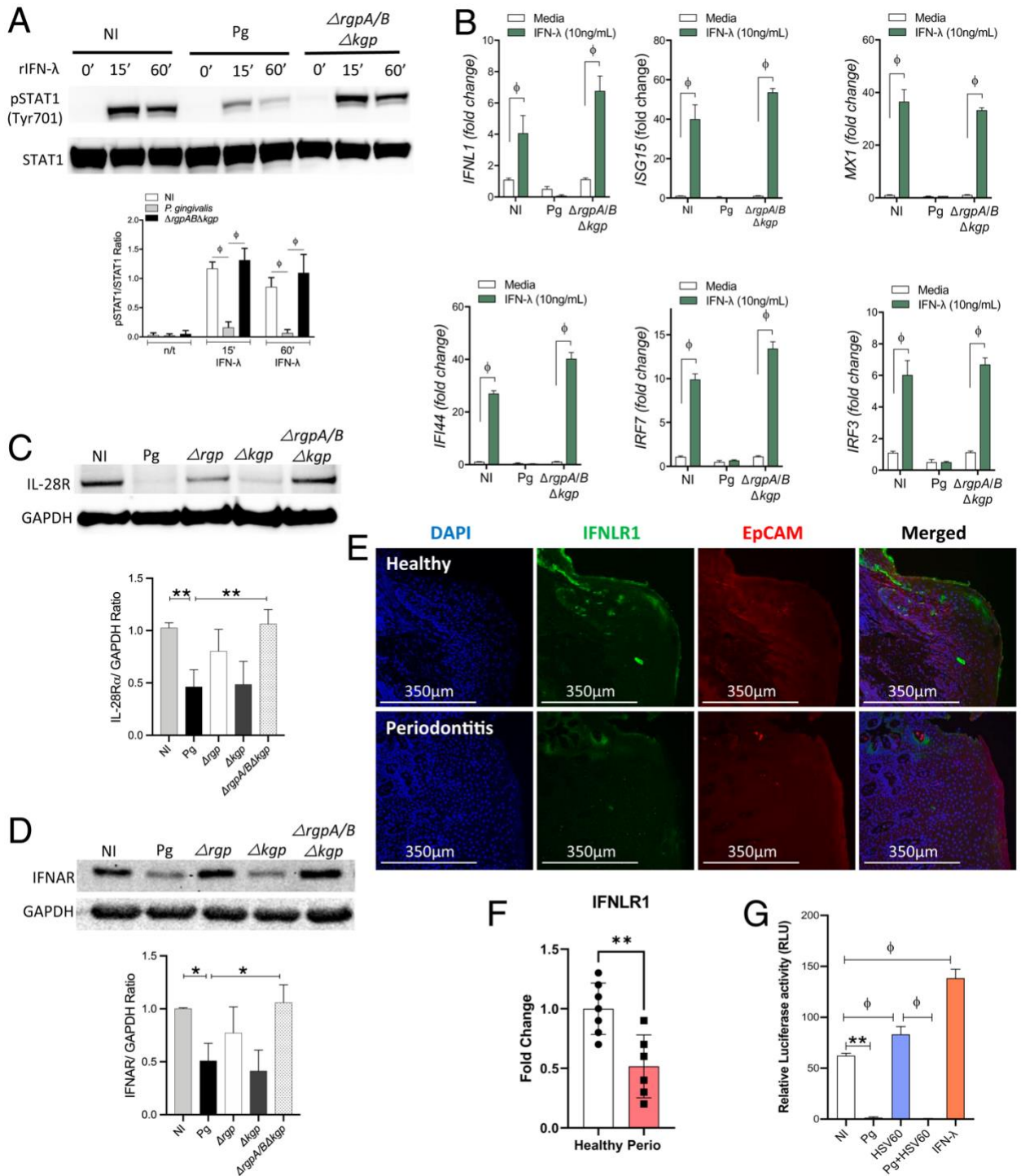
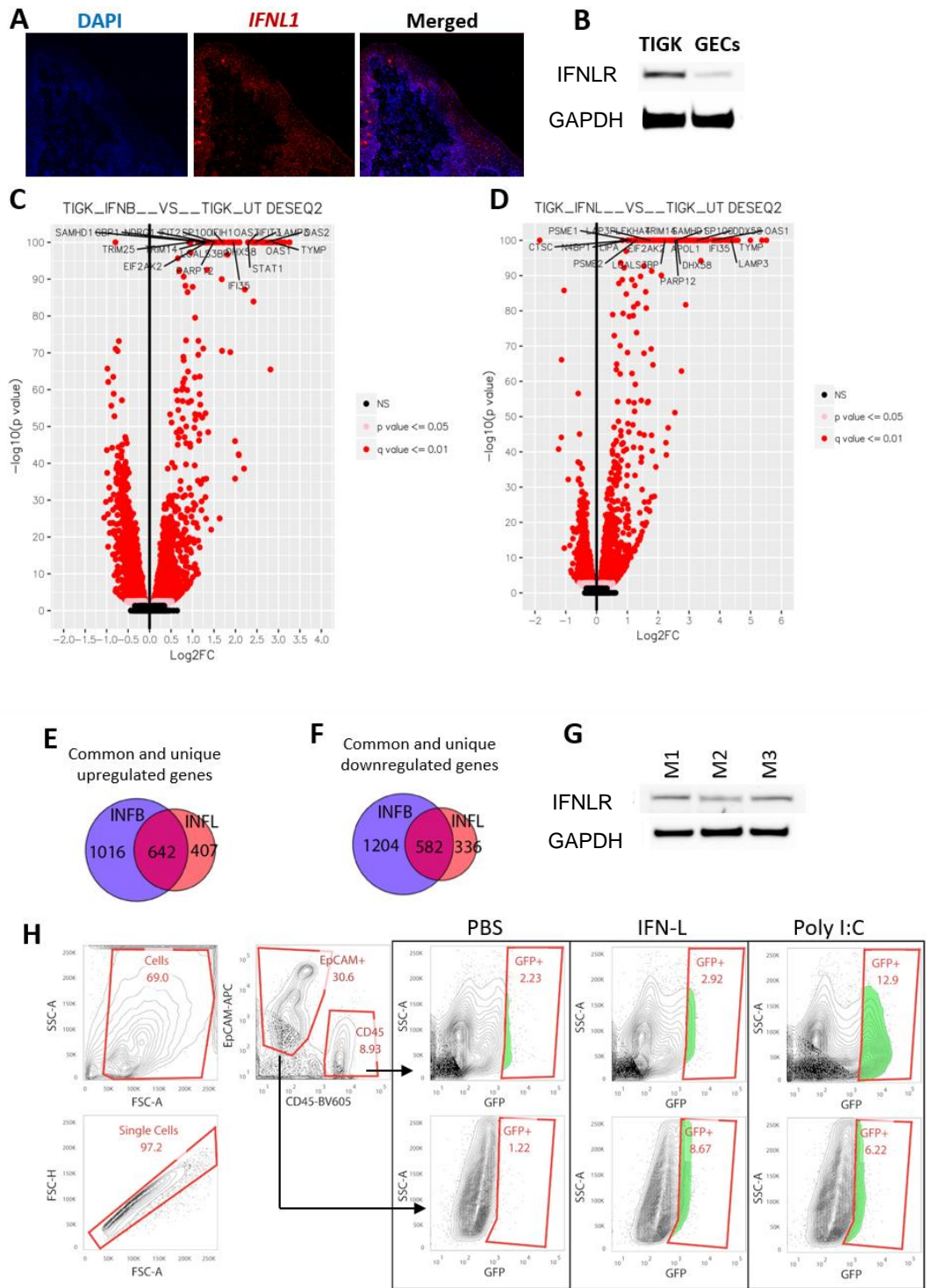


Figure 3.4. *P. gingivalis* infection reduces responsiveness to exogenous IFN- $\lambda$ .

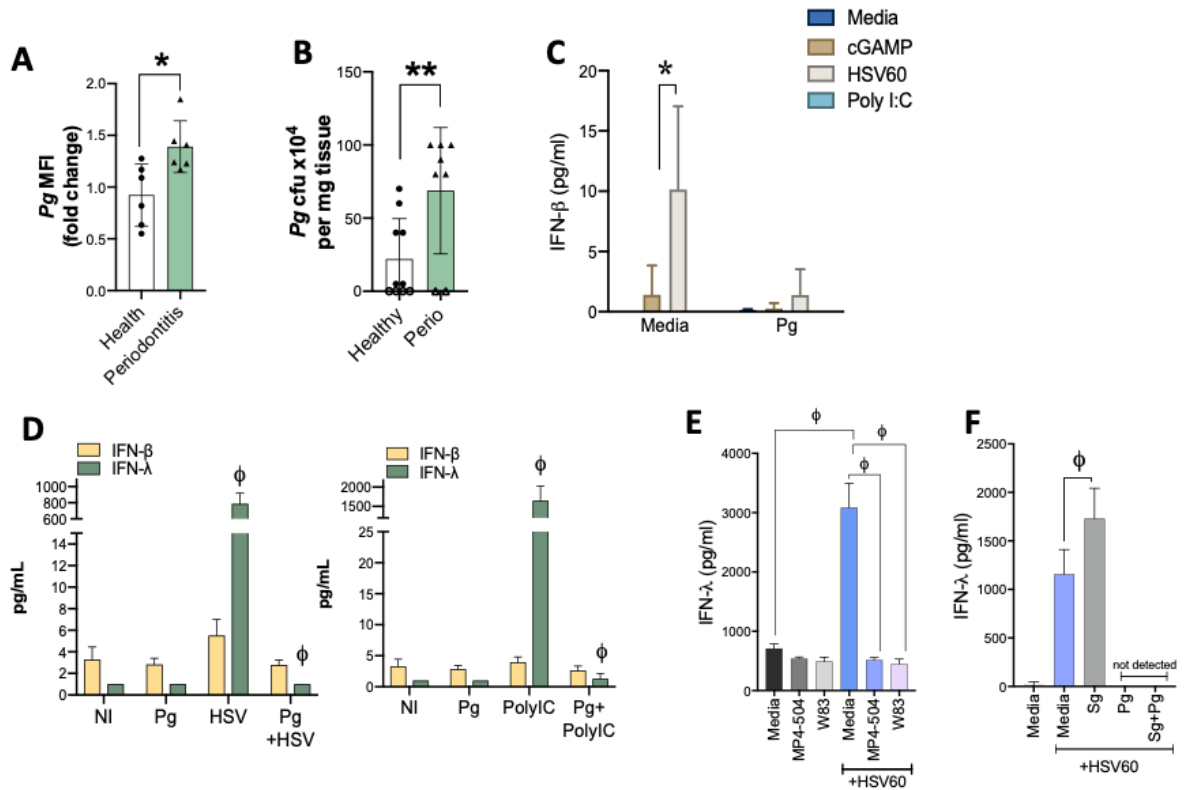
TIGKs were infected with *P. gingivalis* WT or gingipain-null triple mutant ( $\Delta$ rgpAB $\Delta$ kqp) for 1 h and then stimulated with 20 ng/mL IFN- $\lambda$  for indicated timepoints. (A) Phospho-STAT1 (pSTAT1) and total STAT1 expression was determined by Western blotting.

Band intensities were determined, and ratios of pSTAT1 to total STAT1 from three different blots are shown (mean  $\pm$  SD). Statistical differences were determined by one-way ANOVA (\*P < 0.05; \*\*P < 0.01). (B) Changes in transcript levels (mean  $\pm$  SD) of ISG15, MX1, IFI44, IRF7, IRF3, and IFNL1 were determined by qRT-PCR and normalized to GAPDH ( $2^{-\Delta\Delta CT}$ ). Data are shown as mean  $\pm$  SD, and statistical differences were determined by two-way ANOVA ( $\phi$ P < 0.001). TIGKs were infected with *P. gingivalis* WT or gingipain mutant strains  $\Delta$ kgp,  $\Delta$ rgpA/B, and  $\Delta$ rgpAB $\Delta$ kgp for 1 h, and (C) IFNLR (IL-28R), (D) IFNAR, and GAPDH expression was determined in protein lysates by Western blotting. GAPDH was used as a loading control. Densitometry ratios for IL-28R and IFNAR from three different blots are shown as mean  $\pm$  SD. Statistical differences were determined by one-way ANOVA (\*P < 0.05; \*\*P < 0.01). (E) IFNLR (IL-28R) was detected in human gingival tissues from periodontitis patients and healthy controls. (F) Mean fluorescence intensity for IFNLR within the EpCAM-positive region was calculated using Imaris software for seven control (healthy) donors and six periodontitis patients (perio). Statistical differences were determined by Student's t test (\*\*P < 0.01). (G) Dual luciferase reporter analysis of ISRE-Luc activities in GECs under various stimulation conditions. Statistical differences were determined by one-way ANOVA ( $\phi$ P < 0.05; \*\*P < 0.01).



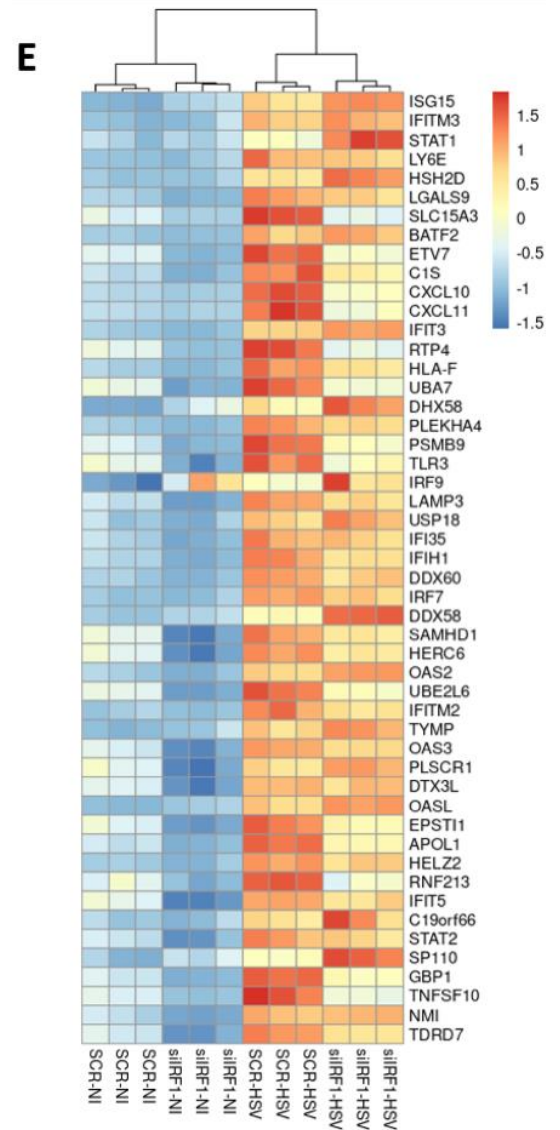
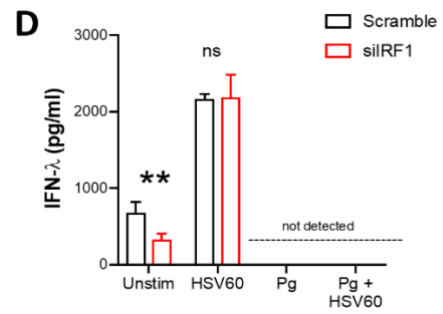
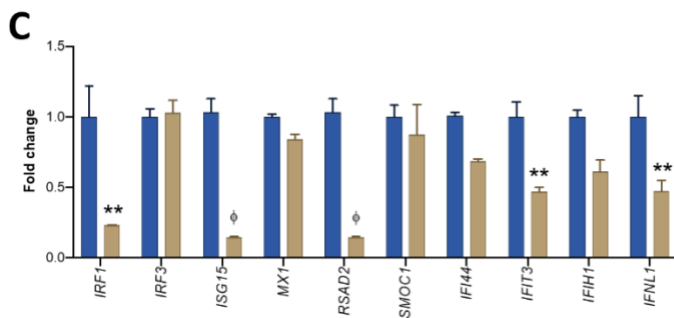
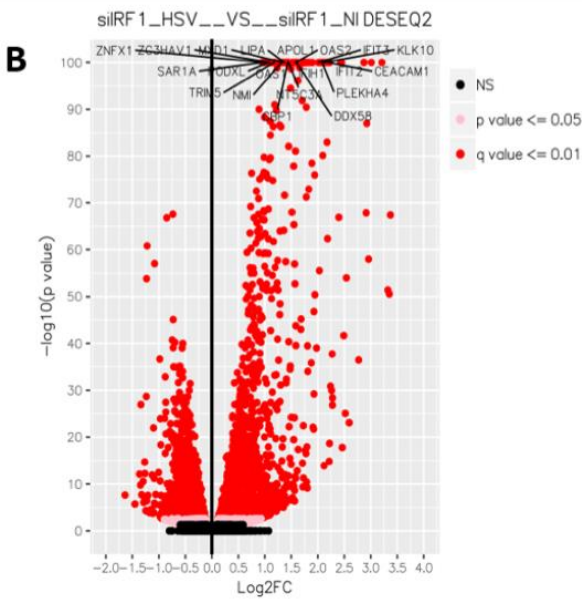
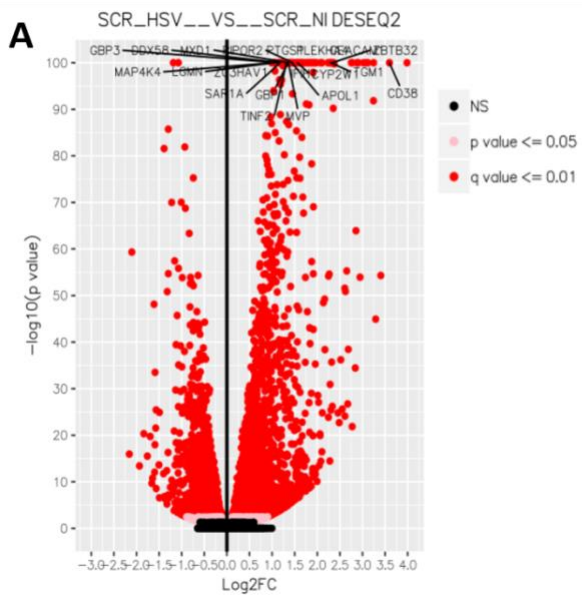
Supplemental Figure 3.1: *IFN-λ* shows bioactivity in oral tissues. A) *IFNL1* transcript expression was determined in fixed human gingival tissues of healthy donors (n=3) by

RNAscope. (B) IFNLR expression in TIGKs and human primary GECs was determined by western blots. Volcano plot of differentially expressed transcripts between GECs incubated with (C) 20 ng/ml IFN- $\lambda$  or (D) 0.2 ng/ml IFN- $\beta$  compared to untreated cells. X-axis shows log-fold change between the two conditions with positive values showing upregulation and negative values showing downregulated genes. Y-axis denotes P values for corresponding genes. Significantly different genes are shown highlighted in red ( $P < 0.05$  as determined using the DESeq package in R). IFN- $\lambda$  treatment resulted in differential expression of 1967 transcripts compared to 3444 after IFN- $\beta$  treatment. Venn Diagrams of unique and differentially upregulated transcripts (E) and downregulated transcripts (F) between the two treatments are shown. (G) To confirm murine gingival tissues, express IFNLR, gingival tissues were isolated from 3 Mx1<sup>gfp</sup> mice, and IFNLR expression determined by immunoblots. (H) Gating strategy for determining GFP expression in gingival cells.



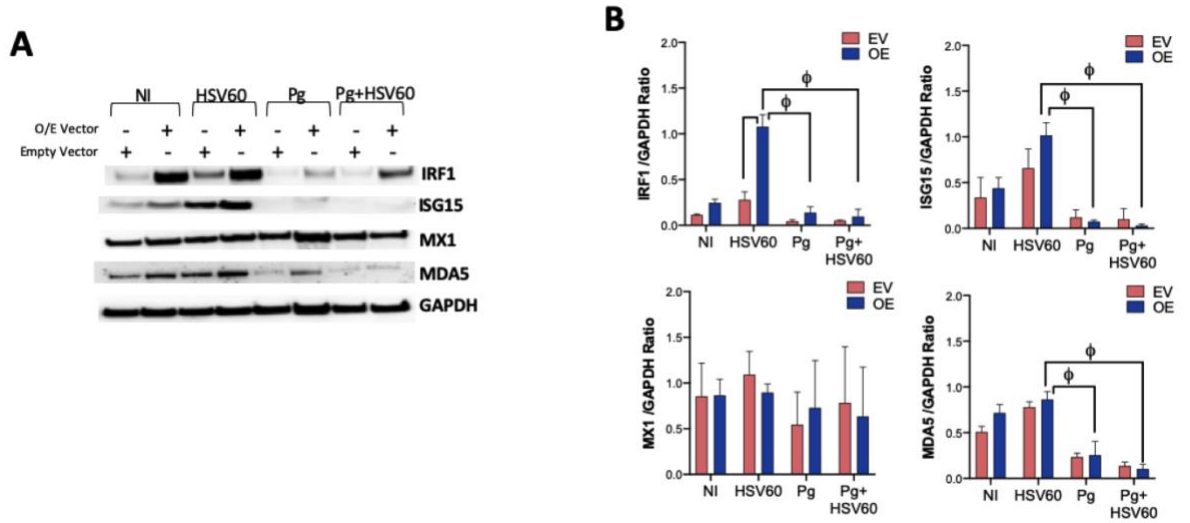
*Supplemental Figure 3.2: Abundance of P. gingivalis in human samples and its effect on IFN production.* (A) Mean fluorescence intensity (fold change) for *P. gingivalis* (*Pg*) staining was estimated in gingival tissue sections from healthy (n=6) and periodontitis (n=6) samples. (B) *P. gingivalis* cfu per mg of tissue were determined by ELISA in gingival tissue homogenates of healthy (n=10) and periodontitis patients (n=8). Open symbols represent samples with values below detection limit). Statistical differences were calculated using students t-test (\*P<0.05). (C) TIGKs were either left untreated or infected with *P. gingivalis* as described above with subsequent stimulation with 50 µg/ml Poly I:C (TLR3 agonist), 5 µg/ml ORN06 (TLR7 agonist), 5 µg/ml HSV60 or 25 µg/ml 2'3'-cGAMP (STING agonist) for 18 h. IFN-β levels in cell free supernatants are shown as mean ± SD. (D) OKF6 cells were infected with *P. gingivalis* for 5h at MOI 100. Cells were washed once with PBS to remove non-internalized bacteria and immediately stimulated with 10 µg/ml HSV60 for 18h. IFN-β (white bars) and IFN-λ (green bars) levels (mean ± SD) in cell free

supernatants were measured by ELISA. For C, D, statistical differences were determined by two-way ANOVA (\*\*P<0.01;  $\phi$ P<0.001) with Holm-Sidak multiple comparison test. TIGKs were infected with *P. gingivalis* W83 or the clinical isolate MP4-504 for 5h at MOI 100 (E) or with a combination of (F) *P. gingivalis* 33277 (MOI 100) and *S. gordonii* (MOI 10) with subsequent stimulation with 5  $\mu$ g/ml HSV60 for 18 h. IFN- $\lambda$  levels in cell free supernatants are shown as mean  $\pm$  SD. Statistical differences were determined by one-way ANOVA with Tukey's multiple comparison test ( $\phi$ P<0.001)

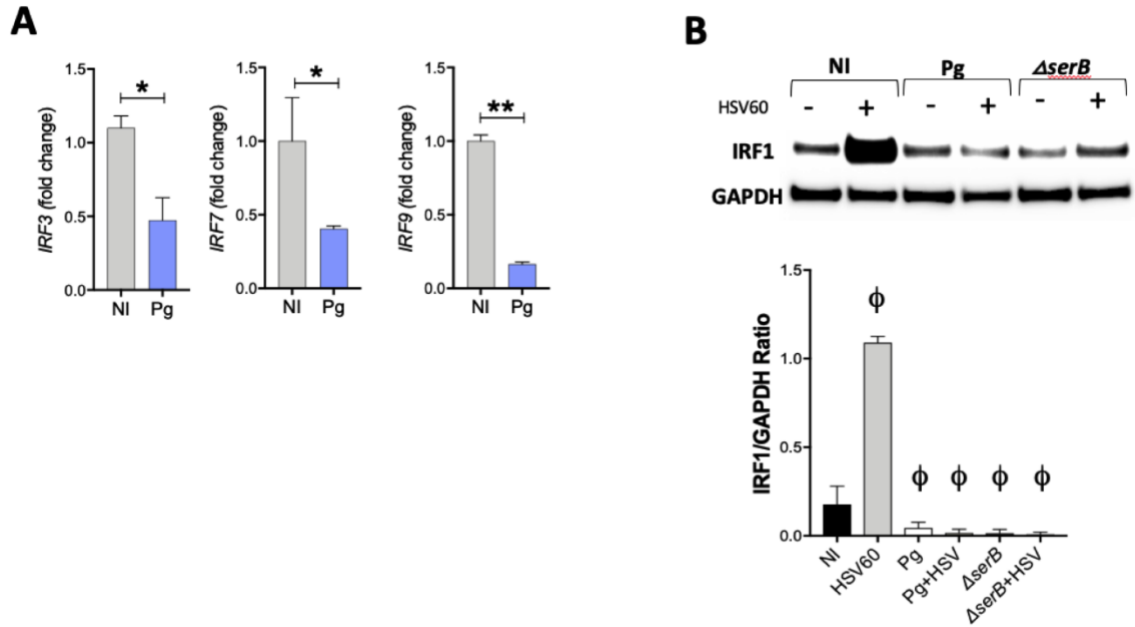


*Supplemental Figure 3.3: Silencing of IRF1 causes suppression of basal ISG expression.* TIGKs were transfected with siIRF1 or scrambled control siRNA for 24 h. Cells were either left non-infected (NI) or stimulated with 5 µg/ml HSV60 for 18h. Volcano plots of differentially expressed transcripts between (A) NI-siIRF1 vs NI-Scrambled control and (B) HSV-siIRF1 vs HSV-scrambled are shown. X-axis shows log-fold change between the two conditions with positive values showing upregulation and negative values showing downregulated genes. Y-axis denotes P values for corresponding genes. Significantly different genes are shown highlighted in red ( $P < 0.05$  as determined using the DESeq package in R). (C) Changes in transcript abundance of select genes from RNA-seq datasets in A, B were confirmed by qRT-PCR, normalized to GAPDH ( $2^{-\Delta\Delta CT}$ ) (blue = SCR-NI; yellow = siIRF1-NI). Data are shown as mean  $\pm$  SD and statistical differences were determined by two-way ANOVA with Holm-Sidak multiple comparison test (\*\* $P < 0.01$ ;  $\phi P < 0.001$ ). (D) TIGKs were transfected with siIRF1 or scrambled control siRNA for 24 h and then stimulated with 5 µg/ml HSV60 with or without *P. gingivalis* infection for 18 h. IFN-I levels in cell free supernatants are shown as mean  $\pm$  SD. Statistical differences were determined by two-way ANOVA with Holm-Sidak multiple comparison test (\*\* $P < 0.01$ ). (E) Hierarchical clustering heatmap (based on log (RPKM) values) of the top 50 IFN stimulated genes (ISGs) under all conditions (siIRF1 Vs scrambled control) are shown. Color intensity denotes level of gene expression.

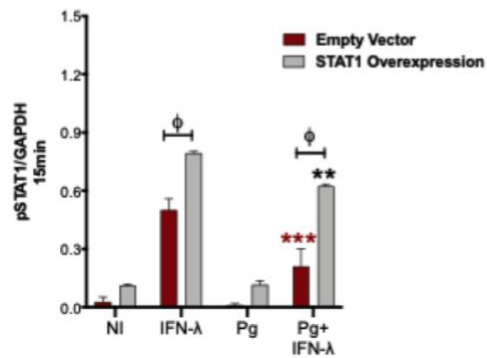
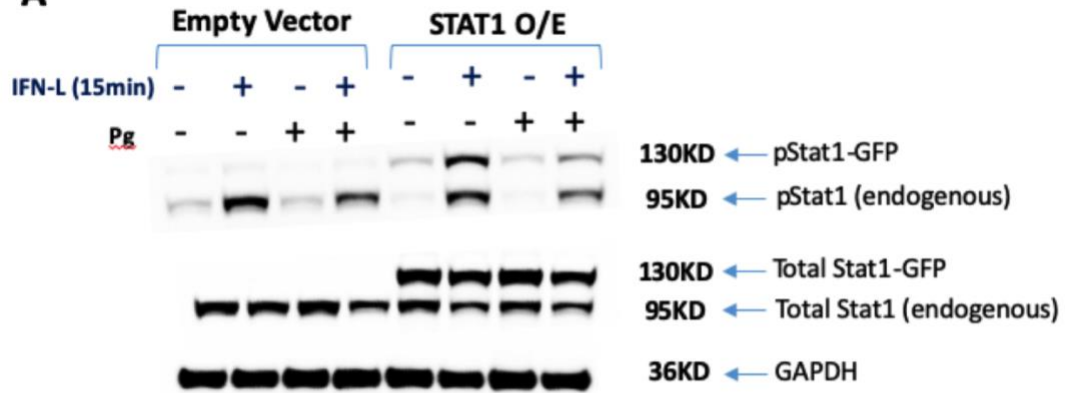
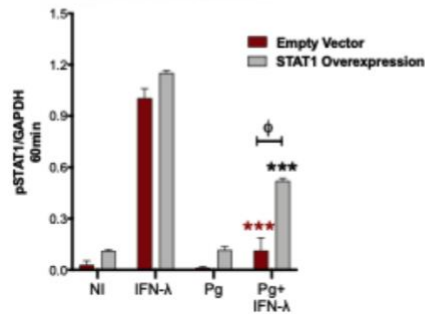
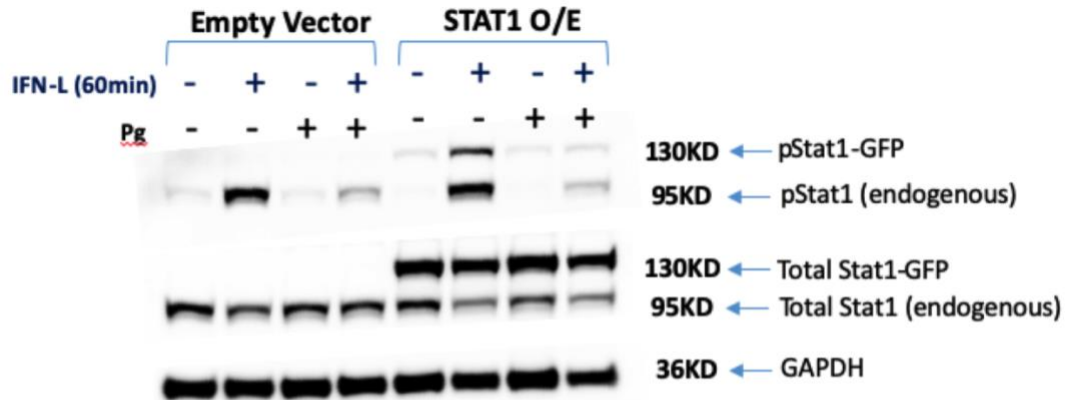




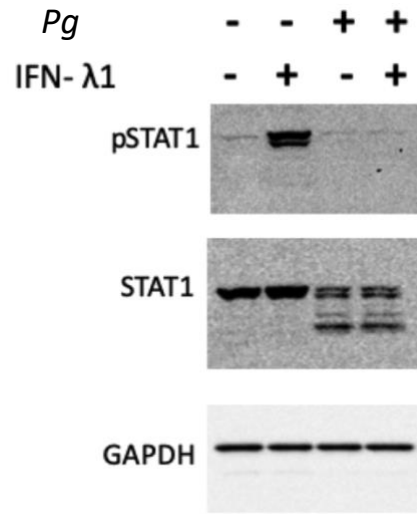
*Supplemental Figure 3.4: Overexpression of IRF1 does not rescue P. gingivalis-dependent suppression of ISGs.* (A) TIGKs were transfected with pCMV-IRF1 overexpression vector (OE) or control empty pCMV vector (EV) and immunoblotted for IRF1, ISG15, MX1, MDA5 and GAPDH after treatment with HSV60 +/- *P. gingivalis*. (B) Band intensities of immunoblots were determined, and ratios of IRF1, ISG15, MX1 and MDA5 to GAPDH from 3 different blots are shown (mean  $\pm$  SD). Statistical differences were determined by two-way ANOVA with Holm-Sidak multiple comparison test ( $\phi$   $P < 0.001$ ).



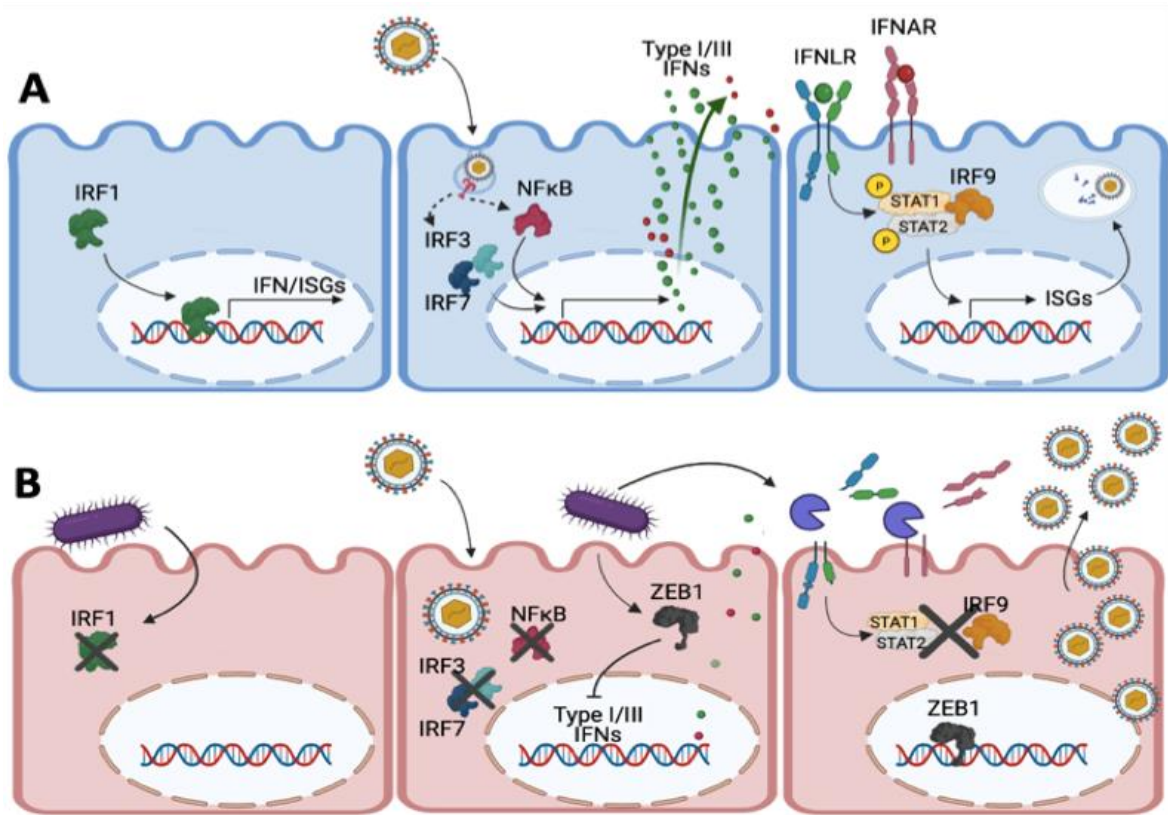
Supplemental Figure 3.5: *P. gingivalis* infection downregulates the expression of members of the IRF family of transcription factors. (A) Transcript levels of *IRF3*, *IRF7* and *IRF9* were determined in unstimulated or *P. gingivalis* challenged TIGKs by qRT-PCR, normalized to GAPDH ( $2^{-\Delta\Delta CT}$ ) and are shown as mean  $\pm$  SD. Statistical differences were determined by student's t-test ( $\phi$   $P < 0.001$ ). (B) TIGKs were infected with *P. gingivalis* WT or SerB deficient isogenic mutant ( $\Delta serB$ ) for 5 h, followed by 5  $\mu$ g/ml HSV DNA for additional 18 h. IRF1 and GAPDH levels were detected by immunoblotting, band intensities were determined and ratios of IRF1 to GAPDH from 3 different blots are shown (mean  $\pm$  SD) in the lower panel. Statistical differences were determined by one-way ANOVA and Tukey's multiple comparison test ( $\phi$   $P < 0.001$ ).

**A****B**

*Supplemental Figure 3.6: Overexpression of STAT1 does not rescue P. gingivalis-dependent suppression of ISGs.* GECs were transfected with STAT1-GFP overexpression plasmid or vector control 24h prior to infection with *P. gingivalis* WT. After 1h of infection, cells were stimulated with 20 ng/ml IFN- $\gamma$  for 15 min (A) and 60 min (B). (A) phospho-STAT1 (pSTAT1) and total STAT1 expression was determined by western blotting. GAPDH was used as the loading control. (B) Band intensities were determined and ratios of pSTAT1 to GAPDH from 3 different blots are shown (mean  $\pm$  SD). Statistical differences were determined at each timepoint by two-way ANOVA (\*\*P<0.05; \*\*\*P<0.01;  $\phi$  P<0.001) ANOVA with Holm-Sidak multiple comparison test. Red and black symbols depict statistical comparisons to the empty vector control and STAT1 overexpression (NI) groups respectively.



*Supplemental Figure 3.7: P. gingivalis degrades STAT1 signaling protein.* A) GECs were infected with *P. gingivalis* MOI 100 for 5 h and stimulated with IFN-λ1 (20 ng/ml) for 5h. Phospho-STAT1 (pSTAT1, total STAT1 and GAPDH expression was determined by western blotting.



Supplemental Figure 3.8: *P. gingivalis* utilizes a multi-hit strategy to suppress IFN signaling in oral epithelium. (A) IRF1 signaling maintains a basal antiviral state in gingival epithelial cells (GECs) via constitutive expression of multiple ISGs. Viral infection in GECs activates several pattern recognition receptors resulting in the preferential induction of Type III IFN that signals via IFN-L receptors to augment ISG expression and antiviral defenses. (B) *P. gingivalis* infection compromises both, constitutive and inducible IFN responses in GECs by degrading or inactivating IFN-inducing transcription factors and cleaving IFN receptors making cells refractory to exogenous IFNs, and inducing a state of broad IFN paralysis. Thus, *P. gingivalis* infection severely compromises anti-viral immunity, providing an early replicative niche for oral viruses.

Table 3.1: Antiviral restriction factors downregulated by *P. gingivalis*

ENSEMBL GENE	GENE SYMBOL	Log2 Fold Change	q_value
ENSG00000183486	<i>MX2</i>	-8.41016	0.001087
ENSG00000137959	<i>IFI44L</i>	-6.85783	0.001087
ENSG00000134321	<i>RSAD2</i>	-6.63744	0.001087
ENSG00000187608	<i>ISG15</i>	-5.87784	0.001087
ENSG00000185885	<i>IFITM1</i>	-4.99342	0.001087
ENSG00000185745	<i>IFIT1</i>	-4.97384	0.001087
ENSG00000138135	<i>CH25H</i>	-4.77437	0.001087
ENSG00000157601	<i>MX1</i>	-4.63737	0.001087
ENSG00000126709	<i>IFI6</i>	-4.57048	0.001087
ENSG00000137965	<i>IFI44</i>	-4.56653	0.001087
ENSG00000119917	<i>IFIT3</i>	-4.06795	0.001087
ENSG00000165949	<i>IFI27</i>	-4.06526	0.001087
ENSG00000185201	<i>IFITM2</i>	-3.94771	0.024228
ENSG00000068079	<i>IFI35</i>	-3.86895	0.001087
ENSG00000111335	<i>OAS2</i>	-3.74836	0.001087
ENSG00000135114	<i>OASL</i>	-3.66909	0.001087
ENSG00000119922	<i>IFIT2</i>	-3.64383	0.002842

## CHAPTER 4:

### BACTERIAL-VIRAL RIVARLY: INVESTIGATING THE RELATIONSHIP BETWEEN PORPHYROMONAS GINGIVALIS AND RESPIRATORY SYNCYTIAL VIRUS IN MUCOSAL DEFENSE

#### 4.1. Introduction

Oral inflammation is now a well-accepted risk factor for several co-morbidities, including chronic inflammatory and autoimmune diseases and cancers [195]. A unifying disease-driving factor linking these diverse sets of disorders is the immune dysregulation caused by periodontal bacterial pathogens residing in dysbiotic oral communities. Of relevance to this chapter are the associations of *P. gingivalis* with exacerbating susceptibility to respiratory diseases.

Recent evidence suggests that oral bacteria can translocate to sites distant from the oral cavity, such as the airways [196-198]. Translocation is facilitated via swallowing, aspiration, or the hematogenous route. *P. gingivalis* has been found in significantly higher numbers in the lung aspirates of patients with aspiration pneumonia, tracheal aspirates of patients with COPD, bronchial alveolar lavage fluid (BALF) of patients with emphysema, and also in several types of lung cancers [190, 199]. Recent studies have also shown that periodontitis can be a risk factor for worse outcomes in respiratory viral infections such as SARS-CoV-2 and



influenza [200, 201]. We previously showed that *P. gingivalis* can suppress epithelial IFN responses anti-viral immunity (Chapter 3 and [135]). We hypothesize that this inhibitory effect on IFN signaling is not confined to the oral epithelium and extends to the respiratory epithelium, enhancing susceptibility to respiratory viruses.

To investigate this, we utilized an in vitro model of Respiratory Syncytial Virus (RSV) infection. RSV infections are a significant health concern in pediatric populations and also in older adults, who also have a higher prevalence of periodontitis [202, 203]. Furthermore, RSV infection triggers the induction of type I and type III IFNs crucial for antiviral defenses [204]. Thus, we investigated whether *P. gingivalis*, a periodontitis associated pathogen, might modulate the host immune response during RSV infection by inhibiting IFN signaling.

#### 4.2. Materials and Methods:

##### *Bacteria.*

*P. gingivalis* 33277 was cultured in trypticase soy broth (TSB) supplemented with hemin (5 µg/mL) and menadione (1 µg/mL) and 1 mg/mL yeast extract. Isogenic mutants were cultured in supplemented TSB with the appropriate antibiotics: major fimbriae mutant ( $\Delta$ fimA)[205] had 10µg/ml erythromycin while the triple gingipain-null mutant ( $\Delta$ kgp $\Delta$ rgpA $\Delta$ rgpB or abbreviated as:  $\Delta$ KRAB)[190] had 10 µg/mL erythromycin, 1 µg/mL tetracycline, and 20 µg/mL chloramphenicol [90]. All strains were grown anaerobically (85% N<sub>2</sub>, 10% H<sub>2</sub>, and 5% CO<sub>2</sub>) at 37 °C.

### *Cell lines Culture.*

A549 human alveolar basal epithelial cell line was cultured in Kaighn's Modification on Ham's F12 medium supplemented with 10% heat inactivated fetal bovine serum (FBS), while the HEP-2 laryngeal cancer cell line was cultured in Eagle's Minimum Essential Medium (EMEM) supplemented with 10% FBS. HEP-2 cell line was cultured in Dubelcco's Modified Eagle's Medium (DMEM) supplemented with 10% FBS. All cultures were grown at 37 °C and 5% CO<sub>2</sub>.

### *Primary well differentiated human bronchial epithelial cultures (HBE)*

HBE progenitors were isolated from donor airways as described previously, grown for a week to confluency and frozen for later use as described [206]. Briefly, progenitor cells were thawed and plated on 0.4 µm pore Transwells (Corning) membranes, 6.5 mm or 12 mm in diameter, fed with ALI medium supplemented with ROCK inhibitor in both the apical and basolateral chambers. Medium in both chambers was replaced with fresh medium every 2–3 days. At 7 days, when the cells were confluent and had formed tight junctions as demonstrated by electrical resistance, the apical medium was removed, and the basal medium was replaced with complete Pneumacult-ALI Medium (STEMCELL Technologies). The medium was replaced with fresh medium, and the apical surface was washed with 100 µL of DMEM every 2–3 days for 3 weeks by which time they had become fully differentiated.

### *Virus production.*

Recombinant GFP-expressing rgRSV224 is based on the A2 laboratory strain of RSV [207]. RSV stocks were grown in HEp-2 cells in DMEM-10% FBS. GFP expressing viruses were serially diluted and titrated on HEp-2 cells by inoculating for 2 h at 37°C and counting GFP foci at 24 hpi.

### *Histology.*

At 48h post infection HBE cultures were fixed with 4% paraformaldehyde for 15min and then transferred to PBS for storage. Tissues were submitted to the Morphology Core at the Abigail Wexner Research center where they were embedded in paraffin, sectioned to 5µm and stained with hematoxylin are eosin.

### *qPCR.*

Total RNA was extracted using the RNAeasy kit (Qiagen) and converted to cDNA using the high-capacity cDNA reverse transcription kit (ThermoFisher). Transcript expression was determined by TaqMan assays using TaqMan mastermix. All prevalidated primer sets and probes were purchased from ThermoFisher. Virus copy number was determined using a standard curve of Quantitative Genomic RNA from human RSV strain A2 (ATCC) after converted to cDNA using the high-capacity cDNA reverse transcription kit (ThermoFisher). Viral quantitative PCR was performed using the Power SYBR Green PCR Master Mix (ThermoFisher) with primers designed to target the nucleocapsid gene. Forward primer: 5'-

GGGAGAGGTAGCTCCAGAATA-3', and reverse primer sequence: 5'-CTCCTAA TCACGGCTGTAAGAC-3'.

#### *ELISA.*

IFN- $\lambda$  (IL-29 and IL-28) ELISA kit was from R&D. Cytokine levels were measured in cell-free supernatants as per the manufacturer's instructions. OD was measured at 450 nm.

#### *RNA-seq.*

RNA was extracted using the RNeasy Mini RNA Isolation kit (QIAGEN). RNA-seq was done at Novogene at a depth of 50,000 paired end reads. Messenger RNA was purified from total RNA using poly-T oligo-attached magnetic beads. After fragmentation, the first strand cDNA was synthesized using random hexamer primers followed by the second strand cDNA synthesis. The library was ready after end repair, A-tailing, adapter ligation, size selection, amplification, and purification. The library was checked with Qubit and real-time PCR for quantification and bioanalyzer for size distribution detection. Quantified libraries will be pooled and sequenced on Illumina platforms, according to effective library concentration and data amount. For the analysis of differentially expressed genes, demultiplexed paired-end fastq files were aligned to reference GRCh38 by top-level assembly with STAR (version 2.6.1). Gene counts were produced by RSEM (version 1.3.1). We used DESeq2 R/Bioconductor package to obtain differential expression between NI\_UT vs. Pg\_UT; NI\_UT vs. NI\_IFN and Pg\_UT vs. Pg\_IFN ( $n = 5$  per

sample). DESeq2 guidelines were used to identify differentially expressed genes, and all *P* values were adjusted for testing multiple genes (Benjamini–Hochberg procedure, alpha = 0.1). For gene set enrichment analysis, we used fgsea Multilevel function from fgsea R/Bioconductor package (<https://doi.org/10.1101/060012>).

### *Statistics.*

Statistical analyses utilized GraphPad Prism 6.0 (GraphPad). A *P* value <0.05 was considered statistically significant. A detailed description of the statistical tests used is stated in each figure legend.

## 4.3. Results

### *P. gingivalis inhibits IFN responses in airway epithelial cells*

We first determined if *P. gingivalis* inhibited IFN signaling pathways in airway epithelial cells. To test this, we co-challenged the airway epithelial cell line A549 with PolyI:C-LyoVec and *P. gingivalis* and determined IFN- $\lambda$  levels by ELISA. Similar to our observations in GECs, *P. gingivalis* infection suppressed IFN- $\lambda$  production in response in the airway epithelium (Fig. 4.1A). Next, we profiled broad transcriptional responses to *P. gingivalis* infection in A549 cells in naïve and IFN- $\lambda$  primed A549 cells. We found that *P. gingivalis* infection alone led to a modest decrease in ISG expression compared to naïve, uninfected A549 cells which was unlike what we observed in GECs (Fig. 4.1A). This was probably related to a lower basal expression of ISGs in A549 cell, which unlike GECs is a transformed

oncogenic cell line. In order to test if *P. gingivalis* was able to dampen ISG expression in cells that expressed ISGs, we primed A549 cells overnight with IFN- $\lambda$  to induce ISG expression and then challenged them with *P. gingivalis* the next day. RNA-seq analysis showed a robust decrease in ISG expression in IFN- $\lambda$  primed cells, indicating that *P. gingivalis* infection can effectively dampen antiviral immunity in the airway epithelial cells (Fig. 4.1B-C).

#### *P. gingivalis* protects HBE cultures against RSV while inhibiting IFN

Next, we determined the impact of *P. gingivalis* mediated suppression of IFN signaling in enhancing susceptibility to RSV infection. We used a model of air-liquid interface cultures of human bronchial epithelial cells (HBE) to test this. Well-differentiated HBE cultures are more representative of the lung microenvironment as these cultures contain ciliated epithelial cells, basal cells, and goblet cells that naturally produce mucus. Moreover, these cultures also have a ciliary beat that is pivotal in airway function and results in syncytia formation during RSV infections that are consistent with the cytopathic effects seen in RSV infections in human lungs [208]. We first infected HBE cultures for 4h *P. gingivalis*, followed by a 2 h challenge with RSV. RSV replication was assessed by measuring green fluorescent protein (GFP) fluorescence in infected wells at 24 and 48 hours post-viral infection (Fig. 4.2A). Similar to our observations in the A549 monolayers, *P. gingivalis* infection resulted in a potent downregulation of IFN- $\lambda$  production in the apical and basal media in HBE transwells (Fig. 4.2B) that correlated with reduced ISG induction (Fig. 4.2C). Since RSV replication and pathogenesis is strongly

restricted by IFN signaling [209], we expected to see higher replication of RSV in wells co-infected with *P. gingivalis*, where IFN- $\lambda$  was absent. However, we found the opposite. RSV replication was significantly less in wells co-infected with *P. gingivalis*, as measured by GFP fluorescence at 24 and 48 h (Fig. 4.2D). In this model, GFP fluorescence at 24 h allows for the quantification of the initial infection round, where groups of infected cells form individual foci. The reduction in infectivity at 24 h indicated that *P. gingivalis* was possibly interfering with RSV's ability to infect cells. At 48 h, we do not see individual foci as the virus replicates and spreads from cell to cell. Instead, we measured GFP mean fluorescent intensity (MFI) and genome copy numbers by qPCR. At 48 h, despite the reduced IFN- $\lambda$  and ISG expression (Fig. 4.2B and C), RSV replication was significantly lower in *P. gingivalis* infected groups (Fig. 4.2F and G).

RSV is an IFN-restricted virus, as indicated by the significant reduction in RSV growth in IFN- $\lambda$ -primed HBE cultures (Fig. 4.3A-D) and, conversely, increased replication in HBE cell pre-treated with a STAT1/2 inhibitor, ruxolitinib (RUX) that would abrogate IFN mediated activation of ISGs (Fig. 4.3A-D). However, RSV replication and initial infection were significantly dampened by *P. gingivalis* in an IFN-depleted microenvironment, which should have been permissive for RSV growth (Fig. 4.3A-D). Thus, we hypothesized that perhaps *P. gingivalis* blocked RSV infection independent of IFN-signaling. H&E staining of HBE cultures showed no overt cytopathic effects in *P. gingivalis* infected wells (Fig. 4.4). In comparison, RSV infected well showed signs of stress characterized by vacuolation and invagination of HBE multi-cellular layers. However, these were

absent on *Pg*-RSV infected wells (Fig. 4.4). Since we did not observe any adverse effects of *P. gingivalis* on HBE layers, we focused our attention on *P. gingivalis* virulence factors that could interfere with viral infection.

We have previously shown that gingipain activity is essential for the enforcement of IFN paralysis in GEC by the proteolytic cleavage of IFN receptors. Gingipains are well known to have a voracious appetite, cleaving multiple proteinaceous substrates such as cellular receptors, extracellular matrix proteins, cytokines, etc. We first determined if gingipain activity negatively impacted RSV infection, possibly by proteolytically inactivating the virus. HBE cultures were coinfecting with the wildtype, or mutant strains of *P. gingivalis* lacking all three gingipains  $\Delta rgpa$ ,  $\Delta rgpb$ ,  $\Delta kgp$  strain abbreviated as  $\Delta KRAB$ ) [190]. We also used the  $\Delta fimA$  mutant that lacks the major fimbriae but gingipain expression is unaffected. Interestingly, despite the lack of key virulence factors, *P. gingivalis* was still able to significantly reduce IFN- $\lambda$  production in HBE cells (Fig. 4.5A). We found that while the wildtype *P. gingivalis* inhibited RSV infection, RSV replication in cells coinfecting with  $\Delta KRAB$  was comparable to the RSV alone group (Fig. 4.5C-E). This indicated that gingipains were essential in mediating the inhibitory effect of *P. gingivalis* on RSV.

Next, we determined whether gingipains inactivated the RSV by cleaving and stripping its surface of critical attachment proteins essential for entry into host cells. Preincubating RSV with RgpB resulted in a precipitous drop of RSV infectivity within 5 minutes of co-incubation (Fig. 4.5F). Thus, our data show that gingipain impaired RSV's infectious capacity.



#### 4.4. Discussion

In the intricate landscape of host-pathogen interactions, the impact of *P. gingivalis* on RSV infection emerges as a multifaceted interplay with profound implications. The air-liquid interface cultures of bronchial epithelium exposed to *P. gingivalis* prior to RSV infection displayed a remarkable suppression of viral replication as measured by reduced GFP expression, fluorescent foci, MFI, and viral genome copies, indicative of its potent interference with the viral life cycle. Notably, RSV inhibition occurred despite *P. gingivalis*' ability to suppress the production of IFN- $\lambda$  and other ISGs. Our findings present a remarkable case where we identify a bacterium capable of dual functionality: inhibiting viral infection while concurrently suppressing the host's IFNs antiviral responses. This novel revelation adds a layer of complexity to our understanding of bacteria-virus interactions. Notably, the existing body of research has shown a spectrum of varied interactions between eukaryotic viruses and bacteria, ranging from symbiotic relationships [210] to antagonistic interactions [211, 212]. Our study contributes to this knowledge by introducing a bacterium that disrupts viral replication while modulating the host's immune response, highlighting the intricate and diverse nature of these interactions.

We hypothesize that *P. gingivalis* may safeguard the airway epithelium by inactivating RSV viral particles, potentially through the action of gingipains. In the context of RSV, it is plausible that gingipains may act on viral envelope proteins, essential for the virus's entry into host cells. By cleaving or modifying these viral

envelope proteins, gingipains could disrupt the fusion process between the virus and the host cell membrane, thereby preventing viral entry and subsequent infection. This interference at the initial stages of the viral life cycle could contribute significantly to the observed reduction in viral replication. Furthermore, gingipains may also exert their effects intracellularly. Once inside the host cell, RSV undergoes replication and assembly processes that involve the synthesis and processing of viral proteins. Gingipains, with their proteolytic capabilities, could potentially interfere with these intracellular processes. By cleaving viral proteins crucial for replication or assembly, gingipains might hinder the production of functional viral progeny, leading to a reduced overall viral load. Understanding the intricate molecular interactions between gingipains and RSV requires targeted experiments and analyses. Techniques such as mass spectrometry, co-immunoprecipitation assays, and proteomic approaches could be employed to identify specific protein targets of gingipains within the context of RSV-infected cells. While our study supports this hypothesis, we acknowledge that there may be additional pathways at play that we have yet to explore. For instance, RSV receptor (CX3CR1) downregulation represents a potential mechanism that could contribute to the observed protection, and further experiments are warranted to investigate this alternative pathway comprehensively.

In summary, the protective effects of *P. gingivalis* against RSV could open avenues for innovative therapeutic strategies in the management of respiratory infections. By leveraging the insights gained from this research, researchers and

clinicians can explore tailored approaches to enhance antiviral defenses, modulate the immune response, and promote respiratory health in a targeted manner.

#### 4.5. Figures:

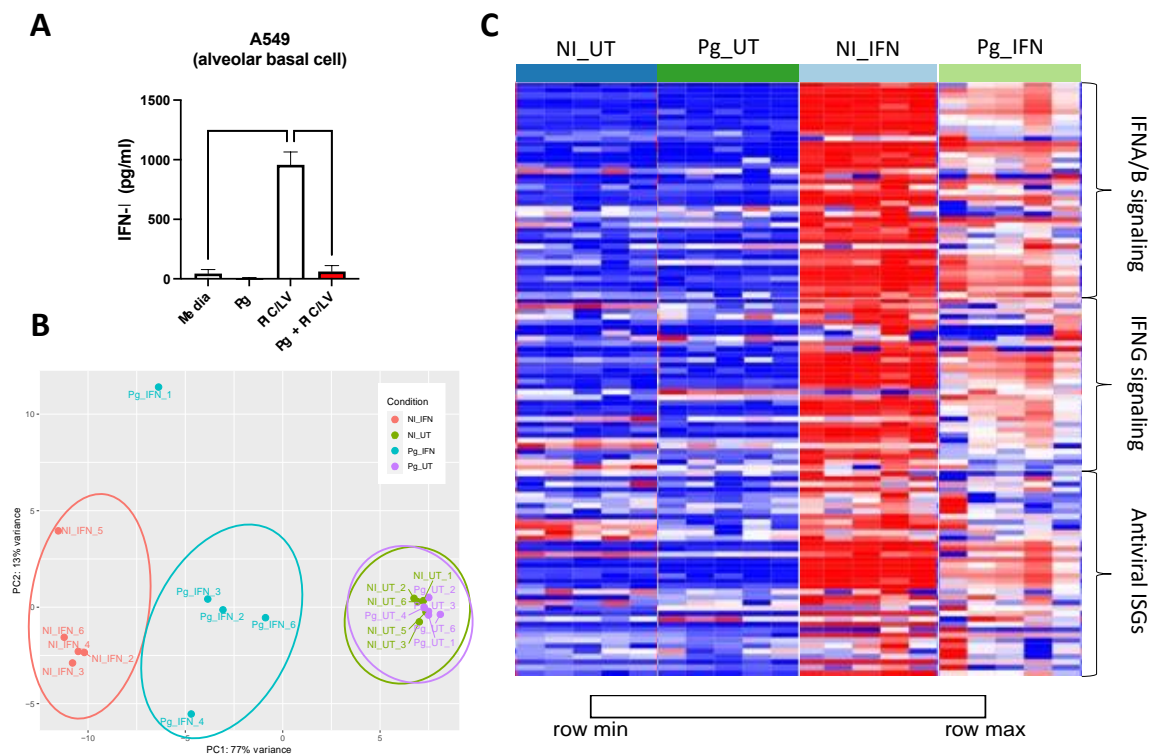


**Figure 4.1. *P. gingivalis* inhibits IFN responses in airway epithelium**

(A) IFN-λ responses were measured by ELISA in A549s challenged either with *P. gingivalis* at MOI 100 for 4h, washed once with PBS, and then stimulated with 500 ng/mL Poly I:C/LyoVec LMW for additional 18 h. IFN-λ levels in cell-free supernatants are shown as mean ± SD. Statistical differences were determined by two-way ANOVA with Tukey's multiple comparison test (\*\* $p < 0.005$ ; \*\*\*\* $p < 0.0001$ ). IFN responses were measured in A549 either primed with 20ng/ml IFN-λ or unstimulated, followed by *P. gingivalis* infection (MOI100) for 4h. Transcripts were harvested at 24h post-infection. (B) The PCA plot depicts the clustering patterns of RNAseq data obtained from distinct cellular stimulations. Each point represents the transcriptional profile of individual samples categorized into four groups: untreated cells (NI\_UT), IFN-primed cells (NI\_IFN), *P. gingivalis*-infected cells

(Pg\_UT), and IFN-primed *P. gingivalis*-infected cells (Pg\_IFN). (C) Gene enrichment analysis of top 300 down-regulated genes was performed as described in Materials and Methods, and hierarchical clustering heatmaps (based on RPKM values) for IFNA/B signaling, IFNG signaling and antiviral ISGs pathways are shown. Color intensity denotes level of gene expression.

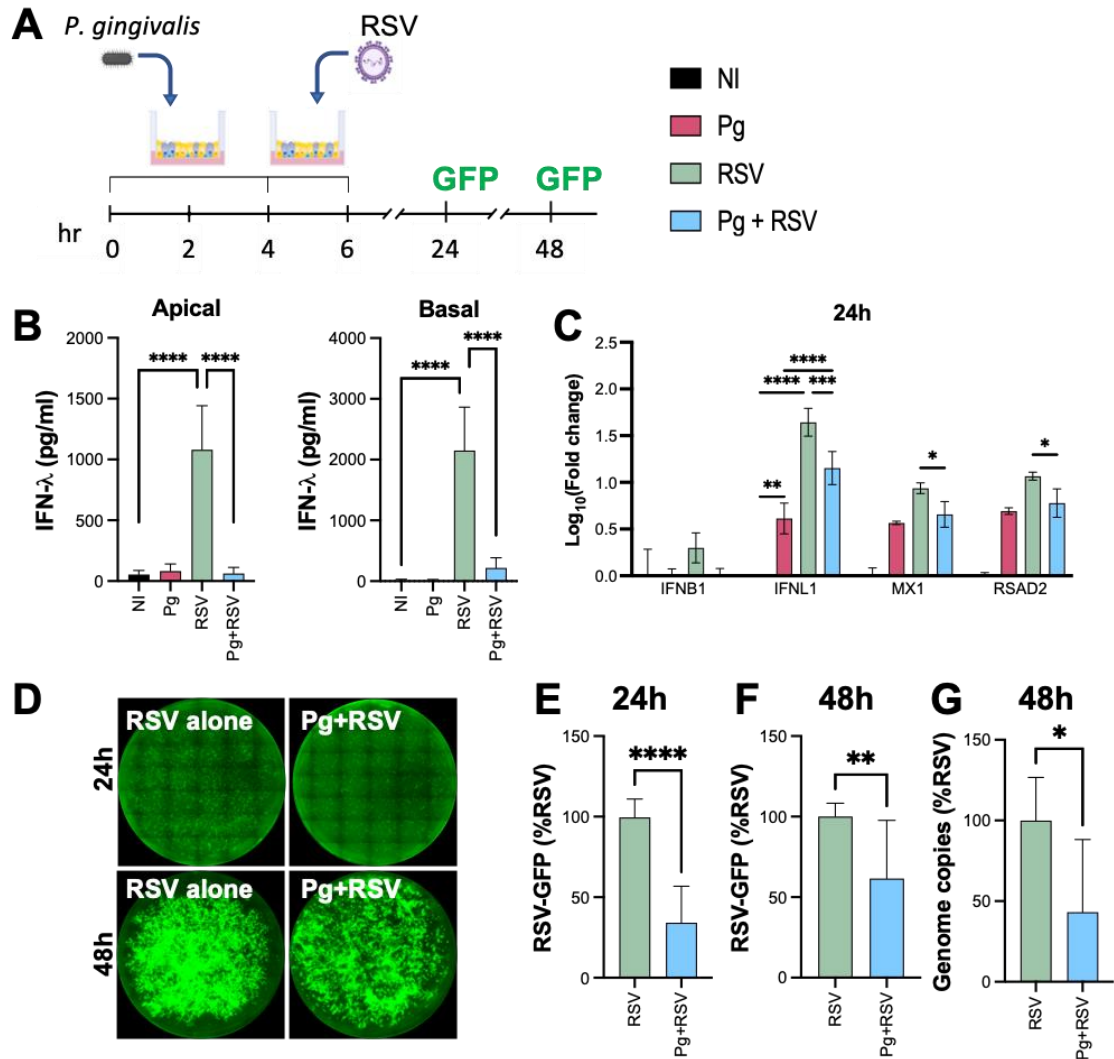


**Figure 4.2.** *P. gingivalis* protects HBE cultures against RSV while inhibiting IFN

Human bronchial epithelial (HBE) cultures were first exposed to *P. gingivalis* (MOI100) for 4 hours and then infected with RSV (1321PFU) for an additional 2 hours, as outlined in (A). IFN- $\lambda$  expression was measured by enzyme-linked immunosorbent assay (ELISA) at the apical (B) and basal (C) surfaces. Data is shown as mean  $\pm$  SD. Statistical differences were determined by One-way ANOVA with Sidak's multiple comparison test (\*\*\*\* $<0.0001$ ). The expression of ISGs was assessed by qPCR at 24h (C) post infection. Data is shown as mean  $\pm$  SD. Statistical differences were determined by two-way ANOVA with Tukey's

multiple comparison test (\* $p < 0.05$ ; \*\* $p < 0.005$ ; \*\*\* $p, 0.0005$ \*\*\*\* $< 0.0001$ ). The EVOS microscope captured representative images of RSV-GFP expression (D). ImageJ software facilitated the quantification of initial infection (fluorescent foci) at 24 hours (E) and replication (MFI) was calculated at 48 hours (F) post-infection. Genome copy number of RSV was determined by qPCR at 48 hours post-infection (G). Data is shown as mean  $\pm$  SD. Statistical differences were determined by Unpaired t test (\* $p < 0.05$ ; \*\* $p < 0.005$ ; \*\*\*\* $< 0.0001$ ). All measurements were conducted on cells subjected to the sequential treatment described in panel A.

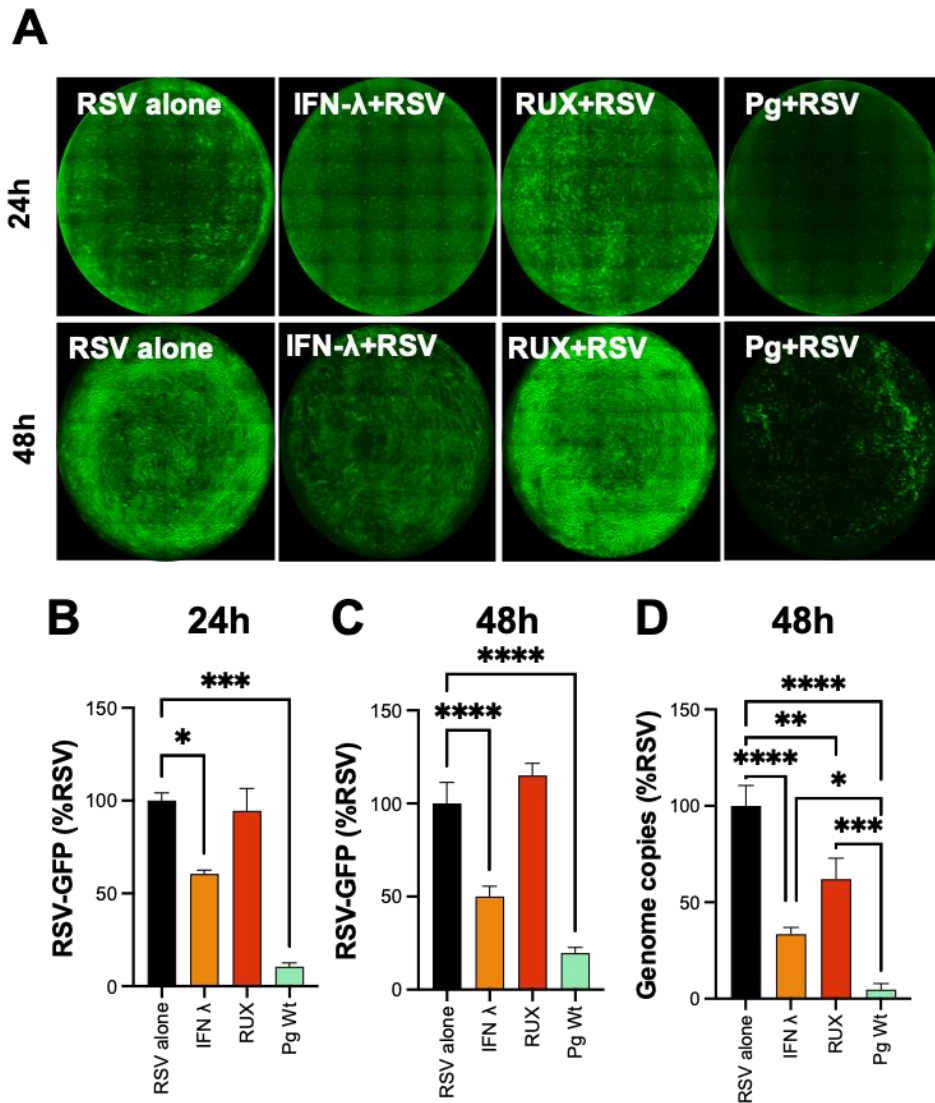
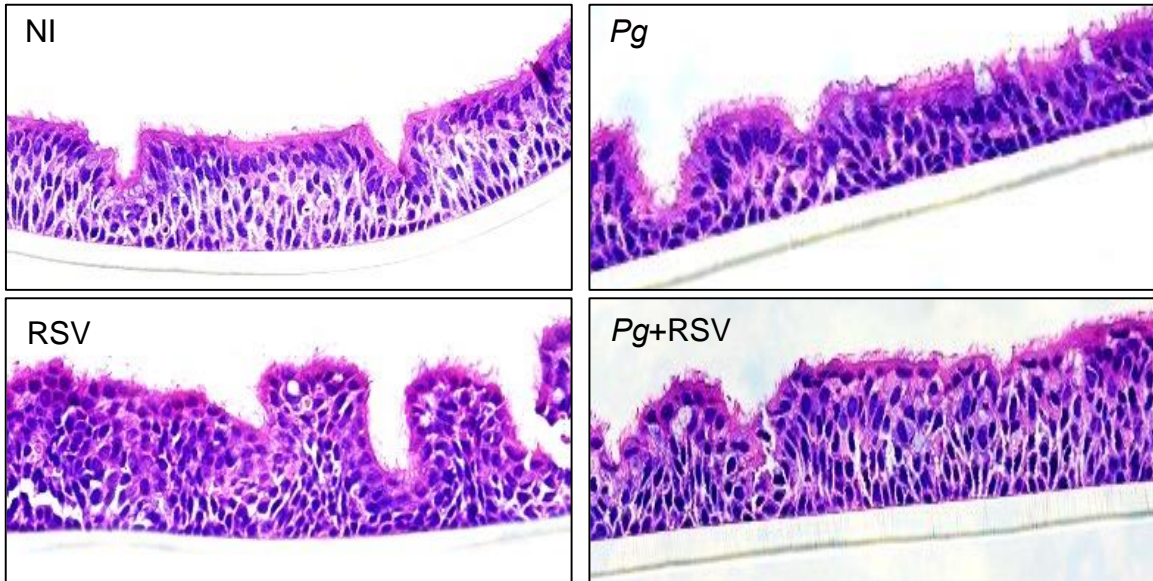


Figure 4.3. *P. gingivalis* protection of HBE cultures against RSV is independent of IFN suppression.

HBE cultures were either primed or left untreated with IFN- $\lambda$  for 24 hours before being infected with *P. gingivalis* (MOI100) for 4 hours, followed by a 2-hour infection with RSV (1321 PFU), and GFP measurements at 24- and 48-hours post-infection. Concurrently, during *P. gingivalis* infection, Ruxolitinib (RUX) was added to the basal media and left for the rest of the experiment. A representative image of RSV-GFP expression was captured



using the EVOS microscope (A). ImageJ software facilitated the quantification of initial infection (B) and replication (C) at 24 and 48 hours post-viral infection, respectively. Data is shown as mean  $\pm$  SD. Statistical differences were determined by One-way ANOVA with Sidak's multiple comparison test (\* $p < 0.05$ ; \*\*\* $p, 0.0005$ ; \*\*\*\* $< 0.0001$ ). RSV genome copy number was determined by qPCR (D). Data is shown as mean  $\pm$  SD. Statistical differences were determined by One-way ANOVA with Tukey's multiple comparison test (\* $p < 0.05$ ; \*\* $p < 0.005$ ; \*\*\* $p, 0.0005$ ; \*\*\*\* $< 0.0001$ ).



*Figure 4.4. Loss of RSV infection in P. gingivalis infected HBE cultures is not due to loss of tissue integrity*

HBE cultures were first exposed to *P. gingivalis* for 4 hours and then infected with RSV for an additional 2 hours, as outlined in Fig. 4.2A. Representative images of sections of HBE cultures at 48h post infection stained with H&E and imaged with a light microscope (40x magnification).

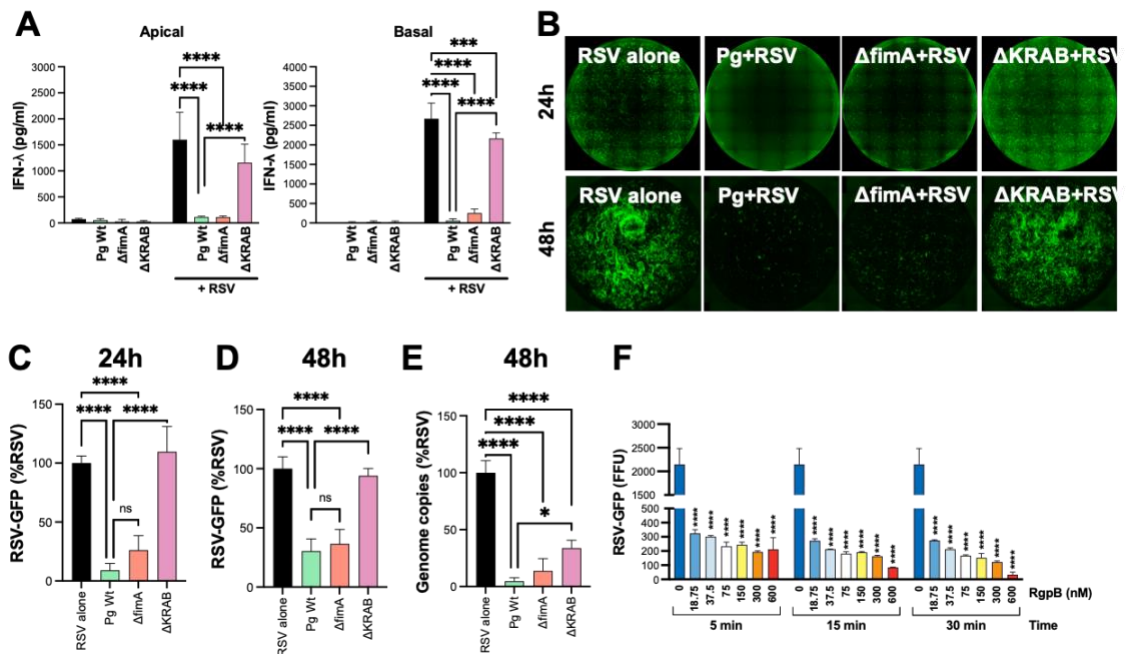


**Figure 4.5. Impact of *P. gingivalis* and Gingipains on RSV Infection**

HBE cultures were infected with different strains of *P. gingivalis* (wild type, fimA mutant, or KRAB mutant) (MOI100) for 4 hours, followed by a 2-hour infection with RSV (1321 PFU), with GFP measurements at 24- and 48-hours post-infection. IFN $\lambda$  expression was measured by ELISA at the apical and basal surfaces (A). Data is shown as mean  $\pm$  SD. Statistical differences were determined by Two-way ANOVA with Sidak's multiple comparison test (\*\* $p < 0.0005$ ; \*\*\*\* $p < 0.0001$ ). A representative image of RSV-GFP expression was captured using the EVOS microscope (B). ImageJ software facilitated the quantification of initial infection (C) and replication (D) at 24 and 48 hours post-viral infection, respectively. RSV genome copy number was determined by qPCR (E). Data is shown as mean  $\pm$  SD. Statistical differences were determined by One-way ANOVA with Sidak's multiple comparison test (\* $p < 0.05$ ; \*\*\* $p < 0.0005$ ; \*\*\*\* $p < 0.0001$ ). To assess the impact of gingipains on RSV infectivity, RSV particles were treated with different

concentrations of gingipains for varying durations before infecting HEp-2 cells, and fluorescent cells were quantified at 24 hours post-infection (F). Data is shown as mean  $\pm$  SD. Statistical differences were determined by comparing to the untreated particles ([RgpB]=0nM) using two-way ANOVA with Dunnetts multiple comparison test (\*\*\*\*<0.0001).

## CHAPTER 5: SUMMARY AND FUTURE DIRECTIONS

My laboratory, along with Dr. Lamont's laboratory, co-discovered IFN- $\lambda$  as the predominant interferon produced by oral epithelial cells in the oral cavity. I explored the factors that modulate IFN- $\lambda$  expression at the oral mucosal barriers and delineated the role for IFN- $\lambda$  in regulating epithelial responses to viral infection. Furthermore, I extended this work to show how oral microbial dysbiosis susceptibility to viral infections in the oral and respiratory epithelium.

IFN- $\lambda$  has potent antiviral activity and serves as a key mediator of host defense against viral infections at various barrier surfaces such as the gastrointestinal and respiratory tracts, blood-brain barrier and skin [77, 79, 213, 214]. My first discovery was showing that similar to other mucosal barriers, IFN- $\lambda$  was the dominant IFN induced produced downstream of multiple PRR in the oral cavity. Furthermore, I showed that IFNL-R are expressed in various oral epithelial cells, keratinocytes, fibroblasts and respond to secreted IFN- $\lambda$  by activating a large number of ISGs that were involved in downstream priming and recruitment of immune cells and directly restraining viral replication.

IFN- $\lambda$  distinguishes itself from Type I and Type II IFNs and is particularly suited for orchestrating potent antiviral defense at various mucosal surfaces without inducing damaging inflammation that would compromise barrier integrity. Unlike type I IFNs, IFN- $\lambda$  triggers a more localized and finely tuned immune response, crucial for combating viral threats while minimizing excessive

inflammation and tissue damage [76]. For example, Broggi et al. showed that IFN- $\lambda$  transcriptionally downregulated inflammatory genes in neutrophils limiting intestinal damage during infection with enteric viruses. Specially, neutrophil priming with IFN- $\lambda$  dampened NADPH oxidase activity and the generation of reactive oxygen species as well as degranulation responses [76]. Neutrophils are essential for oral mucosal tissues homeostasis and are found in high numbers in oral tissues even in the absence of inflammation [215]. It would be interesting to test whether IFN- $\lambda$  generation by epithelial cells was essential for regulating neutrophil responses or oral biofilm bacteria in the oral cavity. I hypothesize that IFN- $\lambda$  could help to minimize inflammatory damage to oral bacteria while still effectively combating viral infections, thus maintaining a delicate balance between immune defense and tissue homeostasis in the oral mucosa.

In addition to elucidating the preferential production of IFN- $\lambda$  in the oral cavity, my research uncovered a significant finding regarding oral dysbiosis, bacterial pathogens, and antiviral immunity and how they intersect. Specifically, we observed that epithelial cells derived from patients with periodontitis displayed a hypo-responsive state when exposed to viral stimuli. This was particularly interesting as periodontitis is an inflammatory disease where interferons can be available from other recruited immune cells. We re-analyzed data from a single cell RNA-seq dataset which was recently published [19] and found that epithelial cell and fibroblasts within the sc-RNA-seq data showed a dampened interferon signature even while exhibiting a statistically significant increase in genes associated with NF- $\kappa$ B, TNF and other inflammatory pathways. Thus our findings

are clinically relevant and might shed insights into how dysbiotic microbial communities associated with periodontitis facilitate the persistence and/or proliferation of viral pathogens.

I found that *P. gingivalis* has the unique ability to suppress IFN responses in oral epithelium. This inhibition occurs at multiple stages, including the downregulation of IRF1 in the basal response, modulation of various factors in the inducible response (such as downregulation of IRFs, inactivation of NF- $\kappa$ B, and upregulation of ZEB1), and the proteolytic degradation of IFN receptors and cytokines. The proteolytic degradation of IFN receptors by *P. gingivalis* renders the cells insensitive to IFN signaling, making them refractory to the antiviral actions of these cytokines, even if they are produced by other cells or administered exogenously as a treatment. As a result, the ability of IFNs to induce an antiviral state and combat viral infections is severely compromised in the presence of *P. gingivalis*-mediated degradation of IFN receptors. These findings highlight the sophisticated strategies employed by *P. gingivalis* to subvert the host's innate immune defenses at different levels, contributing to a comprehensive understanding of the dynamics between oral pathogens and the antiviral immune response.

This study extends the understanding of *P. gingivalis* beyond the oral epithelium, demonstrating its ability to inhibit IFN responses in the airway epithelium, in a similar manner. The decision to investigate the respiratory mucosa stemmed from the recognition of the oral cavity as a potential reservoir for pathogens and immune dysregulation that could impact distant mucosal surfaces

like the respiratory tract. Given the proximity and shared anatomical connections between the oral and respiratory mucosa, exploring the effects of oral pathogens on respiratory immune responses became a crucial aspect of understanding mucosal immunity comprehensively. Transmission of oral bacteria to the airway is supported by data from clinical microbiome sampling studies, indicating at least a transient presence of oral microbes at other mucosae [216]. Thus oral pathogens may impact respiratory immune responses and disease outcomes. By examining the interactions between oral pathogens, such as *P. gingivalis*, and the respiratory mucosa, we aimed to elucidate how dysbiotic conditions in the oral cavity could influence immune responses and susceptibility to respiratory infections. However, while we were able to show the IFN suppressing activity of *P. gingivalis* in a co-challenge model, we were surprised to see that *P. gingivalis* infected airway epithelial cells were somewhat protected from RSV infection. This protection appears to be mediated by gingipains, which play a crucial role by inactivating viral particles. Importantly, the protective effect of *P. gingivalis* against RSV appears to be independent of IFN, emphasizing a distinct pathway through which *P. gingivalis* modulates the host response to viral infections in the airway epithelium.

The contrasting effects of *P. gingivalis* in promoting viral infection in the oral epithelium while exerting a protective role in the airway can be attributed to the complex interplay of host-pathogen interactions within distinct anatomical environments. While both epithelia serve protective roles, the oral epithelium is adapted for the varied functions associated with the oral cavity, including sensory



perception and mechanical protection, while the airway epithelium is tailored for respiratory functions, emphasizing the clearance of respiratory secretions and airborne particles. When observed at the cellular level other differences arise. The gingival epithelium, as part of the oral mucosa, is characterized by a stratified squamous epithelium structure. This epithelium comprises layers of cells, including basal cells responsible for regeneration, keratinocytes providing structural integrity, and various immune cells contributing to local defense mechanisms. In contrast, the bronchial epithelium, lining the respiratory tract, is a pseudostratified columnar epithelium. Its cell composition includes ciliated cells, responsible for mucociliary clearance, goblet cells producing mucus for entrapping particles, basal cells serving as progenitors for epithelial regeneration. Due to the gingiva being *P. gingivalis*'s preferential niche, this bacterium is well adapted to survive in that environment, while the airway epithelium being a completely new environment. The mucus production could potentially trap the bacteria, or the ciliary beating could interfere with *P. gingivalis* attachment. Moreover, our investigation raises the intriguing possibility that *P. gingivalis* might not invade the airway epithelium successfully and perhaps remains extracellular either creating a physical barrier for viral attachment to airway epithelial cell or proteolytically shaving off attachment proteins used by the virus for entry. Thus, we must consider the possibility that *P. gingivalis* creates a bottleneck effect within the epithelial cells, whereby it establishes an inhospitable external environment for viruses to access target cells. Analyzing the degradation of specific viral proteins in gingipain-treated RSV particles through techniques such as Western blotting offers a targeted approach

to deciphering the intricate steps involved in gingipains' interference with viral infections. However, viruses that manage to overcome *P. gingivalis* mediated restriction upon entry into might be able to exploit the IFN devoid environment induced by *P. gingivalis* to thrive within the infected cells.

Taking in consideration that all of our viral data is done in an *in vitro* context, we might need to consider that these effects might not replicate *in vivo*. *In vivo* other considerations have to be considered, such as the microbiome in both mucosal surfaces. Within the oral cavity it has been shown that *P. gingivalis* growth [217] and virulence can be heavily affected by other microbes within the biofilm. Synergistic interactions with other periodontal pathogens, such as *Treponema denticola*, may contribute to the formation of complex biofilms [218]. These biofilms create a conducive environment for the survival and may also enhance the virulence of *P. gingivalis*. Conversely, competitive interactions with beneficial bacteria, including certain strains of Streptococcus and other commensals, may act as a barrier against *P. gingivalis* colonization and infection [219]. The specific identity and abundance of these bacteria, along with the overall microbial community structure, play a critical role in shaping the virulence and pathogenicity of *P. gingivalis* in the oral cavity. Although several reports confirmed the presence of *P. gingivalis* in the airway mucosa [191, 220], not much is known on how this oral pathogen interacts with the respiratory mucosa normal flora. Whether and how the local microbiome in the airways impacts *P. gingivalis* virulence and colonization remains to be determined.

As we delve deeper into the intricate interactions between *P. gingivalis* and oral viruses, the exploration of *in vivo* models becomes imperative for a comprehensive understanding of these complex dynamics. Animal experiments represent a crucial avenue for investigating the interplay between *P. gingivalis* and oral viruses within a more physiological context. Particularly, the use of animal models, such as rodents, can provide valuable insights into the *in vivo* consequences of *P. gingivalis*-virus interactions. The application of a herpes simplex virus type 1 (HSV1) abrasion model presents a promising approach [221], offering a controlled system to study the effects of *P. gingivalis* in the presence of an oral virus. This model allows for the examination of the dynamics between *P. gingivalis* and HSV1, mimicking conditions relevant to oral infections. Additionally, exploring the effect of *P. gingivalis* in respiratory viruses could be facilitated by utilizing a Sendai virus mouse model of infection. Such experiments would not only elucidate the impact of *P. gingivalis* on viral infections but also shed light on potential cooperative or antagonistic relationships between *P. gingivalis* and both oral and respiratory viruses *in vivo*. A compelling future direction in our research involves exploring the impact of co-infection on the protective effect of *P. gingivalis* against RSV in the airway epithelium. Specifically, investigating the interactions between *P. gingivalis* and other lung pathogens or commensals in a co-infection scenario is crucial to unveil the complexities of microbial dynamics in the respiratory mucosa. This exploration could involve introducing co-infections with known lung pathogens or commensals and assessing their influence on *P. gingivalis*' ability to protect against RSV. In conclusion, our ongoing research into

the multifaceted interactions involving *P. gingivalis*, viruses, and potential oral and respiratory implications has unveiled promising avenues for future exploration.

## REFERENCES

1. Squier, C.A. and M.J. Kremer, *Biology of oral mucosa and esophagus*. J Natl Cancer Inst Monogr, 2001(29): p. 7-15.
2. Groeger, S. and J. Meyle, *Oral Mucosal Epithelial Cells*. Front Immunol, 2019. **10**: p. 208.
3. Cimasoni, G., P. de Crousaz, and F. Rebstein, [*Physiology of the gingivo-dental sulcus*]. SSO Schweiz Monatsschr Zahnheilkd, 1977. **87**(8): p. 724-36.
4. Lamont, R.J., D.P. Miller, and J. Bagaitkar, *Illuminating the oral microbiome: cellular microbiology*. FEMS Microbiol Rev, 2023. **47**(4).
5. Zihni, C., et al., *Tight junctions: from simple barriers to multifunctional molecular gates*. Nat Rev Mol Cell Biol, 2016. **17**(9): p. 564-80.
6. Goodenough, D.A. and D.L. Paul, *Gap junctions*. Cold Spring Harb Perspect Biol, 2009. **1**(1): p. a002576.
7. Harris, T.J. and U. Tepass, *Adherens junctions: from molecules to morphogenesis*. Nat Rev Mol Cell Biol, 2010. **11**(7): p. 502-14.
8. Takeichi, M., *Dynamic contacts: rearranging adherens junctions to drive epithelial remodelling*. Nat Rev Mol Cell Biol, 2014. **15**(6): p. 397-410.
9. Hintermann, E., et al., *Discrete proteolysis of focal contact and adherens junction components in Porphyromonas gingivalis-infected oral keratinocytes: a strategy for cell adhesion and migration disabling*. Infect Immun, 2002. **70**(10): p. 5846-56.
10. Vitkov, L., et al., *Breaking the Gingival Barrier in Periodontitis*. Int J Mol Sci, 2023. **24**(5).
11. Lee, G., H.J. Kim, and H.M. Kim, *RhoA-JNK Regulates the E-Cadherin Junctions of Human Gingival Epithelial Cells*. J Dent Res, 2016. **95**(3): p. 284-91.
12. Al-Sadi, R.M. and T.Y. Ma, *IL-1beta causes an increase in intestinal epithelial tight junction permeability*. J Immunol, 2007. **178**(7): p. 4641-9.
13. Bosshardt, D.D. and N.P. Lang, *The junctional epithelium: from health to disease*. J Dent Res, 2005. **84**(1): p. 9-20.
14. Brizuela, M. and R. Winters, *Histology, Oral Mucosa*, in *StatPearls*. 2024: Treasure Island (FL) ineligible companies. Disclosure: Ryan Winters declares no relevant financial relationships with ineligible companies.
15. *Chapter 12 - Oral Mucosa*, in *Ten Cate's Oral Histology (Eighth Edition)*, A. Nanci, Editor. 2013, Mosby: St. Louis (MO). p. 278-310.
16. Ryder, M.I., *Comparison of neutrophil functions in aggressive and chronic periodontitis*. Periodontol 2000, 2010. **53**: p. 124-37.
17. Hovav, A.H., *Dendritic cells of the oral mucosa*. Mucosal Immunol, 2014. **7**(1): p. 27-37.

18. Novak, N., et al., *The immune privilege of the oral mucosa*. Trends Mol Med, 2008. **14**(5): p. 191-8.
19. Williams, D.W., et al., *Human oral mucosa cell atlas reveals a stromal-neutrophil axis regulating tissue immunity*. Cell, 2021. **184**(15): p. 4090-4104 e15.
20. Hans, M. and V. Madaan Hans, *Epithelial antimicrobial peptides: guardian of the oral cavity*. Int J Pept, 2014. **2014**: p. 370297.
21. Hajishengallis, G. and R.J. Lamont, *Dancing with the Stars: How Choreographed Bacterial Interactions Dictate Nososymbiocity and Give Rise to Keystone Pathogens, Accessory Pathogens, and Pathobionts*. Trends Microbiol, 2016. **24**(6): p. 477-489.
22. Kanneganti, T.D., et al., *Critical role for Cryopyrin/Nalp3 in activation of caspase-1 in response to viral infection and double-stranded RNA*. J Biol Chem, 2006. **281**(48): p. 36560-8.
23. Triantafilou, K., et al., *Differential recognition of HIV-stimulated IL-1beta and IL-18 secretion through NLR and NAIP signalling in monocyte-derived macrophages*. PLoS Pathog, 2021. **17**(4): p. e1009417.
24. Lupfer, C. and T.D. Kanneganti, *The expanding role of NLRs in antiviral immunity*. Immunol Rev, 2013. **255**(1): p. 13-24.
25. Rehwinkel, J. and M.U. Gack, *RIG-I-like receptors: their regulation and roles in RNA sensing*. Nat Rev Immunol, 2020. **20**(9): p. 537-551.
26. Ablasser, A., et al., *cGAS produces a 2'-5'-linked cyclic dinucleotide second messenger that activates STING*. Nature, 2013. **498**(7454): p. 380-4.
27. Wu, N., et al., *Race between virus and inflammasomes: inhibition or escape, intervention and therapy*. Front Cell Infect Microbiol, 2023. **13**: p. 1173505.
28. Wang, B., Y. Tian, and Q. Yin, *AIM2 Inflammasome Assembly and Signaling*. Adv Exp Med Biol, 2019. **1172**: p. 143-155.
29. Orzalli, M.H., et al., *cGAS-mediated stabilization of IFI16 promotes innate signaling during herpes simplex virus infection*. Proc Natl Acad Sci U S A, 2015. **112**(14): p. E1773-81.
30. Ashkar, A.A. and K.L. Rosenthal, *Toll-like receptor 9, CpG DNA and innate immunity*. Curr Mol Med, 2002. **2**(6): p. 545-56.
31. Chattopadhyay, S. and G.C. Sen, *dsRNA-activation of TLR3 and RLR signaling: gene induction-dependent and independent effects*. J Interferon Cytokine Res, 2014. **34**(6): p. 427-36.
32. Diebold, S.S., et al., *Innate antiviral responses by means of TLR7-mediated recognition of single-stranded RNA*. Science, 2004. **303**(5663): p. 1529-31.
33. Fuchs, K., et al., *The fungal ligand chitin directly binds TLR2 and triggers inflammation dependent on oligomer size*. EMBO Rep, 2018. **19**(12).
34. Lu, Y.C., W.C. Yeh, and P.S. Ohashi, *LPS/TLR4 signal transduction pathway*. Cytokine, 2008. **42**(2): p. 145-151.
35. Oliveira-Nascimento, L., P. Massari, and L.M. Wetzler, *The Role of TLR2 in Infection and Immunity*. Front Immunol, 2012. **3**: p. 79.
36. Yoon, S.I., et al., *Structural basis of TLR5-flagellin recognition and signaling*. Science, 2012. **335**(6070): p. 859-64.

37. Bi, D., et al., *NOD1 is the innate immune receptor for iE-DAP and can activate NF-kappaB pathway in teleost fish*. Dev Comp Immunol, 2017. **76**: p. 238-246.
38. Dugan, J.W., et al., *Nucleotide oligomerization domain-2 interacts with 2'-5'-oligoadenylate synthetase type 2 and enhances RNase-L function in THP-1 cells*. Mol Immunol, 2009. **47**(2-3): p. 560-6.
39. Grimes, C.L., et al., *The innate immune protein Nod2 binds directly to MDP, a bacterial cell wall fragment*. J Am Chem Soc, 2012. **134**(33): p. 13535-7.
40. Kanneganti, T.D., et al., *Bacterial RNA and small antiviral compounds activate caspase-1 through cryopyrin/Nalp3*. Nature, 2006. **440**(7081): p. 233-6.
41. Satoh, T., et al., *LGP2 is a positive regulator of RIG-I- and MDA5-mediated antiviral responses*. Proc Natl Acad Sci U S A, 2010. **107**(4): p. 1512-7.
42. Joly, S., et al., *Human beta-defensins 2 and 3 demonstrate strain-selective activity against oral microorganisms*. J Clin Microbiol, 2004. **42**(3): p. 1024-9.
43. Xu, D. and W. Lu, *Defensins: A Double-Edged Sword in Host Immunity*. Front Immunol, 2020. **11**: p. 764.
44. Dale, B.A. and L.P. Fredericks, *Antimicrobial peptides in the oral environment: expression and function in health and disease*. Curr Issues Mol Biol, 2005. **7**(2): p. 119-33.
45. Ji, S., et al., *Susceptibility of various oral bacteria to antimicrobial peptides and to phagocytosis by neutrophils*. J Periodontal Res, 2007. **42**(5): p. 410-9.
46. Oren, Z., et al., *Structure and organization of the human antimicrobial peptide LL-37 in phospholipid membranes: relevance to the molecular basis for its non-cell-selective activity*. Biochem J, 1999. **341** ( Pt 3)(Pt 3): p. 501-13.
47. Ross, K.F. and M.C. Herzberg, *Calprotectin expression by gingival epithelial cells*. Infect Immun, 2001. **69**(5): p. 3248-54.
48. Bergman, P., et al., *The antimicrobial peptide LL-37 inhibits HIV-1 replication*. Curr HIV Res, 2007. **5**(4): p. 410-5.
49. Lee, C.J., et al., *Cathelicidin LL-37 and HSV-1 Corneal Infection: Peptide Versus Gene Therapy*. Transl Vis Sci Technol, 2014. **3**(3): p. 4.
50. Zhang, L., et al., *HBD-2 binds SARS-CoV-2 RBD and blocks viral entry: Strategy to combat COVID-19*. iScience, 2022. **25**(3): p. 103856.
51. Schueller, K., et al., *Members of the Oral Microbiota Are Associated with IL-8 Release by Gingival Epithelial Cells in Healthy Individuals*. Front Microbiol, 2017. **8**: p. 416.
52. Darveau, R.P., et al., *Local chemokine paralysis, a novel pathogenic mechanism for Porphyromonas gingivalis*. Infect Immun, 1998. **66**(4): p. 1660-5.
53. Dixon, D.R., B.W. Bainbridge, and R.P. Darveau, *Modulation of the innate immune response within the periodontium*. Periodontol 2000, 2004. **35**: p. 53-74.
54. Chung, W.O., et al., *Expression of defensins in gingiva and their role in periodontal health and disease*. Curr Pharm Des, 2007. **13**(30): p. 3073-83.
55. Easter, Q.T., et al., *Polybacterial intracellular coinfection of epithelial stem cells in periodontitis*. bioRxiv, 2023: p. 2023.08.23.554343.
56. Jauregui, C.E., et al., *Suppression of T-cell chemokines by Porphyromonas gingivalis*. Infect Immun, 2013. **81**(7): p. 2288-95.

57. Montoya, M., et al., *Type I interferons produced by dendritic cells promote their phenotypic and functional activation*. *Blood*, 2002. **99**(9): p. 3263-71.
58. Davidson, S., et al., *Pathogenic potential of interferon alpha in acute influenza infection*. *Nat Commun*, 2014. **5**: p. 3864.
59. Zhou, F., *Molecular mechanisms of IFN-gamma to up-regulate MHC class I antigen processing and presentation*. *Int Rev Immunol*, 2009. **28**(3-4): p. 239-60.
60. Fenimore, J. and A.Y. H, *Regulation of IFN-gamma Expression*. *Adv Exp Med Biol*, 2016. **941**: p. 1-19.
61. Delsing, C.E., et al., *Interferon-gamma as adjunctive immunotherapy for invasive fungal infections: a case series*. *BMC Infect Dis*, 2014. **14**: p. 166.
62. Zhao, C., et al., *Influenza B virus non-structural protein 1 counteracts ISG15 antiviral activity by sequestering ISGylated viral proteins*. *Nat Commun*, 2016. **7**: p. 12754.
63. Lippmann, J., et al., *Dissection of a type I interferon pathway in controlling bacterial intracellular infection in mice*. *Cell Microbiol*, 2011. **13**(11): p. 1668-82.
64. Long, T.M., et al., *Enteropathogenic Escherichia coli inhibits type I interferon- and RNase L-mediated host defense to disrupt intestinal epithelial cell barrier function*. *Infect Immun*, 2014. **82**(7): p. 2802-14.
65. Zhou, Z., et al., *TRIM14 is a mitochondrial adaptor that facilitates retinoic acid-inducible gene-I-like receptor-mediated innate immune response*. *Proc Natl Acad Sci U S A*, 2014. **111**(2): p. E245-54.
66. Perelman, S.S., et al., *Cell-Based Screen Identifies Human Interferon-Stimulated Regulators of Listeria monocytogenes Infection*. *PLoS Pathog*, 2016. **12**(12): p. e1006102.
67. Sun, F., et al., *Topology, Antiviral Functional Residues and Mechanism of IFITM1*. *Viruses*, 2020. **12**(3).
68. Ranjbar, S., et al., *A Role for IFITM Proteins in Restriction of Mycobacterium tuberculosis Infection*. *Cell Rep*, 2015. **13**(5): p. 874-83.
69. Sarkar, R., et al., *Viperin, an IFN-Stimulated Protein, Delays Rotavirus Release by Inhibiting Non-Structural Protein 4 (NSP4)-Induced Intrinsic Apoptosis*. *Viruses*, 2021. **13**(7).
70. Helbig, K.J., et al., *The interferon stimulated gene viperin, restricts Shigella flexneri in vitro*. *Sci Rep*, 2019. **9**(1): p. 15598.
71. Zhao, C., et al., *ISG15 conjugation system targets the viral NS1 protein in influenza A virus-infected cells*. *Proc Natl Acad Sci U S A*, 2010. **107**(5): p. 2253-8.
72. Radoshevich, L., et al., *ISG15 counteracts Listeria monocytogenes infection*. *Elife*, 2015. **4**.
73. Burke, J.M., et al., *RNase L limits host and viral protein synthesis via inhibition of mRNA export*. *Sci Adv*, 2021. **7**(23).
74. Li, X.L., et al., *An essential role for the antiviral endoribonuclease, RNase-L, in antibacterial immunity*. *Proc Natl Acad Sci U S A*, 2008. **105**(52): p. 20816-21.
75. Blazek, K., et al., *IFN-lambda resolves inflammation via suppression of neutrophil infiltration and IL-1beta production*. *J Exp Med*, 2015. **212**(6): p. 845-53.



76. Broggi, A., et al., *IFN-lambda suppresses intestinal inflammation by non-translational regulation of neutrophil function*. Nat Immunol, 2017. **18**(10): p. 1084-1093.
77. Baldridge, M.T., et al., *Expression of Ifnlr1 on Intestinal Epithelial Cells Is Critical to the Antiviral Effects of Interferon Lambda against Norovirus and Reovirus*. J Virol, 2017. **91**(7).
78. Pott, J., et al., *IFN-lambda determines the intestinal epithelial antiviral host defense*. Proc Natl Acad Sci U S A, 2011. **108**(19): p. 7944-9.
79. Good, C., A.I. Wells, and C.B. Coyne, *Type III interferon signaling restricts enterovirus 71 infection of goblet cells*. Sci Adv, 2019. **5**(3): p. eaau4255.
80. Wells, A.I. and C.B. Coyne, *Type III Interferons in Antiviral Defenses at Barrier Surfaces*. Trends Immunol, 2018. **39**(10): p. 848-858.
81. Lazear, H.M., J.W. Schoggins, and M.S. Diamond, *Shared and Distinct Functions of Type I and Type III Interferons*. Immunity, 2019. **50**(4): p. 907-923.
82. Forero, A., et al., *Differential Activation of the Transcription Factor IRF1 Underlies the Distinct Immune Responses Elicited by Type I and Type III Interferons*. Immunity, 2019. **51**(3): p. 451-464 e6.
83. Galani, I.E., et al., *Interferon-lambda Mediates Non-redundant Front-Line Antiviral Protection against Influenza Virus Infection without Compromising Host Fitness*. Immunity, 2017. **46**(5): p. 875-890 e6.
84. Andreakos, E., I. Zanoni, and I.E. Galani, *Lambda interferons come to light: dual function cytokines mediating antiviral immunity and damage control*. Curr Opin Immunol, 2019. **56**: p. 67-75.
85. Drago, F., et al., *Oral and cutaneous manifestations of viral and bacterial infections: Not only COVID-19 disease*. Clin Dermatol, 2021. **39**(3): p. 384-404.
86. La Rosa, G.R.M., et al., *Association of Viral Infections With Oral Cavity Lesions: Role of SARS-CoV-2 Infection*. Front Med (Lausanne), 2020. **7**: p. 571214.
87. Mark Welch, J.L., S.T. Ramirez-Puebla, and G.G. Borisy, *Oral Microbiome Geography: Micron-Scale Habitat and Niche*. Cell Host Microbe, 2020. **28**(2): p. 160-168.
88. Ghosh, S., et al., *Enteric viruses replicate in salivary glands and infect through saliva*. Nature, 2022. **607**(7918): p. 345-350.
89. Rouabhia, M., *Interactions between host and oral commensal microorganisms are key events in health and disease status*. Can J Infect Dis, 2002. **13**(1): p. 47-51.
90. Lee, J.Y., et al., *Maturation of the Mfa1 Fimbriae in the Oral Pathogen Porphyromonas gingivalis*. Front Cell Infect Microbiol, 2018. **8**: p. 137.
91. Hajishengallis, G., *Periodontitis: from microbial immune subversion to systemic inflammation*. Nat Rev Immunol, 2015. **15**(1): p. 30-44.
92. Hajishengallis, G. and R.J. Lamont, *Beyond the red complex and into more complexity: the polymicrobial synergy and dysbiosis (PSD) model of periodontal disease etiology*. Mol Oral Microbiol, 2012. **27**(6): p. 409-19.
93. Huang, N., et al., *SARS-CoV-2 infection of the oral cavity and saliva*. Nat Med, 2021. **27**(5): p. 892-903.

94. Betancourth, M., et al., *Microorganismos inusuales en surcos y bolsas periodontales*. Colombia Médica, 2006. **37**(1): p. 6-14.
95. Costa, C., et al., *Characterization of Oral Enterobacteriaceae Prevalence and Resistance Profile in Chronic Kidney Disease Patients Undergoing Peritoneal Dialysis*. Front Microbiol, 2021. **12**: p. 736685.
96. Dahlen, G. and M. Wikstrom, *Occurrence of enteric rods, staphylococci and Candida in subgingival samples*. Oral Microbiol Immunol, 1995. **10**(1): p. 42-6.
97. Souto, R. and A.P. Colombo, *Detection of Helicobacter pylori by polymerase chain reaction in the subgingival biofilm and saliva of non-dyspeptic periodontal patients*. J Periodontol, 2008. **79**(1): p. 97-103.
98. Newman, M.G., et al., *Carranza's Clinical Periodontology*. 2015: Elsevier Saunders.
99. Lamont, R.J. and G. Hajishengallis, *Polymicrobial synergy and dysbiosis in inflammatory disease*. Trends Mol Med, 2015. **21**(3): p. 172-83.
100. Hasturk, H., et al., *1-Tetradecanol complex reduces progression of Porphyromonas gingivalis-induced experimental periodontitis in rabbits*. J Periodontol, 2007. **78**(5): p. 924-32.
101. Marsh, P.D., *Microbial ecology of dental plaque and its significance in health and disease*. Adv Dent Res, 1994. **8**(2): p. 263-71.
102. Hajishengallis, G. and R.J. Lamont, *Breaking bad: manipulation of the host response by Porphyromonas gingivalis*. Eur J Immunol, 2014. **44**(2): p. 328-38.
103. How, K.Y., K.P. Song, and K.G. Chan, *Porphyromonas gingivalis: An Overview of Periodontopathic Pathogen below the Gum Line*. Front Microbiol, 2016. **7**: p. 53.
104. Lamont, R.J., et al., *Molecules of Streptococcus gordonii that bind to Porphyromonas gingivalis*. Microbiology (Reading), 1994. **140 ( Pt 4)**: p. 867-72.
105. Aleksijevic, L.H., et al., *Porphyromonas gingivalis Virulence Factors and Clinical Significance in Periodontal Disease and Coronary Artery Diseases*. Pathogens, 2022. **11**(10).
106. Sakanaka, A., et al., *Dual lifestyle of Porphyromonas gingivalis in biofilm and gingival cells*. Microb Pathog, 2016. **94**: p. 42-7.
107. Yost, S., et al., *Functional signatures of oral dysbiosis during periodontitis progression revealed by microbial metatranscriptome analysis*. Genome Med, 2015. **7**(1): p. 27.
108. Moutsopoulos, N.M., et al., *Porphyromonas gingivalis promotes Th17 inducing pathways in chronic periodontitis*. J Autoimmun, 2012. **39**(4): p. 294-303.
109. Kitamura, Y., et al., *Gingipains in the culture supernatant of Porphyromonas gingivalis cleave CD4 and CD8 on human T cells*. J Periodontal Res, 2002. **37**(6): p. 464-8.
110. Sochalska, M. and J. Potempa, *Manipulation of Neutrophils by Porphyromonas gingivalis in the Development of Periodontitis*. Front Cell Infect Microbiol, 2017. **7**: p. 197.
111. Moffatt, C.E., et al., *Porphyromonas gingivalis SerB-mediated dephosphorylation of host cell cofilin modulates invasion efficiency*. Cell Microbiol, 2012. **14**(4): p. 577-88.

112. Yilmaz, O., K. Watanabe, and R.J. Lamont, *Involvement of integrins in fimbriae-mediated binding and invasion by Porphyromonas gingivalis*. Cell Microbiol, 2002. **4**(5): p. 305-14.
113. Yilmaz, O., et al., *Gingival epithelial cell signalling and cytoskeletal responses to Porphyromonas gingivalis invasion*. Microbiology (Reading), 2003. **149**(Pt 9): p. 2417-2426.
114. Sztukowska, M.N., et al., *Porphyromonas gingivalis initiates a mesenchymal-like transition through ZEB1 in gingival epithelial cells*. Cell Microbiol, 2016. **18**(6): p. 844-58.
115. Mao, S., et al., *Intrinsic apoptotic pathways of gingival epithelial cells modulated by Porphyromonas gingivalis*. Cell Microbiol, 2007. **9**(8): p. 1997-2007.
116. Fitzsimonds, Z.R., et al., *From Beyond the Pale to the Pale Riders: The Emerging Association of Bacteria with Oral Cancer*. J Dent Res, 2020. **99**(6): p. 604-612.
117. Kuboniwa, M., et al., *P. gingivalis accelerates gingival epithelial cell progression through the cell cycle*. Microbes Infect, 2008. **10**(2): p. 122-8.
118. Qi, Y.J., et al., *Porphyromonas gingivalis promotes progression of esophageal squamous cell cancer via TGFbeta-dependent Smad/YAP/TAZ signaling*. PLoS Biol, 2020. **18**(9): p. e3000825.
119. Zhou, N., et al., *Porphyromonas gingivalis induces periodontitis, causes immune imbalance, and promotes rheumatoid arthritis*. J Leukoc Biol, 2021. **110**(3): p. 461-473.
120. Xie, M., et al., *BMAL1-Downregulation Aggravates Porphyromonas Gingivalis-Induced Atherosclerosis by Encouraging Oxidative Stress*. Circ Res, 2020. **126**(6): p. e15-e29.
121. Dominy, S.S., et al., *Porphyromonas gingivalis in Alzheimer's disease brains: Evidence for disease causation and treatment with small-molecule inhibitors*. Sci Adv, 2019. **5**(1): p. eaau3333.
122. Winkler, E.S. and L.B. Thackray, *A long-distance relationship: the commensal gut microbiota and systemic viruses*. Curr Opin Virol, 2019. **37**: p. 44-51.
123. Odendall, C., et al., *Diverse intracellular pathogens activate type III interferon expression from peroxisomes*. Nat Immunol, 2014. **15**(8): p. 717-26.
124. Walker, F.C. and M.T. Baldrige, *Interactions between noroviruses, the host, and the microbiota*. Curr Opin Virol, 2019. **37**: p. 1-9.
125. Oh, J.E., et al., *Dysbiosis-induced IL-33 contributes to impaired antiviral immunity in the genital mucosa*. Proc Natl Acad Sci U S A, 2016. **113**(6): p. E762-71.
126. Li, N., et al., *The Commensal Microbiota and Viral Infection: A Comprehensive Review*. Front Immunol, 2019. **10**: p. 1551.
127. Baldrige, M.T., et al., *Commensal microbes and interferon-lambda determine persistence of enteric murine norovirus infection*. Science, 2015. **347**(6219): p. 266-9.
128. Uchiyama, R., et al., *Antibiotic treatment suppresses rotavirus infection and enhances specific humoral immunity*. J Infect Dis, 2014. **210**(2): p. 171-82.

129. Eisenreich, W., et al., *How Viral and Intracellular Bacterial Pathogens Reprogram the Metabolism of Host Cells to Allow Their Intracellular Replication*. Front Cell Infect Microbiol, 2019. **9**: p. 42.
130. Young, G.R., et al., *Resurrection of endogenous retroviruses in antibody-deficient mice*. Nature, 2012. **491**(7426): p. 774-8.
131. Gorres, K.L., et al., *Activation and repression of Epstein-Barr Virus and Kaposi's sarcoma-associated herpesvirus lytic cycles by short- and medium-chain fatty acids*. J Virol, 2014. **88**(14): p. 8028-44.
132. Frisan, T., et al., *A bacterial genotoxin causes virus reactivation and genomic instability in Epstein-Barr virus infected epithelial cells pointing to a role of co-infection in viral oncogenesis*. Int J Cancer, 2019. **144**(1): p. 98-109.
133. Van Crombrugge, E., et al., *Bacterial Toxins from Staphylococcus aureus and Bordetella bronchiseptica Predispose the Horse's Respiratory Tract to Equine Herpesvirus Type 1 Infection*. Viruses, 2022. **14**(1).
134. Sugano, N., et al., *Relationship between Porphyromonas gingivalis, Epstein-Barr virus infection and reactivation in periodontitis*. J Oral Sci, 2004. **46**(4): p. 203-6.
135. Rodriguez-Hernandez, C.J., et al., *Microbiome-mediated incapacitation of interferon lambda production in the oral mucosa*. Proc Natl Acad Sci U S A, 2021. **118**(51).
136. Tonoyan, L., et al., *Detection of Epstein-Barr Virus in Periodontitis: A Review of Methodological Approaches*. Microorganisms, 2020. **9**(1).
137. Puletic, M., et al., *Detection rates of periodontal bacteria and herpesviruses in different forms of periodontal disease*. Microbiol Immunol, 2020. **64**(12): p. 815-824.
138. Christersson, L.A., et al., *Subgingival distribution of periodontal pathogenic microorganisms in adult periodontitis*. J Periodontol, 1992. **63**(5): p. 418-25.
139. Imbronito, A.V., et al., *Detection of herpesviruses and periodontal pathogens in subgingival plaque of patients with chronic periodontitis, generalized aggressive periodontitis, or gingivitis*. J Periodontol, 2008. **79**(12): p. 2313-21.
140. Imbronito, A.V., et al., *Detection of Epstein-Barr virus and human cytomegalovirus in blood and oral samples: comparison of three sampling methods*. J Oral Sci, 2008. **50**(1): p. 25-31.
141. Kamma, J.J., A. Contreras, and J. Slots, *Herpes viruses and periodontopathic bacteria in early-onset periodontitis*. J Clin Periodontol, 2001. **28**(9): p. 879-85.
142. Passariello, C., et al., *Evaluation of microbiota associated with Herpesviruses in active sites of generalized aggressive periodontitis*. Ann Stomatol (Roma), 2017. **8**(2): p. 59-70.
143. Chen, C., P. Feng, and J. Slots, *Herpesvirus-bacteria synergistic interaction in periodontitis*. Periodontol 2000, 2020. **82**(1): p. 42-64.
144. Shi, Z., et al., *Segmented Filamentous Bacteria Prevent and Cure Rotavirus Infection*. Cell, 2019. **179**(3): p. 644-658 e13.
145. Kotenko, S.V., et al., *Type III IFNs: Beyond antiviral protection*. Semin Immunol, 2019. **43**: p. 101303.

146. Ingle, H., et al., *Viral complementation of immunodeficiency confers protection against enteric pathogens via interferon-lambda*. *Nat Microbiol*, 2019. **4**(7): p. 1120-1128.
147. Hassan, E. and M.T. Baldrige, *Norovirus encounters in the gut: multifaceted interactions and disease outcomes*. *Mucosal Immunol*, 2019. **12**(6): p. 1259-1267.
148. Grau, K.R., et al., *The intestinal regionalization of acute norovirus infection is regulated by the microbiota via bile acid-mediated priming of type III interferon*. *Nat Microbiol*, 2020. **5**(1): p. 84-92.
149. Thackray, L.B., et al., *Oral Antibiotic Treatment of Mice Exacerbates the Disease Severity of Multiple Flavivirus Infections*. *Cell Rep*, 2018. **22**(13): p. 3440-3453 e6.
150. Moffatt-Jauregui, C.E., et al., *Establishment and characterization of a telomerase immortalized human gingival epithelial cell line*. *J Periodontal Res*, 2013. **48**(6): p. 713-21.
151. Miller, D.P., et al., *Genes Contributing to Porphyromonas gingivalis Fitness in Abscess and Epithelial Cell Colonization Environments*. *Front Cell Infect Microbiol*, 2017. **7**: p. 378.
152. Barth, K. and C.A. Genco, *Microbial Degradation of Cellular Kinases Impairs Innate Immune Signaling and Paracrine TNFalpha Responses*. *Sci Rep*, 2016. **6**: p. 34656.
153. Shihan, M.H., et al., *A simple method for quantitating confocal fluorescent images*. *Biochem Biophys Rep*, 2021. **25**: p. 100916.
154. Uccellini, M.B. and A. Garcia-Sastre, *ISRE-Reporter Mouse Reveals High Basal and Induced Type I IFN Responses in Inflammatory Monocytes*. *Cell Rep*, 2018. **25**(10): p. 2784-2796 e3.
155. Hertzog, J., et al., *Infection with a Brazilian isolate of Zika virus generates RIG-I stimulatory RNA and the viral NS5 protein blocks type I IFN induction and signaling*. *Eur J Immunol*, 2018. **48**(7): p. 1120-1136.
156. Sokoloski, K.J., et al., *Identification of Interactions between Sindbis Virus Capsid Protein and Cytoplasmic vRNA as Novel Virulence Determinants*. *PLoS Pathog*, 2017. **13**(6): p. e1006473.
157. Linden, J., et al., *Interferon-lambda Receptor Expression: Novel Reporter Mouse Reveals Within- and Cross-Tissue Heterogeneity*. *J Interferon Cytokine Res*, 2020. **40**(6): p. 292-300.
158. Contreras, A., H. Nowzari, and J. Slots, *Herpesviruses in periodontal pocket and gingival tissue specimens*. *Oral Microbiol Immunol*, 2000. **15**(1): p. 15-8.
159. Contreras, A., et al., *Relationship between herpesviruses and adult periodontitis and periodontopathic bacteria*. *J Periodontol*, 1999. **70**(5): p. 478-84.
160. Naqvi, A.R., et al., *Herpesviruses and MicroRNAs: New Pathogenesis Factors in Oral Infection and Disease?* *Front Immunol*, 2018. **9**: p. 2099.
161. Hajishengallis, G., et al., *Low-abundance biofilm species orchestrates inflammatory periodontal disease through the commensal microbiota and complement*. *Cell Host Microbe*, 2011. **10**(5): p. 497-506.
162. Borisy, G.G. and A.M. Valm, *Spatial scale in analysis of the dental plaque microbiome*. *Periodontol 2000*, 2021. **86**(1): p. 97-112.

163. Ximenez-Fyvie, L.A., A.D. Haffajee, and S.S. Socransky, *Comparison of the microbiota of supra- and subgingival plaque in health and periodontitis*. J Clin Periodontol, 2000. **27**(9): p. 648-57.
164. Hornung, V., et al., *OAS proteins and cGAS: unifying concepts in sensing and responding to cytosolic nucleic acids*. Nat Rev Immunol, 2014. **14**(8): p. 521-8.
165. Takeuchi, O. and S. Akira, *Pattern recognition receptors and inflammation*. Cell, 2010. **140**(6): p. 805-20.
166. Fensterl, V. and G.C. Sen, *Interferon-induced Ifit proteins: their role in viral pathogenesis*. J Virol, 2015. **89**(5): p. 2462-8.
167. Wang, Y., et al., *Periodontal disease increases the host susceptibility to COVID-19 and its severity: a Mendelian randomization study*. J Transl Med, 2021. **19**(1): p. 528.
168. Marouf, N., et al., *Association between periodontitis and severity of COVID-19 infection: A case-control study*. J Clin Periodontol, 2021. **48**(4): p. 483-491.
169. Honda, K., A. Takaoka, and T. Taniguchi, *Type I interferon [corrected] gene induction by the interferon regulatory factor family of transcription factors*. Immunity, 2006. **25**(3): p. 349-60.
170. Jefferies, C.A., *Regulating IRFs in IFN Driven Disease*. Front Immunol, 2019. **10**: p. 325.
171. Griffiths, S.J., et al., *A systematic analysis of host factors reveals a Med23-interferon-lambda regulatory axis against herpes simplex virus type 1 replication*. PLoS Pathog, 2013. **9**(8): p. e1003514.
172. Caine, E.A., et al., *Interferon lambda protects the female reproductive tract against Zika virus infection*. Nat Commun, 2019. **10**(1): p. 280.
173. Yamane, D., et al., *Basal expression of interferon regulatory factor 1 drives intrinsic hepatocyte resistance to multiple RNA viruses*. Nat Microbiol, 2019. **4**(7): p. 1096-1104.
174. Nair, S., et al., *Interferon Regulatory Factor 1 Protects against Chikungunya Virus-Induced Immunopathology by Restricting Infection in Muscle Cells*. J Virol, 2017. **91**(22).
175. Matsuyama, T., et al., *Targeted disruption of IRF-1 or IRF-2 results in abnormal type I IFN gene induction and aberrant lymphocyte development*. Cell, 1993. **75**(1): p. 83-97.
176. Siegel, R., J. Eskdale, and G. Gallagher, *Regulation of IFN-lambda1 promoter activity (IFN-lambda1/IL-29) in human airway epithelial cells*. J Immunol, 2011. **187**(11): p. 5636-44.
177. Iwanaszko, M. and M. Kimmel, *NF-kappaB and IRF pathways: cross-regulation on target genes promoter level*. BMC Genomics, 2015. **16**: p. 307.
178. Takeuchi, H., et al., *The serine phosphatase SerB of Porphyromonas gingivalis suppresses IL-8 production by dephosphorylation of NF-kappaB RelA/p65*. PLoS Pathog, 2013. **9**(4): p. e1003326.
179. Yang, J., et al., *Epigenetic silencing of IRF1 dysregulates type III interferon responses to respiratory virus infection in epithelial to mesenchymal transition*. Nat Microbiol, 2017. **2**: p. 17086.

180. Ye, L., D. Schnepf, and P. Staeheli, *Interferon-lambda orchestrates innate and adaptive mucosal immune responses*. Nat Rev Immunol, 2019. **19**(10): p. 614-625.
181. Nakayama, M., et al., *Attenuation of the phosphatidylinositol 3-kinase/Akt signaling pathway by Porphyromonas gingivalis gingipains RgpA, RgpB, and Kgp*. J Biol Chem, 2015. **290**(8): p. 5190-202.
182. Stafford, P., et al., *Gingipain-dependent degradation of mammalian target of rapamycin pathway proteins by the periodontal pathogen Porphyromonas gingivalis during invasion*. Mol Oral Microbiol, 2013. **28**(5): p. 366-78.
183. Zhou, Y., et al., *Noncanonical activation of beta-catenin by Porphyromonas gingivalis*. Infect Immun, 2015. **83**(8): p. 3195-203.
184. Hwang, S., et al., *Conserved herpesviral kinase promotes viral persistence by inhibiting the IRF-3-mediated type I interferon response*. Cell Host Microbe, 2009. **5**(2): p. 166-78.
185. Laurent-Rolle, M., et al., *The interferon signaling antagonist function of yellow fever virus NS5 protein is activated by type I interferon*. Cell Host Microbe, 2014. **16**(3): p. 314-327.
186. Grant, A., et al., *Zika Virus Targets Human STAT2 to Inhibit Type I Interferon Signaling*. Cell Host Microbe, 2016. **19**(6): p. 882-90.
187. Lubick, K.J., et al., *Flavivirus Antagonism of Type I Interferon Signaling Reveals Prolidase as a Regulator of IFNAR1 Surface Expression*. Cell Host Microbe, 2015. **18**(1): p. 61-74.
188. Nakajima, M., et al., *Oral Administration of P. gingivalis Induces Dysbiosis of Gut Microbiota and Impaired Barrier Function Leading to Dissemination of Enterobacteria to the Liver*. PLoS One, 2015. **10**(7): p. e0134234.
189. Kageyama, S., et al., *Characteristics of the Salivary Microbiota in Patients With Various Digestive Tract Cancers*. Front Microbiol, 2019. **10**: p. 1780.
190. Benedyk, M., et al., *Gingipains: Critical Factors in the Development of Aspiration Pneumonia Caused by Porphyromonas gingivalis*. J Innate Immun, 2016. **8**(2): p. 185-98.
191. Okuda, K., et al., *Involvement of periodontopathic anaerobes in aspiration pneumonia*. J Periodontol, 2005. **76**(11 Suppl): p. 2154-60.
192. Terpenning, M.S., et al., *Aspiration pneumonia: dental and oral risk factors in an older veteran population*. J Am Geriatr Soc, 2001. **49**(5): p. 557-63.
193. Muir, A.J., et al., *A randomized phase 2b study of peginterferon lambda-1a for the treatment of chronic HCV infection*. J Hepatol, 2014. **61**(6): p. 1238-46.
194. Prokunina-Olsson, L., et al., *COVID-19 and emerging viral infections: The case for interferon lambda*. J Exp Med, 2020. **217**(5).
195. Hajishengallis, G., *Interconnection of periodontal disease and comorbidities: Evidence, mechanisms, and implications*. Periodontol 2000, 2022. **89**(1): p. 9-18.
196. Kageyama, S., et al., *High-Resolution Detection of Translocation of Oral Bacteria to the Gut*. J Dent Res, 2023. **102**(7): p. 752-758.

197. Shigdel, R., et al., *Oral bacterial composition associated with lung function and lung inflammation in a community-based Norwegian population*. *Respir Res*, 2023. **24**(1): p. 183.
198. Wang, N. and J.Y. Fang, *Fusobacterium nucleatum, a key pathogenic factor and microbial biomarker for colorectal cancer*. *Trends Microbiol*, 2023. **31**(2): p. 159-172.
199. Shi, T., et al., *Periodontopathogens Porphyromonas gingivalis and Fusobacterium nucleatum and Their Roles in the Progression of Respiratory Diseases*. *Pathogens*, 2023. **12**(9).
200. Brock, M., S. Bahammam, and C. Sima, *The Relationships Among Periodontitis, Pneumonia and COVID-19*. *Front Oral Health*, 2021. **2**: p. 801815.
201. Tada, A. and H. Senpuku, *The Impact of Oral Health on Respiratory Viral Infection*. *Dent J (Basel)*, 2021. **9**(4).
202. Falsey, A.R. and E.E. Walsh, *Respiratory syncytial virus infection in elderly adults*. *Drugs Aging*, 2005. **22**(7): p. 577-87.
203. Linder, K.A. and P.N. Malani, *RSV Infection in Older Adults*. *JAMA*, 2023. **330**(12): p. 1200-1200.
204. Selvaggi, C., et al., *Interferon lambda 1-3 expression in infants hospitalized for RSV or HRV associated bronchiolitis*. *J Infect*, 2014. **68**(5): p. 467-77.
205. Love, R.M., et al., *Coinvasion of dentinal tubules by Porphyromonas gingivalis and Streptococcus gordonii depends upon binding specificity of streptococcal antigen I/II adhesin*. *Infect Immun*, 2000. **68**(3): p. 1359-65.
206. Fulcher, M.L., et al., *Well-differentiated human airway epithelial cell cultures*. *Methods Mol Med*, 2005. **107**: p. 183-206.
207. Kwilas, S., et al., *Respiratory syncytial virus grown in Vero cells contains a truncated attachment protein that alters its infectivity and dependence on glycosaminoglycans*. *J Virol*, 2009. **83**(20): p. 10710-8.
208. King, T., et al., *The larger attachment glycoprotein of respiratory syncytial virus produced in primary human bronchial epithelial cultures reduces infectivity for cell lines*. *PLoS Pathog*, 2021. **17**(4): p. e1009469.
209. Hijano, D.R., et al., *Role of Type I Interferon (IFN) in the Respiratory Syncytial Virus (RSV) Immune Response and Disease Severity*. *Front Immunol*, 2019. **10**: p. 566.
210. Kuss, S.K., et al., *Intestinal microbiota promote enteric virus replication and systemic pathogenesis*. *Science*, 2011. **334**(6053): p. 249-52.
211. Boyd, M.R., et al., *Discovery of cyanovirin-N, a novel human immunodeficiency virus-inactivating protein that binds viral surface envelope glycoprotein gp120: potential applications to microbicide development*. *Antimicrob Agents Chemother*, 1997. **41**(7): p. 1521-30.
212. O'Keefe, B.R., et al., *Potent anti-influenza activity of cyanovirin-N and interactions with viral hemagglutinin*. *Antimicrob Agents Chemother*, 2003. **47**(8): p. 2518-25.
213. Lazear, H.M., et al., *Interferon-lambda restricts West Nile virus neuroinvasion by tightening the blood-brain barrier*. *Sci Transl Med*, 2015. **7**(284): p. 284ra59.



214. Wolk, K., et al., *IL-29 is produced by T(H)17 cells and mediates the cutaneous antiviral competence in psoriasis*. *Sci Transl Med*, 2013. **5**(204): p. 204ra129.
215. Scott, D.A. and J. Krauss, *Neutrophils in periodontal inflammation*. *Front Oral Biol*, 2012. **15**: p. 56-83.
216. Dong, J., et al., *Relationships Between Oral Microecosystem and Respiratory Diseases*. *Front Mol Biosci*, 2021. **8**: p. 718222.
217. Shu, Y., et al., *Spent culture supernatant of Streptococcus gordonii mitigates inflammation of human periodontal cells and inhibits proliferation of pathogenic oral microbes*. *J Periodontol*, 2023. **94**(4): p. 575-585.
218. Tan, K.H., et al., *Porphyromonas gingivalis and Treponema denticola exhibit metabolic symbioses*. *PLoS Pathog*, 2014. **10**(3): p. e1003955.
219. Xie, H., et al., *Streptococcus cristatus ArcA interferes with Porphyromonas gingivalis pathogenicity in mice*. *J Periodontal Res*, 2012. **47**(5): p. 578-83.
220. Irani, S., et al., *Evidence for graft colonization with periodontal pathogens in lung transplant recipients. A pilot study*. *Schweiz Monatsschr Zahnmed*, 2011. **121**(12): p. 1144-9.
221. Kollias, C.M., et al., *Animal models of herpes simplex virus immunity and pathogenesis*. *J Neurovirol*, 2015. **21**(1): p. 8-23.

## CURRICULUM VITAE

Carlos Josué Rodríguez Hernández  
University of Louisville School of Medicine  
505 S. Hancock St., Louisville, KY 40202  
Louisville, KY 40202  
EMAIL: cjrodr04@louisville.edu

### EDUCATION

- 2012-2017 B.S. in Biomedical Sciences, university of Puerto Rico, Ponce, PR  
2017-2018 Post-Baccalaureate Research Education Program, University of Rochester, Rochester, NY  
2018-current Ph.D. in Microbiology and Immunology, University of Louisville, Louisville, KY

### RESEARCH EXPERIENCE

- 2016-2017 Undergraduate Research Assistant; University of Puerto Rico, Ponce, PR  
Project: *Determined the therapeutic effects of Resveratrol on colony formation and proliferative capacity of different human breast carcinoma cell lines.*  
Mentor: Abigail Ruiz
- 2017-2018 Post-Baccalaureate Research Education Program Trainee; University of Rochester, Rochester, NY  
Project: *Developed a novel orthotopic mouse model to study the influence of conventional radiotherapy affect the immune response to colon cancer.*  
Mentor: Edith Lord
- 2018-current Graduate Student; University of Louisville, Louisville, KY  
Projects: *Determined the novel role of type III interferons (interferon lambda) in modulating antiviral responses at the oral mucosal barrier.*  
*Determined how dysbiotic oral microbiome disengaged antiviral immunity in murine models of oral and respiratory viral infections.*  
Mentor: Juhi Bagaitkar

## TEACHING EXPERIENCE

- 2015-2016     Physics tutor. Academic Support Center for Students and Faculty, University of Puerto Rico, Ponce, PR  
Course/Role: Provide academic support to undergraduate students at the University Physics and Fundamentals and Development of Physics Sciences courses.
- 2020            Louisville Science Pathways (LSP), Invited Lecturer  
                  LSP is a competitive high school summer research program designed to expose high school students to research and future career opportunities in the STEM fields.  
                  Topic: Immune cells and how to find them: Introduction to Flow cytometry.
- 2021            MBIO610: Research Methods in Microbiology and Immunology, Lecturer  
                  Invited Guest Lecturer; Topic: Flow Cytometry
- 2021            Dental Microbiology (OIID604); University of Louisville School of Dentistry, Louisville, KY;2021
- 2024            Invited Guest Lecturer; Topic: Endodontic microbiology and Pathogenesis: A Scientific Review

## AWARDS AND HONORS

- 2013-2017     University of Puerto Rico Member of the Dean's List
- 2018-2020     University of Louisville Graduate School Diversity Fellow
- 2021            ASM Kentucky/Tennessee Branch Meeting - 3<sup>rd</sup> Place – PhD student category.
- 2022            ID consortium Symposium – Best Trainee Oral Abstract
- 2022            Gordon Research Conference – Phagocytes 2022 Meeting – Outstanding Poster Award
- 2023            ABRCMS 2022 – Travel Award
- 2023            Oral-GI Research Affinity Group, student travel award, Nationwide Children's Hospital

## GRANTS

- 2020-2022:    T32 fellow: Inflammation and Pathogenesis T32 Training Grant; NIH/NIAID-T32 AI132146-01A1

## RESEARCH SKILLS

- Animal Surgery: Orthotopic rectal tumor implantation, Intratracheal instillation, Oral ligature model of periodontitis, Subcutaneous coil chamber implantation, Organ and tissue harvest and processing, lymph node and gingival dissection.
- Animal treatment and management: Genotyping, conditional KO mice breeding, inducible mouse model induction, intranasal infection, injections (ip, sc, iv).

- Immunology: Multi-color Flow with experience in panel design, Spectral flow, Immunohistochemistry, immunofluorescence.
- Molecular biology: Confocal Microscopy, Immunoblotting, qPCR, Fluorescent *in situ* Hybridization, bacterial and eukaryotic primer design, ELISA, tissue embedding and processing.
- Culture: Colony formation assays, Cell culture, Human Epithelial cell Isolation and culture, aseptic bacterial culture, air-liquid interface culture.
- Viral assays: Viral handling and expansion, quantification by fluorescence (FFU) or by PCR methods
- Language: Spanish (native), English
- Computational: FlowJo, Office, Graphpad Prism, ADOBE Illustrator, IMARIS, ImageJ, LAS X, Volocity.

#### PUBLICATIONS:

1. Fitzsimonds ZR, Rodriguez-Hernandez CJ, Bagaitkar J, Lamont RJ. "From Beyond the Pale to the Pale Riders: The Emerging Association of Bacteria with Oral Cancer". *J Dent Res*. 2020 Jun;99(6):604-612. doi: 10.1177/0022034520907341. Epub 2020 Feb 24. PMID: 32091956; PMCID: PMC7243420.
2. Uccello TP, Kintzel SA, Mills BN, Murphy JD, Garrett-Larsen J, Battaglia NG, Rodriguez CJ, Drage MG, Ye J, Love TMT, Johnston CJ, Repasky EA, Qiu H, Linehan DC, Lord EM, Gerber SA. "Development of an Orthotopic Murine Model of Rectal Cancer in Conjunction With Targeted Short-Course Radiation Therapy". *Adv Radiat Oncol*. 2021 Dec 9;7(2):100867. doi: 10.1016/j.adro.2021.100867. PMID: 35036637; PMCID: PMC8749199.
3. Rodriguez-Hernandez CJ, Sokoloski KJ, Stocke KS, Dukka H, Jin S, Metzler MA, Zaitsev K, Shpak B, Shen D, Miller DP, Artyomov MN, Lamont RJ, Bagaitkar J. "Microbiome-mediated incapacitation of interferon lambda production in the oral mucosa". *Proc Natl Acad Sci U S A*. 2021 Dec 21;118(51):e2105170118. doi: 10.1073/pnas.2105170118. PMID: 34921113.

#### ORAL PRESENTATIONS

1. 2018 PREP Symposium. "Development of an Orthotopic Colorectal Cancer Mouse Model for Radiation Therapy Studies." Carlos J. Rodriguez, Nicholas Battaglia, Scott Gerber & Edith Lord
2. University of Louisville Microbiology and Immunology Departmental Seminar (2020). "Novel role of Interferon Lambda at the oral mucosal barrier." Carlos J. Rodriguez-Hernandez, Richard Lamont & Juhi Bagaitkar.
3. American Society for Microbiology (ASM), Kentucky/Tennessee Branch meeting (2021) "Paving the Road: *Porphyromonas gingivalis* abolishes antiviral immunity in the oral epithelium." Carlos J. Rodriguez-Hernandez, Shunying Yin, Kevin Sokoloski, Richard Lamont & Juhi Bagaitkar
4. University of Louisville Microbiology and Immunology Departmental Seminar (2022). "Interferon interference: Bacterial pathogen blocks IFN-λ responses in the

oral cavity.” Carlos J. Rodriguez-Hernandez, Shunying Yin, Kevin Sokoloski, Richard Lamont & Juhi Bagaitkar.

5. Infectious Disease Consortium Symposium (2022). “Pathogenic shift increases susceptibility to viral infection by dampening antiviral immunity.” Carlos J. Rodriguez-Hernandez, Shunying Yin, Kevin Sokoloski, Richard Lamont & Juhi Bagaitkar
6. Inflammation and Pathogenesis T32 Colloquium (2022). “Regulation and manipulation of the Type III IFN responses at the oral epithelium.” Carlos J. Rodriguez-Hernandez, Shunying Yin, Kevin Sokoloski, Richard Lamont & Juhi Bagaitkar
7. University of Louisville Microbiology and Immunology Departmental Seminar (2023). “Oral dysbiosis and the suppression of antiviral immunity.” Carlos J. Rodriguez-Hernandez, Shunying Yin, Kevin Sokoloski, Richard Lamont & Juhi Bagaitkar.

#### POSTER PRESENTATIONS

1. AAI Immunology Conference (2018) “Development of an Orthotopic Colorectal Cancer Mouse Model for Radiation Therapy Studies.” Carlos J. Rodriguez, Nicholas Battaglia, Scott Gerber & Edith Lord
2. Gordon Research Conference and Seminar– Phagocytes (2022) “*P. gingivalis* enhances susceptibility to viral infections by inactivating type III interferons at the oral mucosal epithelium” Carlos J. Rodriguez-Hernandez, Kevin J. Sokoloski, Himabindu Dukka, Shunying Jin, Daniel P. Miller, Maxim N. Artyomov, Richard J. Lamont, and Juhi Bagaitkar.
3. Infectious Disease Consortium (2022) “*P. gingivalis* enhances susceptibility to viral infections by inactivating type III interferons at the oral mucosal epithelium” Carlos J. Rodriguez-Hernandez, Kevin J. Sokoloski, Himabindu Dukka, Shunying Jin, Daniel P. Miller, Maxim N. Artyomov, Richard J. Lamont, and Juhi Bagaitkar.
4. Annual Biomedical Research Conference for Minoritized Scientists (ABRCMS) (2023) “Interfering with Interferons: Oral pathogen inhibits interferon responses in different mucosal epithelium, leading to enhanced viral susceptibility” Carlos J. Rodriguez-Hernandez, Kevin J. Sokoloski, Himabindu Dukka, Shunying Jin, Daniel P. Miller, Maxim N. Artyomov, Richard J. Lamont, and Juhi Bagaitkar.
5. Gordon Research Conference – Biology of Acute Respiratory Infection (2024) “Dysbiosis associated incapacitation of IFN responses and antiviral immunity” Carlos J. Rodriguez-Hernandez, Chandra Shrestha, Phylip Chen, Mark E. Peeples, Mitchell H. Grayson, Richard J. Lamont, and Juhi Bagaitkar.

#### MEMBERSHIPS

2013-2017 Honor Program Student Association, Active Member  
2013-2017 National Biological Honor Society βββ Zeta Kappa Chapter, Active Member  
2018-current The American Association of Immunologists, Student Member  
2019 Society for Leukocyte Biology, Student Member  
2021-current American Society for Microbiology, Student Member

COMMUNITY OUTREACH AND SERVICE

2020            Louisville Regional Science & Engineering Fair, Ambassador  
2021            Louisville Regional Science and Engineering Fair, Judge  
2022            NCH Research Retreat, Judge  
2022-2023      Summer Student Poster Day, Judge  
2023            The Ohio Academy of Science (virtual), Judge